Quaternary environmental changes in central Chukotka (NE Siberia, Russia) inferred from Lake El'gygytgyn pollen record and biome reconstruction

Inaugural-Dissertation

Zur

Erlangung des Doktorgrades
der Mathematisch-Naturwissenschaftlichen Fakultät
der Universität zu Köln

Vorgelegt von
Wenwei Zhao
aus Shanxi, China

Köln 2017

Berichterstatter	Prof. Dr. Martin Melles (Universität zu Köln)
(Gutachter)	apl. Prof. Dr. Bernd Wagner (Universität zu Köln)
	apl. Prof. Dr. Pavel Tarasov (Freie Universität Berlin)
Vorsitzender der	
Prüfungskommission:	Prof. Dr. Frank Schäbitz (Universität zu Köln)

Tag der mündlichen Prüfung: November 13, 2017

Contents

1 Introduction

1.1 Research background, objectives, methodology, and thesis structure

For more than a century the cause of Quaternary glacial/interglacial cycles has remained a research focus. Hays et al. (1976) first provided evidence to the Milankovitch hypothesis and suggested that the cyclic variations in the earth's orbit around the sun corresponded to variations in Earth's climate over the late Quaternary. Shackleton and Opdyke (1976) extended the record of orbital-scale variability spanning the entire Pleistocene based on a benthic $\delta^{18}O$ record from marine core V28-239 in the equatorial Pacific Ocean. The studies demonstrate that the oscillation between glacial and interglacial climates is the most fundamental characteristic of the Quaternary environment (past 2.588 Myr; International Commission on Stratigraphy, 2013). The cyclic pattern of glacial-interglacial climates was primarily forced by earth's orbital parameters: the precession (23-ka cycle), eccentricity (100-ka cycle), and obliquity (41-ka cycle). This proposal is supported by numerous geological archives of various depositional environments, e.g., deep ocean sediments (e.g. Shackleton and Opdyke, 1976; Shackleton et al., 1995), continental margin depositional sequences (e.g. Cronin et al., 1994; Naish et al., 1997, 1998), and continental records such as loess (e.g. Ding et al., 2002) and lacustrine sediments (e.g. Singh et al., 1981; Prokopenko et al., 2006). For instance, the long-term periodic ice-sheet changes were registered by the oxygen isotopic composition of marine foraminiferas (Lisiecki and Raymo, 2005). A number of international research projects are involved, e.g., Deep Sea Drilling Project (DSDP; 1968-1983), Ocean Drilling Program (ODP; 1985-2003), Integrated Ocean Drilling Program (IODP; since 2003), Greenland Ice Sheet Project (GRIP; 1989-1992), and International Continental Scientific Drilling Program (ICDP; since 1996).

Despite the enormous progress obtained from the marine and ice-core records concerning the relationship between climate cycles and orbital parameters, long continental records spanning the whole Quaternary period are scarce. The Arctic is highly sensitive to climate variations and is thus a key region for understanding the present and past climate changes on land. In the context of global climate changes, it is vital to investigate the response of the most vulnerable ecosystems such as forest tundra, shrub tundra, and steppe in the northern Siberia.

As a powerful tool for reconstructing the paleovegetation, pollen analysis is applied to the Lake El'gygytgyn (Northeastern Siberia) sediments. The palynological investigation of the

Lake El'gygytgyn sediments was initiated by Shilo et al. (2001). Since then, a number of localities in the lake have been studied palynologically. For instance, the *c.* 13 m long sediment core PG1351 were retrieved from the central part of the lake and the obtained pollen spectra (Lozhkin et al., 2007) were dated back to 250 ka (Nowaczyk et al., 2007). The pollen results prove the capacity of pollen spectra documenting vegetation and climate changes in the central Chukotka, Northeast Siberia (Lozhkin et al., 2007). In addition, 310 modern lacustrine samples were collected from the Northeast Siberia and Alaska and were analyzed to facilitate the interpretation of fossil pollen data (Anderson and Brubaker, 1993; Lozhkin et al., 2001, 2002; Anderson et al., 2002a, b).

Between 2008 and 2009, the deep-drilled composite core ICDP 5011-1 retrieved 318-m Lake El'gygytgyn (Melles et al., 2011) dated back to 3.58 Ma (Melles et al., 2012; Nowaczyk et al., 2013). Andreev et al. (2014, 2016) present the pollen result of the lower 216-m sediments documenting the vegetation and climate changes during the Late Pliocene and Early Pleistocene (*c.* 3.58-2.15 Myr). For the same sediment core, Lozhkin and Amderson (2013) compare the pollen spectra of the postglacial thermal maximum (PGTM) and MIS 5 with the "super" interglaciations (MIS 11 and 31; Melles et al., 2012). Recently, Lozhkin et al. (2017) published a new pollen result from core 5011-1 encompassing a period of the mid-Pleistocene (MIS 19-11; 374-790 ka).

This thesis aims to provide new insights into the Quaternary paleovegetation and its response to climate forcings in the Northeast Siberia. To achieve this, the thesis includes palynological investigation of the Lake El'gygytgyn sediment core 5011-1 concerning the intervals of ~2150 to 2100 ka (MIS 82-79), ~1091 to 715 ka (MIS 31-18), and ~240.5 to 181.5 ka (MIS 7.5-6.6). Pollen-based biome reconstruction (also known as biomization) was performed following the numerical method described by Prentice et al. (1996). The approach was first developed in order to produce a global vegetation map for the Last Glacial Maximum and Holocene period, which was a major task of the BIOME 6000 project (Prentice and Webb III, 1998). For reconstructing past vegetation dynamics of a region, the biomization method introduces the calculation of biome affinity scores for each pollen sample using a standard equation. Fluctuations in the biome affinity scores can provide information regarding the changes in the significance of a specific biome in the region. The method has been utilized in fossil pollen studies of different regions and was proved successful (e.g., Williams et al., 2004; Rudaya et al., 2009; Müller et al., 2010). Tarasov et al. (2013) verified the reliability of the biomization approach based on 43 modern surface pollen samples of the Lake El'gygytgyn area (Matrosova, 2009) and applied biome reconstruction to previously investigated Lake

El'gygytgyn core 5011-1 fossil pollen samples (Andreev et al., 2014, 2016; Lozhkin and Amderson, 2013). Additionally, the pollen-based index landscape openness is employed for indicating the regional vegetation cover.

The detailed objectives of this thesis are:
(i) to reconstruct the vegetation and environmental history in the Siberian Arctic during the intervals of ~2150 to 2100 ka (including the Réunion Subchron polarity reversal event; chapter 2), ~1091 to 715 ka (encompassing the Mid-Pleistocene Transition; chapter 3), and ~240.5 to 181.5 ka (the penultimate interglacial; chapter 4);
(ii) to discover the pattern of vegetation succession during glacials and interglacials based on qualitative and quantitative pollen analysis;
(iii) to infer the response of Arctic vegetation to changes in orbital forcings by a detailed comparison between the pollen data and astronomical parameters;
(iv) to reveal possible mechanisms driving climatic variations in the high latitudes during the Quaternary.

At last, chapter 5 synthesizes pollen data presented in chapters 2, 3, and 4. It compares vegetation successions during different stages of the Quarternary, probes into the environmental settings of characteristic interglaciations and glaciations, and attempts to reveal the dynamics of earth's orbital and internal forcings influencing Arctic vegetation and climate over the Quaternary.

1.2 Study region

1.2.1 Lake El'gygytgyn

Lake El'gygytgyn, located ~100 km to the north of the Arctic Circle in Northeast Russia (67°30′N, 172°05′E), was formed by a meteorite impact ~3.58 Myr ago (Layer, 2000). The lake is 170-m deep and ~12 km in diameter (Melles et al., 2012). The meteorite crater is a ~18 km-diameter flat-bottom circular basin that is located on the southeastern slope of the Akademik Obruchev Ridge in the central Chukotka. The surrounding crater rim is 100-130 m above lake level. The vegetation of the Lake El'gygytgyn basin is dominated by lichen and herbaceous taxa and is often discontinuous, especially on higher slopes (Kozhevnikov, 1993).

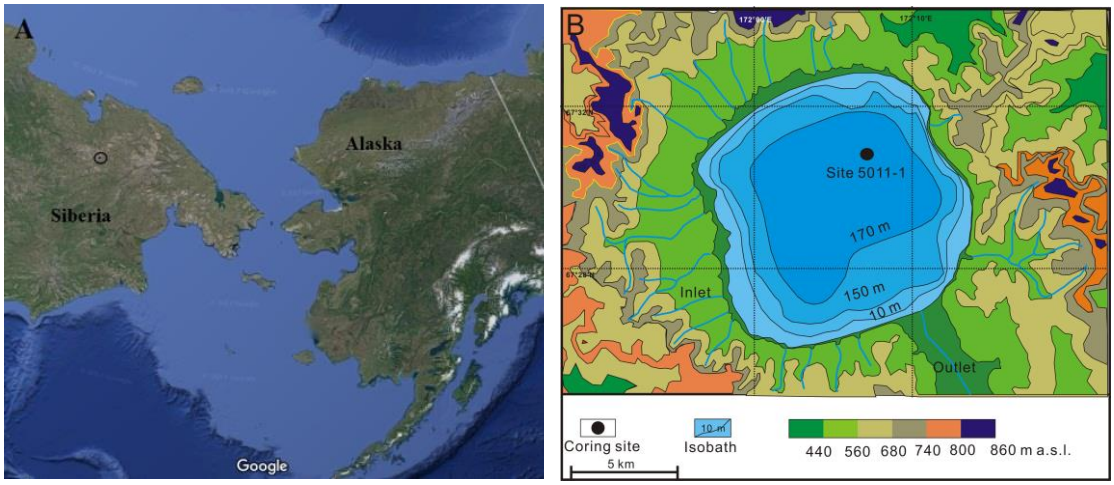

Fig. 1.1 Map of the study region: (A) location of Lake El'gygytgyn marked by a circle, (B) bathymetric map of Lake El'gygytgyn and topography of its catchment, after Swann et al. (2010). The drilling site 5011-1 is indicated as a black dot.

The lake has a surface area of 110 km^2 and a relatively small catchment of 293 km^2, with ~50 creeks discharging into the lake and the Enmyvaan River outlet flowing southeastward to the Bering Sea (Nolan and Brigham-Grette, 2007). The lake is covered by seasonal ice between mid-October and July (Nolan et al., 2002). The inlets deliver ~350 t yr^{-1} of sediments into the lake, with spring and early summer being the main periods of sediment influx. Discharge of the Enmyvaam River is limited to the summer months and is estimated to be *c.* 0.05 km^3 yr^{-1} (Fedorov et al., 2013). The residence time of the lake water is *c.* 100 years (Fedorov et al., 2013; Fig. 1.1).

1.2.2 Climate

The climate of the northern Siberia is characterized by long cold winters and short hot summers. The thermal regimes are mainly controlled by the geographical setting of high latitude and continental location (Shahgedanova, 2002). The winters in the region are marked by cold air mass brought by the strong Aleutian highs over the Beaufort and Chukchi Seas. In contrast, during the summers, warm Pacific air is transported into the lake area (Nolan and Brigham-Grette, 2007).

In the crater region, the mean annual air temperature is low and displays an increasing trend over the last half-century (Fig. 1.2). Air temperatures data between 1948 and 2002 (Kalnay et al., 1996) for this region show a mean annual air temperature of -8.3 ℃. The mean air

temperature ranges from -35 ℃ in winter to 8 ℃ in summer. Extremely high summer temperature can reach as high as 26 ℃.

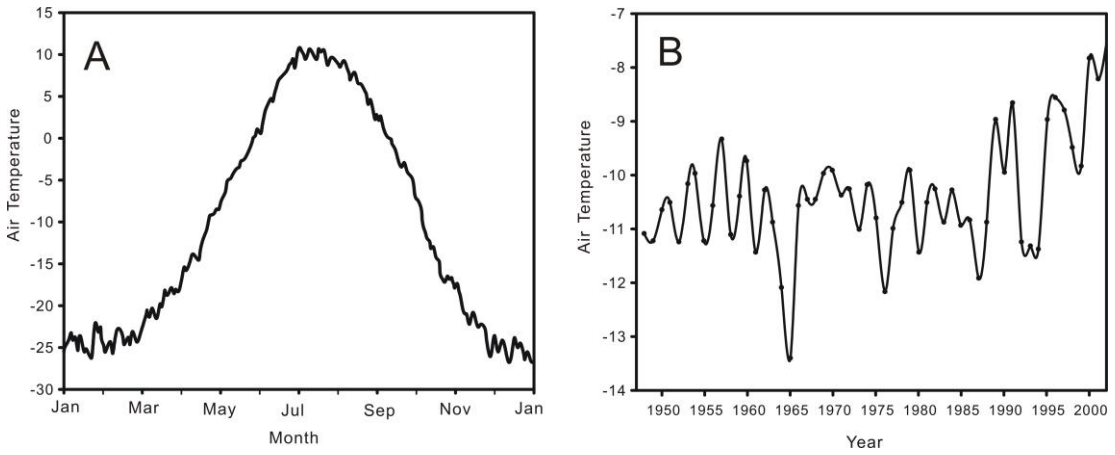

Fig. 1.2 (A) Mean daily average air temperatures for the period 1948-2002, (B) mean annual air temperatures from 1948 to 2002, after Nolan and Brigham-Grette (2007).

The El'gygytgyn crater is generally dry, which is typical of the Arctic region. The mean annual precipitation is ~200 mm yr^{-1}, with ~80 mm occurring during summers (from June to September) and ~110 mm as snowfall during other seasons. Extreme climate events, e.g., in 2002, showed that air temperatures between mid-May and late-September dropped to nearly 0 ℃ and the snowfall (>5 cm) started in mid-July and accumulated to *c.* 0.40 m in 2002. Strong winds are characteristic of the region. In winter, particularly, the wind speed averages 17.8 m s^{-1} (Nolan and Brigham-Grette, 2007).

1.2.3 Vegetation

In the Arctic region, not only the harsh climate but also the existence of polar day and night play dominant roles on the vegetation (Lavrushin and Alekseev, 2005). In the following, information of the Siberian and Alaskan plant communities are summarized mainly according to the description by Viereck et al. (1992), Viereck and Little (1975), and Lozhkin et al. (2007; Fig. 1.3).

The low-lying areas of the crater slopes and lake terraces is primarily covered by hummock tundra with *Eriophorum vaginatum, E.callitrix, E.polystachion, Pedicularis pennellii, P. albolabiata, Carex rotundata, C. lugens, Salix fuscescens, S.reticulata, Senecio atropurpureus,* and *Vaccinium uliginosum.* In the higher elevations of the crater slopes, moss-lichens tundra occurs and is mainly composed of *Cassiope tetragona, Rhododendron*

parvifolium, *Senecio resedifolus*, *Ermania parryoides*, *Silene stenophylla*, *Dryas octopetala*, *Potentilla elegans*, and *Anderosace ochotensis*. The upper mountain plains are covered by sterile tundra, where *Salix phlebiphylla*, *Artemisia furcate*, and *Saxifraga serpyllifolia* are found (Lozhkin et al., 2001).

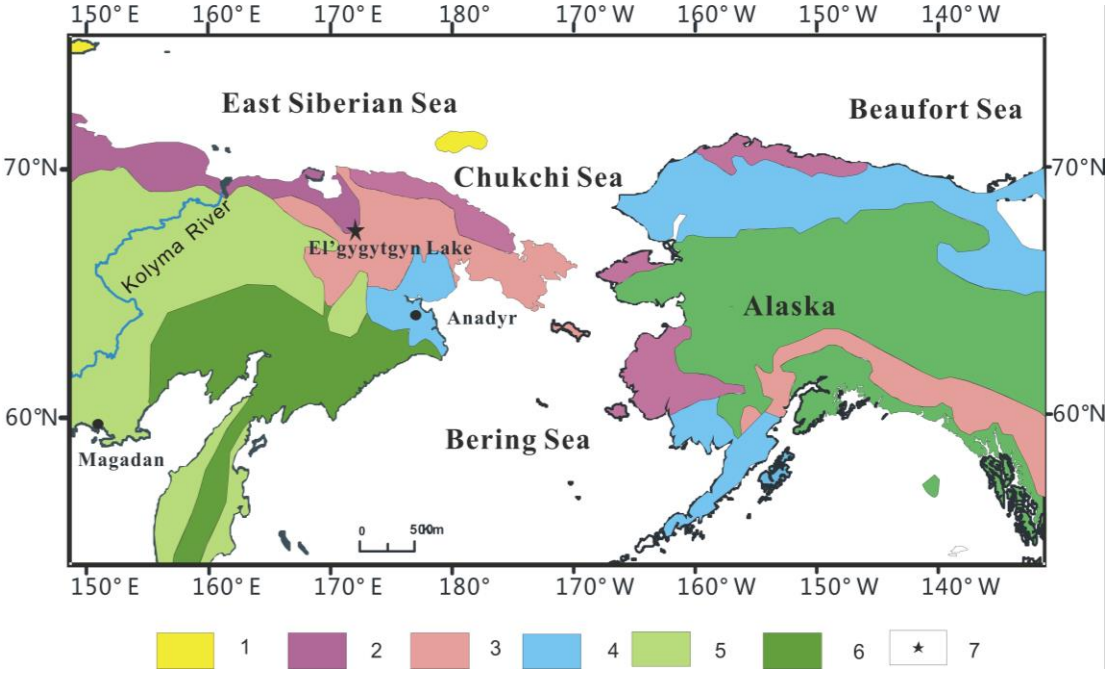

Fig. 1.3 Key to the vegetation, after Lozhkin et al. (2007): (1) polar desert with discontinuous herb-dominated vegetation, (2) wet arctic tundra dominated by *Eriophorum spp.* with some low-growth shrubs, (3) upland and mesic tundra, (4) moist tundra often with low to mid-sized shrubs and Cyperaceae, (5) boreal forest dominated by *Larix gmelinii* and *Pinus pumila*, (6) high shrub tundra, and (7) location of Lake El'gygytgyn.

Riparian plants, especially along the Enmyvaam River and large inlet creeks, are mainly low shrubs of willow communities, e.g. *Salix tschuktschorum, S. saxatilis, Androsace ochotensis, Empetrum subholarcticum, Pleuropogon sabinii, Polemonium spp., Beckwithia chamissonis, Saussurea tilesii,* and *Chamerion latifolium* (Belikovich, 1994).

In terms of the regional vegetation, a sparse tundra interspersed by a few low shrub species is the most widespread in the Chukchi uplands. Low shrubs such as *Salix krylovii* and *S.alaxensis* are found in the valleys. *Betula exilis* is restricted to better organically accumulated areas such as alpine valleys, terraces, and saddles. In the southern Chukchi uplands, common shrubs are *Pinus pumila* and *Alnus fruticosa* (~2 to 3 m).

Nearest coniferous forest appears ~150 km to the south and west of Lake El'gygytgyn. The main body of the forests is at a ~300 km distance, with *Larix dahurica* being the most

widespread deciduous trees. The vegetation of the northeastmost Siberia, located ~600 km to Lake El'gygytgyn, is a discontinuous herb-dominated tundra and polar desert. The only shrub species (*Salix.* spp.) typically grows in prostrate form (~1 m) in protected valleys (Lozhkin et al., 2007).

1.3 The Lake El'gygytgyn sediment core 5011-1

1.3.1 Drilling campaign and sediment cores

The drilling operation was conducted by the U.S. consortium DOSECC using a modified GLAD 800 drilling system (Russian FLAD 800; Melles et al., 2011). LacCore at the University of Minnesota handled core curation. The research is financed by International Continental Scientific Drilling Program (ICDP), the U.S. National Science Foundation (NSF), the German Federal Ministry of Education and Research (BMBF), Alfred Wegener Institute (AWI) and GeoForschungsZentrum Potsdam (GFZ), the Russian Academy of Sciences Far East Branch (RAS FEB), the Russian Foundation for Basic Research (RFBR), and the Austrian Federal Ministry of Science and Research (BMWF; Melles et al., 2011).

Three parallel holes were drilled at ICDP Site 5011-1 in the central part of Lake El'gygytgyn (Fig. 1.1). The drilling penetrated all the sediments deposited since the formation of the lake. A composite sediment profile of 318 m is obtained by correlating magnetic susceptibility measurements of the parallel cores (Melles et al., 2011). The uppermost sediment gaps was filled by comparing with the 16-m sediment core (Lz1024) drilled in 2003. The resultant composite core sediments display no signs of hiatuses (i.e., no evidence of basin glacial or desiccation). The lacustrine sediments are mainly clastic and highly variable in composition, with five different lithofacies being assigned to specific depositional conditions (for details see Melles et al. (2012)). Event indicators include the occurrence of prominent MMD (Sauerbrey et al., 2013), tephra layers (van den Bogaard et al., 2014), and fossil redox layers (Wennrich et al., 2014).

1.3.2 Chronology

The timing of the El'gygytgyn impact was dated by $^{40}Ar/^{39}Ar$ to 3.58±0.04 Ma ago on the impact-melted rocks derived from the crater rim (Layer, 2000). The age is also confirmed by

paleomagnetic data measured on the impact breccia and bedrock material recovered by core 5011-1C (Maharaj et al., 2013). Paleomagnetic measurements on U-channels and discrete samples yielded distinct down-core variations in inclination of the ChRM that could be addressed to three polarity chrons (Gauss, Matuyama, and Brunhes) and five subchrons (Jaramillo, Olduvai, Réunion, Kaena, and Mamooth; Melles et al., 2012; Fig. 1.4). The geomagnetic reversals and age of the impact were used as first order tie points for the composite profile of core 5011-1.

The second order tie points were obtained by correlating the XRF-scanning-based Si/Ti ratios and Ti contents and the Fourier transform infrared spectroscopy (FTIRS) derived biogenic silica (BSi) contents with the global marine isotope stack LR04 record (Lisiecki and Raymo, 2005). The third order tie points were a result of comparing the variations in the total organic carbon (TOC) contents and the magnetic susceptibility (MS) with the cumulative 65 °N summer insolation (Laskar et al., 2004). Subsequently, an iterative tuning approach was applied to the tie points of all three orders to refine the age/depth model (Nowaczyk et al., 2013).

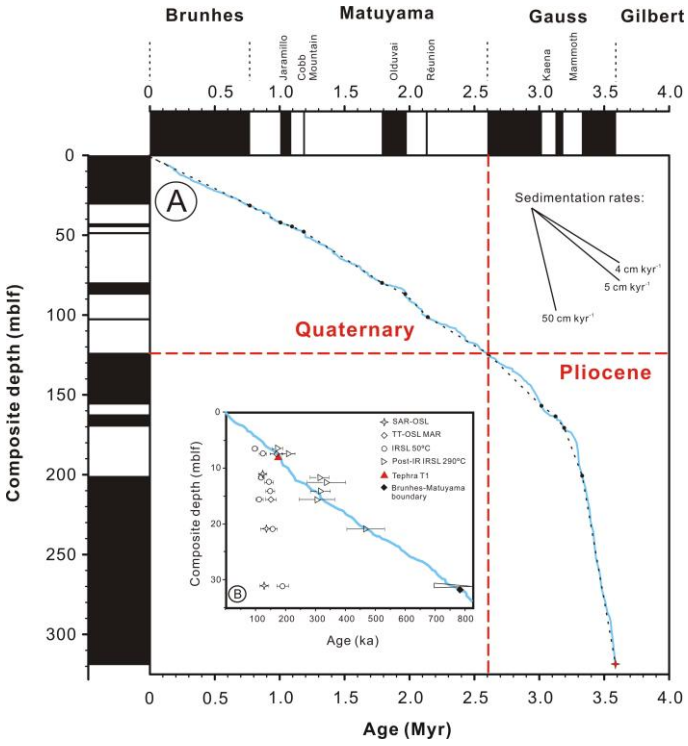

Fig. 1.4 (A) Age/depth model for the Lake El'gygytgyn ICDP 5011-1 composite core, after Melles et al. (2012). The black dots indicate the first-order tie points and the blue curve denotes the second- and third-order tie points. The red cross marks the time of the meteorite impact at 3.58 ±0.04 Ma. The black and white bars along the age and depth axes denote normal and reversed polarity, respectively, (B) age/depth model of the uppermost 35 m for the ICDP 5011-1 composite core (the blue curve) with a consolidation of luminescence ages, after Wennrich et al. (2016). Ages of tephra T1 (van den Bogaard et al., 2014; red triangle) and the Brunhes/Matuyama polarity change

(Haltia and Nowaczyk, 2014; black diamond) are also indicated. The extended triangle in the lower right corner correlates with the sample from the B/M boundary and illustrates a pIRIR290 age of >700 ka.

Age/depth model of the uppermost 35 m was consolidated by luminescence ages determined by different dating protocols on the fine-grained quartz and the polymineral fraction (Zander and Hilgers, 2013). The dating protocols involved a multiple aliquot additive dose IRSL protocol and a single aliquot regeneration dose (SAR)-IRSL protocol, which have been successfully applied to the cores PG1351 (Forman et al., 2007) and Lz1024 (Juschus et al., 2007) of Lake El'gygytgyn sediments younger than 300 ka.

To conclude, the Lake El'gygytgyn sediment core 5011-1 yields great opportunities for filling the gap of a continuous Quaternary vegetation history in the high latitudes. With multi-proxy analysis (e.g., Melles et al., 2012; Brigham-Grette et al., 2013; Francke et al., 2013; Tarasov et al., 2013; Wennrich et al., 2013, 2016), it is possible to comprehensively understand the long-term environmental change and its climate forcings.

2 The Réunion Subchron vegetation and climate history of the northeastern Russian Arctic inferred from the Lake El'gygytgyn pollen record*

Abstract

The 318-m-thick sediment record from Lake El'gygytgyn provides unique opportunities for a detailed examination of environmental changes during the Réunion Subchron polarity reversal event (2.1384-2.1216 Myr BP) in the northeastern Russian Arctic. The paper describes vegetation and climate fluctuations between ~2.150 and 2.100 Myr BP as inferred from palynological data. Biome reconstructions indicate that throughout this interval the tundra (TUND) biome generally has higher affinity scores as compared to cold steppe (STEP) or cold deciduous forest (CLDE). An exception is the climatic optimum between ~2.139-2.131 Myr BP, coinciding with Marine Isotope Stage 81 (approximately the Réunion Subchron), when the CLDE biome has the highest scores. Landscape-openness indices suggest that more closed vegetation characterized most of the interval between 2.146-2.127 Myr BP, when deciduous forest and shrubs expanded in the regional vegetation and climate was relatively warm and wet. Peaks in green algal colonies (*Botryococcus*) and *Zygnema*-type spores ~2.150-2.146, ~2.131-2.123, and ~2.112-2.102 Myr BP indicate expansions of shallow-water habitats and lowered lake levels. Comparisons with biome reconstructions from other interglacial intervals at Lake El'gygytgyn suggest that precession-related summer insolation intensity and obliquity-related duration of summer daylight are major controls on the onset of interglaciations, whereas obliquity probably plays a more significant role on vegetation succession at northern high latitudes during the Pleistocene.

Keywords: Pollen, Early Pleistocene, Biome, Orbital forcing, Northeastern Russian Arctic

* This chapter is based on Zhao, W.W., Andreev, A.A., Wennrich, V., Tarasov, P.E., Anderson, P., Lozhkin, A.V., Melles, M., 2015. The Réunion Subchron vegetation and climate history of the northeastern Russian Arctic inferred from the Lake El'gygytgyn pollen record. Palaeogeography, Palaeoclimatology, Palaeoecology 436, 167-177.

2.1 Introduction

Lake El'gygytgyn, located in northeastern Russia (67°30' N, 172°05' E; Fig. 2.1), hosts the oldest continuous terrestrial sediment record from the Arctic (Melles et al., 2012; Brigham-Grette et al., 2013). In spring 2009, a 318-m-thick composite record was recovered in the center of the lake (ICDP Site 5011-1, Fig. 2.1), penetrating the last 3.6 Myr BP, with full recovery down to 2.8 Myr BP (Melles et al., 2011). A suite of multi-disciplinary studies on this record has been reported previously (Melles et al., 2012; Brigham-Grette et al., 2013; special issue of Climate of the Past: http://www.clim-past.net/special_issue48.html), including ones using palynological data to reconstruct past vegetation and climate (Lozhkin et al., 2007; Lozhkin and Anderson, 2013; Tarasov et al., 2013; Andreev et al., 2014). These earlier studies revealed a number of major shifts in vegetation, perhaps none more noteworthy than those of the Late Pliocene to Early Pleistocene (3.575-2.150 Myr BP). Until ~2.93 Myr BP, the vegetation was dominated by taxon-rich, cool-mixed and cool-conifer forests, Pliocene remnants representing climates significantly warmer and wetter than the present. After ~2.725 Myr BP, cold deciduous forests and tundra characterized the El'gygytgyn region. Beginning ~2.6 Myr BP, the cool conifer and cold deciduous forests were gradually replaced by tundra. Despite the onset of glaciation in the northern hemisphere (Brigham-Grette et al., 2013), warmer-than-present Arctic summers persisted at Lake El'gygytgyn until ~2.2 Myr BP, when glacial episodes started to gradually increase in frequency (Melles et al., 2012; Brigham-Grette et al., 2013).

The Lake El'gygytgyn sediments indicate clear polarity zonations and thus provide 12 first-order tie points to pin down the age of the longest paleoclimate record from the continental Arctic (Haltia and Nowaczyk, 2014). The mean sedimentation rate decreases rapidly from ~50 cm ka^{-1} to 4-5 cm ka^{-1} at the onset of the Pleistocene, when polarity shifts from the Gauss Chron to the Matuyama Chron. This reversal likely was associated with the reorganization of circumpolar atmospheric circulation through climate changes that have caused variations in sediment deposition (Haltia and Nowaczyk, 2014; Fig. 2.2). The Réunion Subchron, which is the first polarity reversal within the Quaternary recognized in the Lake El'gygytgyn sediment record, provides exceptionally good age control for early Quaternary deposits. This quality allows the unequivocal identification of glacial and interglacial events the specific orbital parameters associated with these climate shifts.

It is well documented that oscillations in glacial and interglacial periods since the onset of the Pleistocene (~2.6 Myr) have been controlled by the astronomical parameters of eccentricity,

obliquity, and precession (Milankovitch, 1941; Hays et al., 1976). Obliquity and precession are dominant influences on the duration of climatic cycles, whereas eccentricity only "paces" rather than "drives" climatic change (Maslin and Ridgwell, 2005). Obliquity at high latitudes has a profound effect on seasonal insolation (Berger and Loutre, 2004; Liu and Herbert, 2004), although precession is the dominant factor at lower latitudes (Ruddiman and McIntyre, 1984; Shakleton et al., 1999; Ruddiman, 2003; Liu and Herbert, 2004; Maslin and Ridgwell, 2005; Joannin et al., 2011). According to grain-size data from the Lake El'gygytgyn record, the glacial-interglacial cycles during the Early Pleistocene in that area are mainly controlled by the 41 ka (obliquity) cycle, whereas after ~ 0.67 Myr BP the 100 ka (eccentricity) cycle is dominant (Francke et al., 2013).

Several studies have examined the relationship of long-term vegetation change during the Pleistocene and relevant astronomical forcing (e.g., Tzedakis et al., 1997; Bar-Matthews et al., 2003; Prokopenko, et al., 2006; Joannin et al., 2007, 2008, 2011). However, most of these studies are limited to middle-to-low latitudes of the northern hemisphere. In this paper, we present the Réunion Subchron pollen data from the composite core of Lake El'gygytgyn in Chukotka. The objectives of this study are (1) to provide the first high-resolution Réunion Subchron pollen record in the high Arctic and (2) to evaluate the relative importance and influence of the obliquity-related duration of seasonal sunlight and precession-related levels of summer insolation on regional vegetation and climate changes by comparing the study interval with MIS 5 and MIS 11 pollen records.

2.2 Study region and site description

Lake El'gygytgyn, located in northeastern Russia, was formed by a meteorite impact ~3.58 Myr ago (Layer, 2000; Fig. 2.2). The meteorite crater is a *c.* 18 km-diameter flat-floored circular basin that is located in the central part and southeastern slope of the Akademik Obruchev Ridge in central Chukotka. The lake floor is bowl-shaped with a diameter of ~12 km and a maximum water-depth of ~170 m. The surrounding crater rim is 100~130 m above lake level.

The lake has a relatively small catchment of 293 km^2, with ~50 creeks discharging into the lake and the Enmyvaan River outlet flowing to the southeast (Nolan and Brigham-Grette, 2007). Lake El'gygytgyn is an oligotrophic to ultra-oligotrophic and cold-monomictic lake (Cremer and Wagner, 2003) with 9-10 months ice-cover resulting in a very short open-water

season (Nolan et al., 2003). The inlets deliver ~350 t yr^{-1} of sediment into the lake, with spring and early summer being the main times of sediment influx (Fedorov et al., 2013). Considerable phytoplankton growth also takes place in winter time beneath the ice cover and contributes to the sedimentation (Cremer et al., 2005).

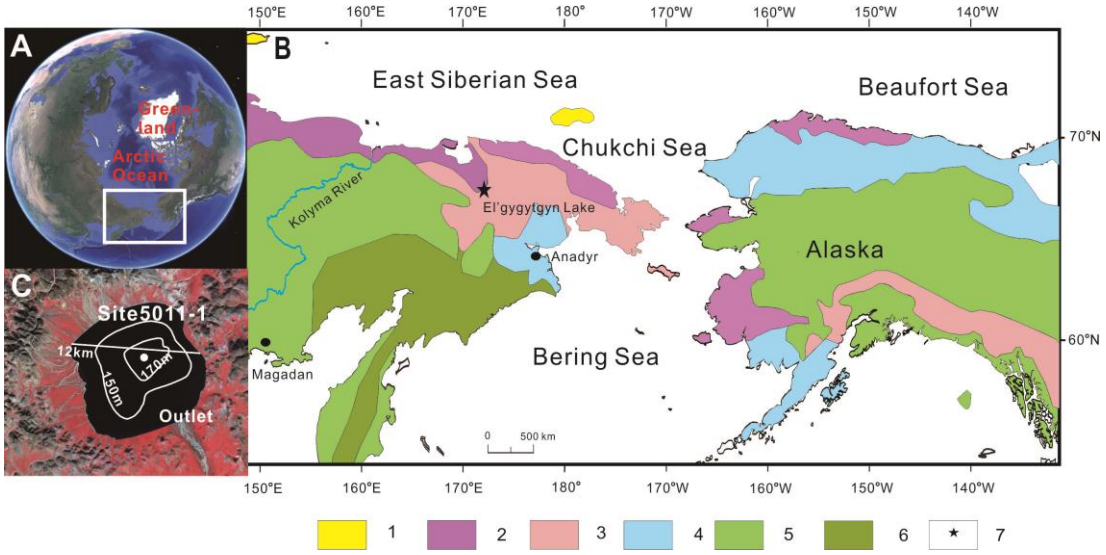

Fig. 2.1 Map showing the location of Lake El'gygytgyn and a simplified distribution of the major vegetation types in northeastern Russia. (A) Location of the study site (image source: Google Earth). (B) Key to the vegetation (modified from Lozhkin et al., 2007) with (1) polar desert with discontinuous herb-dominated vegetation, (2) wet arctic tundra dominated by *Eriophorum* spp. with some low-growth shrubs, (3) upland and mesic tundra, (4) moist tundra often with low to mid-sized shrubs and Cyperaceae, (5) boreal forest dominated by *Larix gmelinii* and *Pinus pumila*, (6) high shrub tundra, and (7) location of El'gygytgyn Lake. (C) Satellite image of the El'gygytgyn crater showing the location of the drilling site 5011-1 (image source: http://www.geo.umass.edu/lake_e/media.html).

Lake El'gygytgyn is situated within the zone of continuous permafrost, exhibiting a mean annual ground temperature of -10 ℃ at 12.5 m depth (Schwamborn et al., 2008). The region is characterized by extremely harsh climate with mean annual air temperature (MAT) of *c.* -10 ℃ and average July and January temperatures of 8 ℃, and -35 ℃, respectively. Mean annual precipitation is ~200 mm yr^{-1} with 80 mm summer rainfall (June-September) and ~110 mm water-equivalent in snowfall (Nolan and Brigham-Grette, 2007).

The modern vegetation in the El'gygytgyn Crater is generally sparser with fewer shrub species as compared to the surrounding Chukchi uplands (Lozhkin et al., 2001; Lozhkin and Anderson, 2013). Low-shrub and herb-dominated tundra populate the uplands surrounding the crater. They are mainly composed of *Salix polaris, Cassiope tetragona, Carex tripartite, Phippsia algida, Koenigia islandica, Saxifraga hyperborean, Eritrichium villosum, Primula tschuktschorum, Hierochloe pauciflora,* together with small populations of *Pinus pumila* and

Alnus fruticosa (Belikovich, 1994; Andreev et al., 2012). Scattered stands of *Larix gmelinii* and *Pinus pumila* appear ~100 km to the south and west of Lake El'gygytgyn, while the main body of the forest is ~300 km away.

The carter is covered primarily by Cyperaceae-hummock and moss-lichen tundra that is dominated by herbaceous and lichen species (e.g., *Eriophorum spp., Pedicularis spp., Carex spp., Salix spp., Senecio atropurpureus, Ledum decumbens, Andromeda polifolia, Vaccinium uliginosum, Cassiope tetragona, Rododendron parvifolium, Ermannia parryoides, Silene stenophylla, Dryas octopetala, Crepis nana, Potentilla elegans,* and *Androsace ochotensis)*. Small thickets of *Alnus fruticosa* (shrub alder) are found ~10 km to the south of the Enmyvaan River (Fig. 2.1C).

2.3 Methods

2.3.1 Laboratory methods and age model

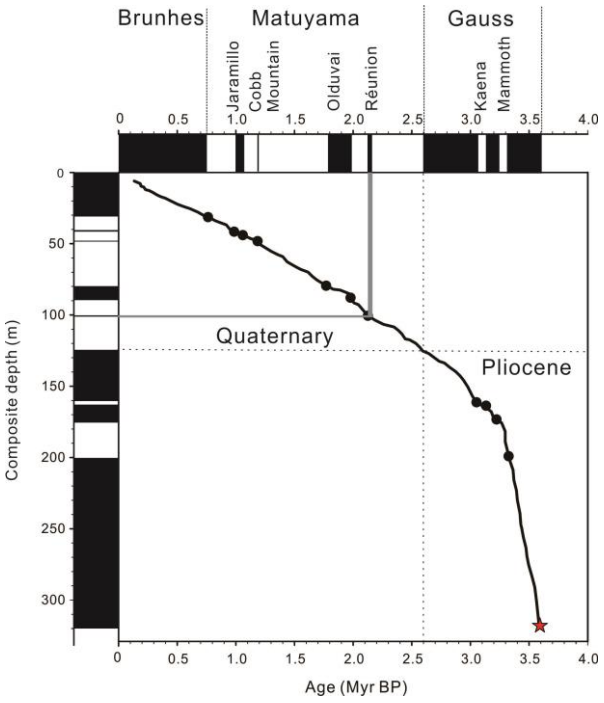

Fig. 2.2 Age/depth model with resulting sedimentation rates for the ICDP 5011-1 core composite from Lake El'gygytgyn, based on magnetostratigraphy and correlation between sediment proxy data, the LR04 marine isotope stack (Lisiecki and Raymo, 2005), and regional spring and summer insolation (Laskar et al., 2004). Initial first-order tie points are indicated by black dots; second- and third-order tie points are denoted by the black curve. The red star marks the time of the impact inferred from $^{40}Ar/^{39}Ar$ dating at 3.58 Ma (Layer, 2000). Black and white bars denote normal and reversed polarity, respectively. The gray bar indicates the studied interval. This figure is adapted from Melles et al. (2012).

Pollen subsamples of ~1.5 g were taken at ~1000 yr (1 ka) increments from 101.91 to 99.59 m depth in the composite core 5011-1 from Lake El'gygytgyn. This core interval according to the age model provided by Melles et al. (2012) and Nowaczyk et al. (2013) encompasses a period of ~50,000 years between ~2.15 and 2.10 Myr BP (Fig. 2.2).

Samples were processed following standard techniques (Fægri and Iversen, 1989), with additional fine sieving to remove clay-sized particles. A tablet containing *Lycopodium clavatum* spores was added to each sample for calculation of pollen concentrations and pollen accumulation rates (PAR; Stockmarr, 1971). The pollen concentrate was mounted in water-free glycerol. Palynomorphs were identified at 400× magnification, with the aid of several pollen keys and atlases (Kupriyanova and Alyoshina, 1972, 1978; Bobrov et al., 1983; Reille, 1992, 1995, 1998). In this paper, the so-called non-pollen-palynomorphs (NPPs) include spores, fungi, and algal colonies, which were identified and counted according to van Geel (2001). In most samples, >250 terrestrial pollen grains were identified, with this sum used to calculate the percentages of tree, shrub, and herb pollen. Percentages of NPPs are based on terrestrial pollen counts plus sums of the respective NPP category (e.g., $spore_{type1}$ percentage equals to $spore_{type1}$ counts divided by sum of pollen and spore). Poor pollen concentration in some samples resulted in insufficient counts to provide reliable percentages. These samples are excluded from further analysis. Pollen accumulation rates (grains cm^{-2} yr^{-1}) of each taxon are computed by multiplying pollen concentration (grains ml^{-1}) by the sedimentation rate (cm yr^{-1}).

2.3.2 Reconstructing biomes and landscape openness

Reconstructing plant biomes (a process also known as "biomization") was done following the techniques of Prentice et al. (1996) that include calculating biome or affinity scores for each pollen sample using their standard equation. This method has been applied successfully to the Late Pliocene-Early Pleistocene part of the Lake El'gygytgyn pollen record (Tarasov et al., 2013). Pollen taxa and their associated biomes are summarized in Table 2.1. The taxa-to-biome assignment and biome score calculations used in this study follow the matrix presented in Tarasov et al. (2013).

Landscape openness is another criterion that has proved useful in paleovegetation reconstructions (Tarasov et al., 2013). This method provides a qualitative assessment of changes in vegetation cover by evaluating the difference between maximum forest biome

(MFBS) and maximum open biome (MOBS) scores. In our study, the forest biome is represented by cold deciduous (CLDE), taiga (TAIG), cool conifer (COCO), and cool mixed (COMX) biomes; more open vegetation is indicated by tundra (TUND) and steppe (STEP) biomes. Biomes and landscape openness were also calculated for two other intervals in the Lake El'gygytgyn record that center on the MIS 11c super interglacial (Lozhkin and Anderson, 2013) and the MIS 5e interglacial (Lozhkin et al., 2007). Each of these intervals encompasses *c.* 50,000 yr. All results were compared qualitatively to examine the relationship of vegetation change to variations in orbital parameters.

Table 2.1 Terrestrial pollen taxa identified in the Quaternary part of the Lake El'gygytgyn record and their associated biome assignments. Among MIS 81, MIS 11 and MIS 5, the biomes TAIG and COCO are only recognized during the superinterglacial MIS 11. Taxa, whose percentages in the biome-taxon matrix are <0.5% (threshold suggested by Prentice et al., 1996) and which do not influence the results of the biome reconstruction, are marked with an asterisk between ~2.15 and 2.10 Myr BP.

Biome	**Terrestrial pollen taxa**
TUND/Tundra	*Alnus fruticosa*-type (shrub), *Betula* sect. *Albae*-type (tree)*, *B.sect. Nanae*-type (shrub), *B.* undif, Cyperaceae, Ericales, Poaceae, Polemoniaceae, Polygonaceae, *Rubus chamaemorus*, *Salix*, Saxifragaceae, Valerianaceae
CLDE/Cold deciduous forest	*Alnus fruticosa*-type (shrub), *Betula* sect. *Albae*-type (tree)*, *B.* sect. *Nanae*-type (shrub), *B.* undif, Ericales, *Larix/Pseudotsuga*, *Pinus subgenus Haploxylon*, Pinaceae undif, *Rubus chamaemorus*, *Salix*
TAIG/Taiga	*Alnus sp*, *Abies**, *Betula* sect. *Albae*-type (tree)*, *B.* sect. *Nanae*-type (shrub), *B.* undif, Ericales, *Larix/Pseudotsuga*, *Picea**, *Pinus* s/g *Haploxylon*, Pinaceae undif, *Rubus chamaemorus*, *Salix*
COCO/Cool conifer forest	*Alnus sp*, *Abies**, *Betula* sect. *Albae*-type (tree)*, *B.* sect. *Nanae*-type (shrub), *B.* undif, *Carpinus*-type*, *Corylus**, Ericales, *Larix/Pseudotsuga*, *Picea**, *Pinus subgenus Haploxylon*, Pinaceae undif, *Salix*, *Tilia**, *Tsuga**
STEP/Cold steppe	*Artemisia*, Asteraceae, Asteraceae Cichorioideae*, Caryophyllaceae, *Cannabis*-type, Chenopodiaceae, Fabaceae, Lamiaceae, Onagraceae, Papaveraceae, Poaceae, Polygonaceae, Ranunculaceae, Rosaceae*, *Thalictrum*, Valerianaceae

2.4 Results

2.4.1 Pollen

A total of 69 pollen, spore and NPP types have been identified in the 47 samples investigated (Fig. 2.3 and 2.4). Major trends in the taxa are described in Table 2.2. The diagrams have been subdivided into 7 pollen zones (PZ), based on stratigraphically constrained cluster analysis (CONISS) and visual inspection of the percentages. PZ numbers are assigned following those in Andreev et al. (2014) to insure chronological continuity and compatibility of comparison. Four general pollen assemblages characterize the record between ~2.15 and 2.10 Myr BP: (i) herb dominated (PZ-58), (ii) deciduous shrub-graminoid dominated (PZ-61, PZ-62, PZ-63, PZ-64), (iii) deciduous shrub dominated (PZ-59), and (iv) *Pinus*/deciduous shrub dominated (PZ-60). Note that *Larix* pollen occurs in all zones except PZ-58.

2.4.2 Biome reconstructions

Four samples with low counts (<50 terrestrial pollen grains; Fig. 2.3) were excluded from biomization. The results obtained on the remaining samples show that the Lake El'gygytgyn record between 2.15 and 2.10 Myr BP is characterized by tundra (TUND), cold steppe (STEP), and cold deciduous forest (CLDE) (Fig. 2.5). Tundra and cold deciduous forest (i.e., larch forest) are common in northeastern Siberia today (Fig. 2.1), while all three biomes are found in neighboring areas of eastern Siberia. The TUND biome has the highest affinity scores throughout our record, and tundra biomes predominate (Fig. 2.5A, B). The exceptions are two short intervals at 2.138-2.131 and ~2.111 Myr BP, with CLDE and STEP biome, respectively. Relatively high CLDE affinity scores occurred at 2.145-2.127 and 2.117-2.112 Myr BP. Between 2.123 and 2.117 Myr BP, the affinity scores of CLDE and STEP are close.

The landscape around Lake El'gygytgyn was relatively open for most of the 2.150-2.099 Myr BP interval (Fig. 2.5C). An exception occurred between 2.138 and 2.131 Myr BP, when pollen of *Pinus* s/g *Haploxylon* (Fig. 2.5D) was abundant.

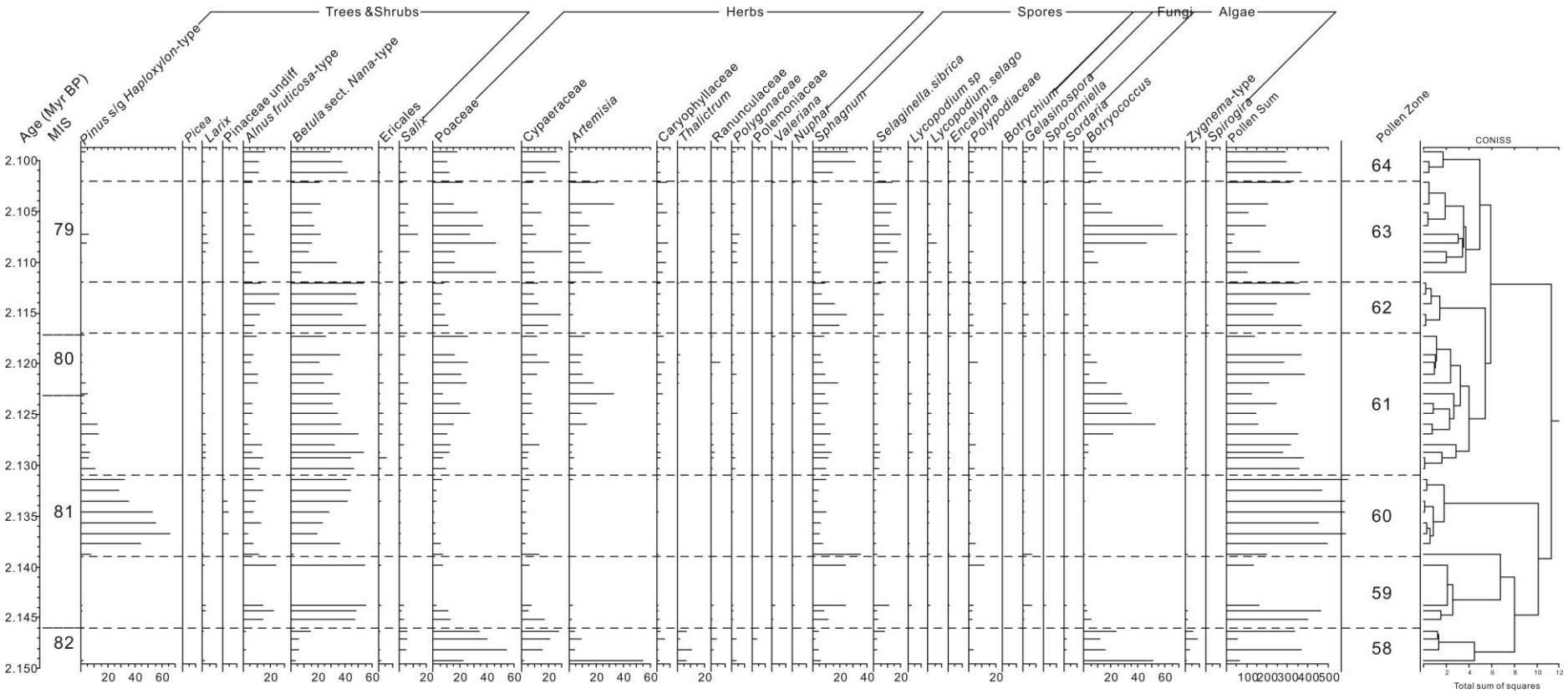

Fig. 2.3 Summary diagram showing percentages of major pollen, spore, fungal and algal taxa between ~2.15 and 2.10 Myr BP in Lake El'gygytgyn.

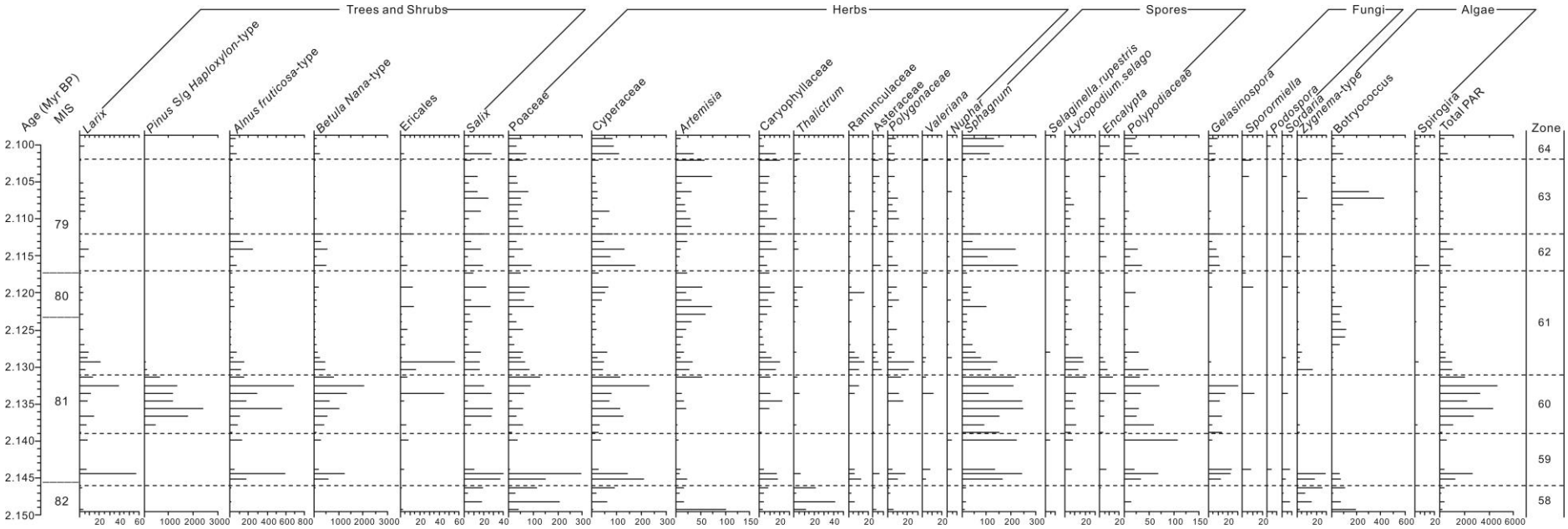

Fig. 2.4 Summary diagram of pollen accumulation rates (grains cm^{-2} yr^{-1}) for major taxa between ~2.15 and 2.10 Myr BP in Lake El'gygytgyn.

Table 2.2 Description of the pollen zones that occur in the sediments of Lake El'gygygyn formed between 2.150 and 2.099 Myr BP. PZ=pollen assemblage zone, AP=arboreal pollen, NAP=non-arboreal pollen, LB=lower boundary, NPP=non-pollen-palynomorph.

PZ	Age (Myr BP)	Features	PAR
Deciduous shrub taxa PZ-64	2.099-2.102	**AP**: predominance of *Betula* sect. *Nanae*-type and *Alnus* **NAP**: predominance of Cyperaceae **NPP**: higher values of *Sphagnum* **LB**: increase of *Artemisia* (>20%) and decrease of *Sphagnum* (<4%)	**AP**: low PAR **NAP**: high PAR of Poaceae, Cyperaceae and Polygonaceae **NPP**: high PAR of *Sphagnum* and *Gelasinospora*
Herbaceous taxa PZ-63	2.102-2.112	**AP**: remarkable amounts of *Larix* and *Salix* **NAP**: predominance of Poaceae, Cyperaceae and *Artemisia*, some Caryophyllaceae **NPP**: higher values of *Selaqinella rupestris* and *Botryococcus* **LB**: decrease of *Artemisia* and *Selaqinella rupestris* and *Botryococcus*	**AP**: relatively high PAR of *Larix* and *Salix* **NAP**: high PAR of Poaceae, Cyperaceae, *Artemisia* and Caryophyllaceae **NPP**: higher *Botryococcus*
Deciduous shrub taxa PZ-62	2.112-2.117	**AP**: predominance of *Betula* sect. *Nanae*-type and *Alnus* **NAP**: low values of *Artemisia* a Poaceae **NPP**: higher values of *Sphagnum* **LB**: increase of *Artemisia* and Poaceae	**AP**: high PAR of *Larix*, *Betula* sect. *Nanae*-type, *Alnus* and *Salix* **NAP**: high PAR of Poaceae, Cyperaceae and Caryophyllaceae **NPP**: high values of *Sphagnum* and *Gelasinospora*
Mixed herb- and shrub- taxa PZ-61	2.117-2.131	**AP**: predominance of *Betula* sect. *Nanae*-type and *Alnus* **NAP**: the opposite trend of AP in Poaceae, Cyperaceae and *Artemisia* **NPP**: higher values of *Botryococcus* **LB**: increase of *Pinus* s/g. *Haploxylon*	**AP**: high PAR of *Larix*, Ericales and *Salix* **NAP**: high PAR of Poaceae, Cyperaceae, *Artemisia*, Caryophyllaceae, Ranunculaceae and Polygonaceae **NPP**: high values of *Sphagnum* and *Botryococcus*
Deciduous forest taxa PZ-60	2.131-2.139	AP: highest values of *Pinus* s/g. *Haploxylon* (>40%) NAP: low values of herbaceous taxa NPP: remarkable *amounts of Sphagnum* LB: decrease of *Pinus* s/g. *Haploxylon* to 7%	AP: high PAR of *Larix*, *Pinus* s/g. *Haploxylon*, *Alnus*, *Betula* sect. *Nanae*-type and *Salix* NAP: high herbs PAR NPP: high values of *Sphagnum*, Polypodiaceae and *Gelasinospora*

PZ	Age (Myr BP)	Features	PAR
Deciduous shrub taxa PZ-59	2.139-2.146	**AP**: predominance of *Betula* sect. *Nanae-type* and *Alnus* **NAP**: low values of *Artemisia* **NPP**: predominance of *Sphagnum* **LB**: decrease of *Betula* sect. *Nanae*-type (<10%) and *Alnus* (<2%)	**AP**: high PAR of *Larix, Alnus, Betula* sect. *Nanae*-type and *Salix* **NAP**: high herbs PAR **NPP**: high values of *Sphagnum*, Polypodiaceae, *Gelasinospora*, *Botryococcus* and *Zygnema*
Herbaceous taxa PZ-58	2.146-2.150	**AP**: absent **NAP**: remarkable percentage peaks of Poaceae, *Artemisa* and *Thalictrum* **NPP**: higher values of *Botryococcus* and *Zygnema* **LB**: see PZ-58 in previous study (Andreev et al., 2014)	**AP**: high PAR of *Salix* **NAP**: high PAR of Poaceae, *Artemisia*, Caryophyllaceae and *Thlictrum* **NPP**: high values of *Botryococcus* and *Zygnema*

Table 2.2 Continued

2.5 Interpretation and discussion

To describe the vegetation history of the Lake El'gygytgyn region, it is necessary to address several caveats when interpreting the pollen record. The first concerns the taxonomic ambiguity associated with *Pinus* pollen. Currently, three species of pine grow in northern Siberia: *P. pumila*, *P. sibirica* and *P. sylvestris*. The latter produces *P.* s/g *Dyploxylon*-type pollen which is a taxon not found in this part of the Lake El'gygytgyn core. *P.* s/g *Haploxylon*-type pollen, a key component of our record, is produced by both *P. pumila* and *P. sibirica*. Dwarf stone pine (*P. pumila*) is found as (1) an understory shrub in larch forests (*Larix gmelinii*); (2) a component of lowland shrub tundra; (3) a number of shrub tundra communities found above the altitudinal tree limit. Today the coniferous shrub is located ~100 km to the south and west of Lake El'gygytgyn (Galanin et al., 1997). Siberian pine (*P. sibirica*) and *Picea obovata* are typical members of the conifer forests across much of Siberia. These evergreen forests benefit from a relatively warm climate and generally are restricted to lowland and valley settings (Lozhkin and Anderson, 2013). Stone pine can survive under cooler temperatures and a wider range of elevations as compared to Siberian pine. Given the absence of *Picea* pollen during the interval studied, and the wide range of elevations represented in the Lake El'gygytgyn record, we think it is most likely that the *P.* s/g *Haploxylon*-type pollen was produced by stone and not by Siberian pine.

A second consideration is that of *Larix* pollen, which is known both for its short-distance dispersal from the larch tree and for its poor preservation (Andreev et al., 2001; Kataoka et al., 2003). Thus, *Larix* pollen is often considered the equivalent of a plant macrofossil. Consequently, we interpret the low but consistent presence of the taxon in our fossil pollen spectra to indicate the presence of larch in the lake crater and/or the surrounding uplands.

Thirdly, *Betula* sect. *Nanae*-type pollen is characteristic of modern pollen assemblages from tundra habitats in many areas of Siberia (Kunes et al., 2008; Andreev et al., 2012 and references therein). Dwarf birches do grow today with shrub alder (*Alnus fruticosa*-type pollen) in mesic settings, but these birches also can be found to the north and east of the current alder distribution occurring in more severe tundra landscapes.

2.5.1 Environmental conditions at Lake El'gygytgyn during ~2.15-2.10 Myr BP

The vegetation history provided in this paper is based on the qualitative interpretations of pollen-vegetation-climate relationships and the more quantitative assessments of plant biomes and landscape openness (Fig. 2.3 to 2.6).

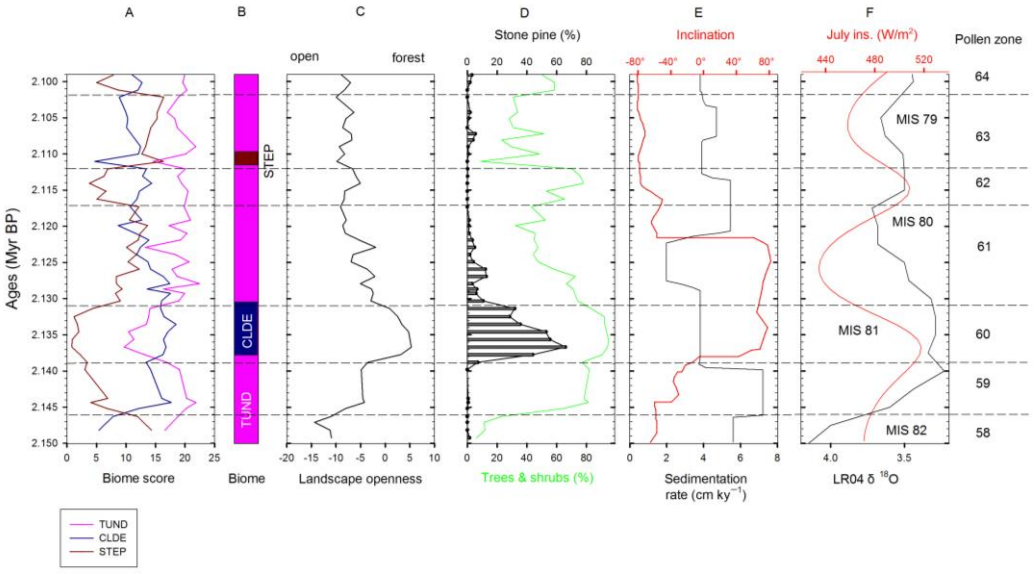

Fig. 2.5 Summary diagram for 2.15-2.10 Myr BP showing: (A) time series of individual biomes, (B) dominant biomes, (C) qualitative characteristic of landscape openness reflected by the difference between the maximum score of forest biomes (MSFB) and the maximum score of open biomes (MSOB) at each level, (D) tree and shrub pollen percentages (green line) compared with percent pine pollen (black histogram), (E) inclination of the characteristic remanent magnetization (Nowaczyk et al., 2013) with the positive (negative) value indicate normal (reversed) polarity and sedimentation rate in the sediment record, and (F) LR04 global marine isotope stack (black dots and line, Liesecki and Raymo 2005) and mean July insolation for 67.5 ºN (red line, Laskar et al., 2004).

Between 2.150 and 2.146 Myr BP (PZ-58; late MIS 82), the vegetation was dominated by graminoid communities that included drought- and cold-tolerant herbs (e.g., *Artemisia*, *Thalictrum*, Caryophyllaceae, Ranunculaceae). The predominance of herb taxa and low PAR suggest open habitats. However, one sample includes *Larix* pollen, thus suggesting a possible presence of small stands in protected areas of the catchment. Woody taxa were certainly limited in distribution, with *Salix* being most common. Although PZ-58 dates to late MIS 82, the paleobotanical data are similar to those that prevailed throughout the isotope stage (2.163-2.150 Myr BP), when Poaceae, Cyperaceae, and *Artemisia* communities likely were common around the lake and climates were inferred to be extremely dry and cold (Lozhkin et al., 2007; Andreev et al., 2014). According to the biomization (Fig. 2.5A), STEP biome scores are relatively high at one level (Fig. 2.5A, B, C), but TUND scores are dominant, suggesting the presence of tundra-steppe. Numerous remains of green algal colonies (*Botryococcus*) and spores of *Zygnema*-type algae indicate the widespread occurrence of shallow-water habitats and relatively low lake-levels, as previously concluded also for the early MIS 82 (Andreev et al., 2014).

Between 2.146 and 2.139 Myr BP (PZ-59), increased pollen percentages and PAR of *Betula* sect. *Nanae*-type and *Alnus*, low values for Poaceae and *Artemisia* pollen, and higher PAR for *Salix* indicate that shrub tundra became common regionally. These changes reflect the beginning of climatic amelioration within MIS 81. The more consistent appearance of *Larix* pollen suggests the local establishment of this tree, probably in isolated and scattered stands. Increases in CLDE and TUND scores, from low values occurring in PZ-58, suggest the onset of wetter and warmer conditions. A moister climate, resulting in locally mesic substrates, is also indicated by higher percentages of *Sphagnum* spores. The interpretation of a temperature increase at the beginning of MIS 81 is supported by a change towards a sedimentary facies B that reflects only semi-permanent lake-ice coverage (Melles et al., 2012).

The pollen spectra between 2.139 and 2.131 Myr BP (PZ-60, MIS 81) are characterized by the highest percentages and PAR of *Pinus* s/g *Haploxylon* and the highest total PAR in this portion of the El'gygytgyn record. Sedimentation rate of this period is lower than that at PZ-59. *Alnus* and *Betula* sect. *Nanae*-type, although remaining important components of the pollen assemblages, are lower in PZ-60 than in PZ-59. *Larix* pollen has a low but consistent presence and relatively high PAR. The shift in the pollen spectra between PZ-59 and PZ-60 indicates the establishment of larch forest with stone pine-birch-alder shrub communities in the understory and at higher elevations beyond the altitudinal treeline. The dominance of woody taxa is reflected in an increase of CLDE scores to the highest in the record. Reductions

in steppe and tundra communities and the widespread presence of larch forests with a rich shrub understory clearly mark the presence of wet and warm summer climates, associated with the MIS 81 thermal optimum (Fig. 2.5F). The relatively high sedimentation rates coeval with PZ-59 (Fig. 2.5E) suggest more terrestrial material was transported into the lake by inlet streams (Fedorov et al., 2013; Wennrich et al., 2013). Subsequently, the increased vegetation cover leads to less soil erosion and mud flows, contributing to markedly low sedimentation rate during the Réunion Subchron (*c.* 3.8 cm/ka), which covers the period from the MIS 81 climate optimum to the MIS 81/80 transition (2.138-2.122 Myr BP; Fig. 2.5E).

The transition from PZ-60 into PZ-61 at 2.131 to 2.123 Myr BP (representing the latter part of MIS 81) documents the return to shrub tundra-dominated landscapes as the climate cooled towards the MIS 80 glaciation. This shift is evident in the decline in *P.* s/g *Haploxylon* pollen percentages and PAR, the decrease in total PAR, and the increase in herb pollen (mainly Poaceae and *Artemisia*). Birch and alder were the dominant shrub species, possibly with scattered thickets of stone pine. *Larix* PAR suggests that during early PZ-61 larch forests persisted but were reduced to isolated stands by *c.* 2.128 Myr BP. This shift may have been gradual, as suggested by the landscape-openness scores (Fig. 2.5C). Biomization results show an increase in STEP scores and a reduction in CLDE scores (Fig. 2.5A), although TUND scores predominant. These trends are consistent with a cooling and drying climate.

The peak in *Artemisia* percentages at ~2.123 Myr BP also reflects cooler and drier conditions than before and coincides with the transition to MIS 80. A peak in *Botryococcus* green algal colonies between 2.126 and 2.121 Myr BP implies expanded shallow-water habitats, most likely associated with drier conditions. This suggestion is supported by the lowest sedimentation rates in the entire record at the same time, indicating declined inflow. A simultaneous decline in *P.* s/g *Haploxylon* pollen suggests that this drying may reflect a decline in effective moisture during the cool seasons, as stone pine requires a sufficient snow cover to protect the evergreen shrub from winter desiccation.

In PZ-62 (between 2.117 and 2.112 Myr BP, early MIS 79), relatively high percentages and modest PARs of *Alnus* and *Betula* sect. *Nanae*-type pollen indicate that shrub tundra communities were characteristic of the regional vegetation. *Larix* percentages and PAR suggest the continued albeit restricted presence of larch. Percentages of Poaceae and *Artemisia* are lower than those of MIS 80. However, Cyperaceae PAR and, to a lesser extent, its percentages and the greater values for *Sphagnum* spores suggest that mesic conditions occurred locally. Higher CLDE scores support the presence of conditions sufficiently warm to

allow the widespread distribution of deciduous shrubs. The climate inferred for PZ-62 resembles that of PZ-59, which represents the glacial-interglacial transition from MIS 82 to MIS 81.

Between 2.112 and 2.102 Myr BP (PZ-63, central MIS 79), individual taxon and total PAR generally are low. Although *Betula* pollen percentages are lower than in PZ-62, the values are still sufficiently high to suggest the shrub's presence. However, *Betula* PAR and *Alnus* percentages and PAR suggest these shrubs were not common, making willow the only significant shrubby taxa in the regional landscape. Small increases in *Pinus* s/g *Haploxylon* and *Larix* pollen suggest that larch stands accompanied by shrub birch and shrub alder were scattered in protected sites such as valley bottoms. Compared to trees and shrubs, herb taxa (particularly Poaceae and *Artemisia*) generally have higher PAR. *Selaginella rupestris* spores, a taxon associated with well-drained, dry habitats, also have high abundances. At that time, stadial herb communities were common in the region, thus characterizing a rather cool and particularly dry climate. A significant peak in *Botryococcus* algae between ~2.110 and 2.105 Myr BP suggests an increase in shallow-water habitats consistent with drier conditions. High TUND and STEP biome scores are indicative of open vegetation dominated by arctic herb tundra.

The PZ-64 (2.102-2.099 Myr BP, upper MIS 79) pollen assemblages contain similar spectra to those of PZ-62, with (1) relatively high percentages of *Alnus*, *Betula* sect. *Nanae*-type, and Cyperaceae pollen; (2) low percentages of *Artemisia* pollen; and (3) high percentages of *Sphagnum* spores. Although herb tundra still dominated the landscape, a reduction in STEP affinity scores suggests the climate was more favorable than before.

2.5.2 Response of biomization-inferred vegetation successions to orbital forcing

The oscillation between glacial and interglacial climates, which is the most fundamental characteristic of the Pleistocene, is controlled primarily by changes in the Earth's orbital parameters (Hays et al., 1976). Milankovitch (1941) argued that the intensity of summer insolation at 65 ℃N was a critical influence in regulating glacial-interglacial cycles. In other words, when summer insolation at 65 ℃N was reduced sufficiently to minimize summer snow-melt, then ice sheets would eventually form. As to the orbital parameters themselves, precession mediates the Earth-Sun distance and thus is the dominant influence on insolation intensity and also closely correlates to incoming July insolation (Berger et al., 1999; Maslin

and Ridgwell, 2005; Fig. 2.6C, D). Changes in obliquity also play an important role; for example an increase in obliquity results in a greater seasonal difference in duration of daylight that in turn leads to warmer summers and colder winters. Hence, regional vegetation changes at high latitudes should show responses to variations both in precession-related levels of summer insolation and obliquity-related duration of seasonal sunlight. However, it should be noted that modeling results indicate that precession is clearly stronger than obliquity in driving the 65 ºN summer insolation in northern and central Eurasia (Ruddiman, 2003).

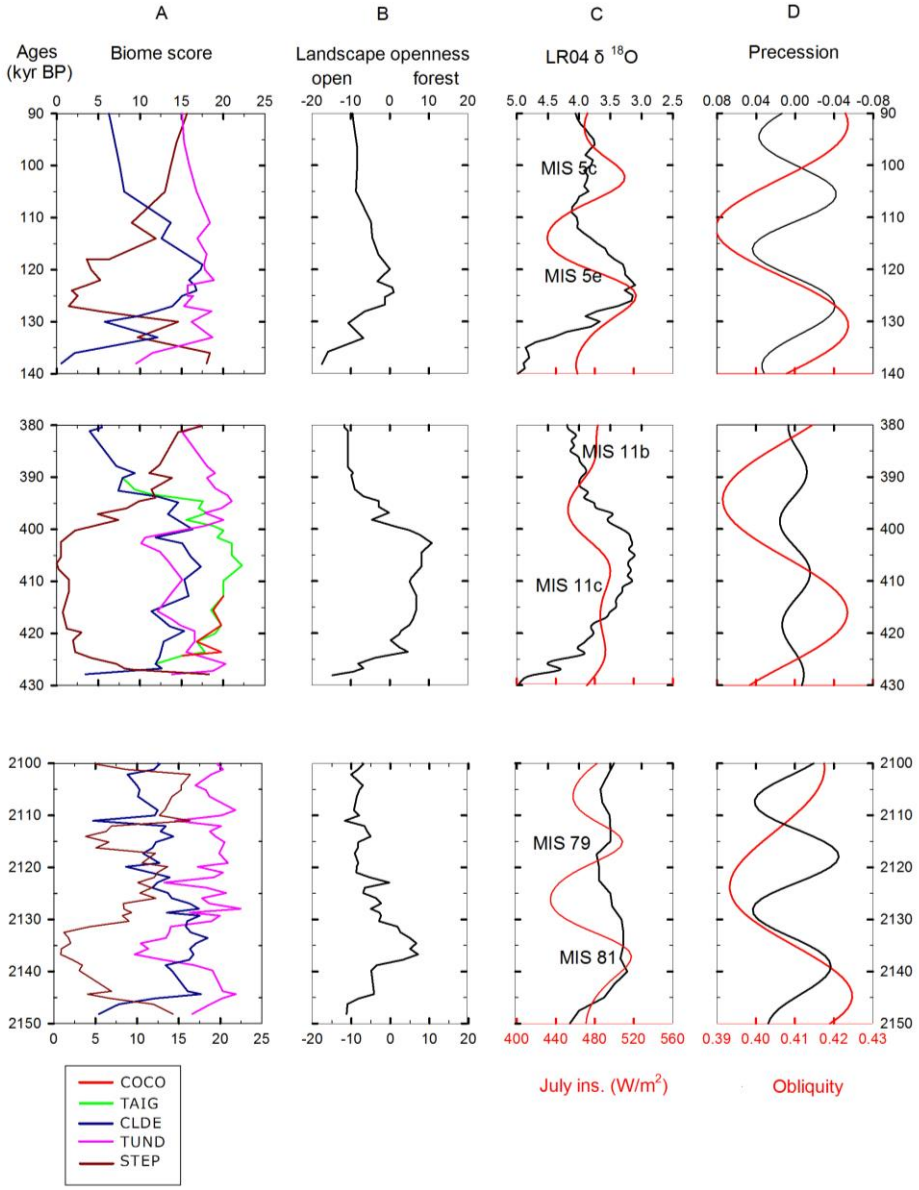

Fig. 2.6 Summary diagrams showing the relationship between biomes with: (A) biome reconstruction for 2.15-2.10 Myr BP (this study), 90-140 ka BP and 370-420 ka BP (Tarasov et al., 2013), (B) landscape openness calculated as the difference between MSOB and MSFB, (C) LR04 global marine isotope stack (Liesecki and Raymo, 2005) and mean July insolation for 67.5 ºN (red line, Laskar et al., 2004), and (D) precession curve (black line) and obliquity curve (red line) from Laskar et al. (2004).

Given the importance of the above parameters, we examined more closely selected interglacials/interstadials at Lake El'gygytgyn in order to assess possible similarities or dissimilarities in patterns of vegetation change as they relate to precession, obliquity and July insolation (Fig. 2.6). We draw examples from this study (late MIS 82 to MIS 79), the MIS 11 super-interglacial (Melles et al., 2012; Lozhkin and Anderson, 2013) and MIS 5 (Lozhkin et al., 2007). Each of these intervals represents ~50,000 yr.

The vegetation succession and astronomical configuration ~2.150-2.100 Myr BP displays a pattern similar to those for MIS 5. At first, open vegetation (TUND and/or STEP) characterized the late glacial stages (~2.150-2.146 Myr BP and ~140-135 ka BP, respectively), when the precession-related summer-insolation intensity and obliquity values were relatively low. During the glacial-interglacial transitions (~2.146-2.139 Myr BP and ~135-128 ka BP, respectively) the CLDE biome increased in significance. The onset of interglacial conditions is correlated with rising summer-insolation intensity and higher obliquity values. High CLDE affinity scores occur ~2.146-2.127 Myr BP and ~128-115 ka BP, although the TUND biome in both cases remained an important landscape component. CLDE scores reach maximum values ~2.139-2.131 Myr BP and ~125-123 ka BP, reflecting the presence of optimal warm and moist climates. These interglacial optima are represented by high summer-insolation intensity and high obliquity.

The ~2.127-2.117 Myr BP and ~115-105 ka BP intervals are characterized by a progressive decrease in CLDE and an accompanying increase in STEP scores, although the TUND biome was still dominant, marking the onset of glacial conditions. Abrupt declines in CLDE scores coincide with both low summer insolation intensity and low obliquity. The interglacial/interstadial MIS 79 (~2.117-2.100 Myr BP) and MIS 5c (105-92 ka BP) are similar in that both show the replacement of CLDE by STEP biome, except during early MIS 79 (~2.117-2.112 Myr BP), when CLDE scores are higher than STEP scores.

The onset and end of MIS 81 and MIS 5e both correspond to the high-amplitude downward trend of precession and obliquity, from peak to trough, respectively. This phenomenon is also recorded in the Mediterranean Sea (Joannin et al., 2008; 2011) and Lake Baikal (Prokopenko et al., 2006). Peaks of obliquity-related daylight duration and precession-related summer insolation intensity lead to the peak annual mean temperature, which triggered the onset of interglaciation and forest expansion. When the obliquity and precession move to the trough, herbaceous components increase in significance due to a deteriorated climate. The succeeding interglacial/interstadial MIS 79 and MIS 5c do not witness such a prominent change in

vegetational landscape, which possibly was induced by a combination of peak precession-related summer insolation intensity but relatively low obliquity values.

The vegetation history of super interglacial MIS 11 to differs from those of MIS 5 and of this study in terms of both the biome types involved and the duration of the optimal conditions. Two additional biomes (taiga, TAIG and cold coniferous forest, COCO) established during the super interglacial. The glacial-interglacial transition is marked by a decrease in STEP and an increase in TUND, TAIG, CLDE and COCO scores within a rather short time (~430-424 ka BP as compared to the ~135-128 ka BP and ~2.146-2.139 Myr BP transitions in MIS5 and MIS81, respectively). The TUND biome is dominant and during this interval low-amplitude changes in precession result in relatively stable and high summer-insolation. Therefore, the rapid vegetation succession likely responds primarily to the increasing obliquity values. A "plateau" of TAIG and CLDE scores occurs between 424 and 399 ka BP (MIS 11c), whereas high COCO scores exist between 424 and 415 ka BP. This pattern was mainly influenced by the presence of *Corylus* pollen, which was likely subject to long-distance transport (Lozhkin and Anderson, 2013). However, mixed spruce-larch-birch-alder forest certainly was widespread in the region. The maximum summer temperatures and annual precipitation values of MIS 11c are estimated to be ~4 ℃ to 5 ℃ and ~300 millimeters higher than those of MIS 5e by employing pollen-based modern analogue approach (Melles et al., 2012). Between 399 and 395 ka BP, coniferous forest declined slightly, whereas shrub tundra increased on the landscape. Around ~395 ka BP, TUND and STEP scores return to high values. Roughly at the same time, summer insolation and obliquity were both minimal. Since 390 ka BP, the TAIG biome has been absent. Declining CLDE and TUND scores and increasing STEP scores indicate a gradual cooling and drying of climate with the beginning of MIS 11b.

During all interglacial optima (MIS 81, 11c and 5e) high forest biome scores correlate well with respective patterns in precession-related high summer-insolation intensity and high obliquity values. MIS 11c is clearly the warmest and longest of the three interglacial optima (Melles et al., 2012). This character of super interglacial MIS 11c is widely shared by records from North Atlantic marine sediment cores (Voelker et al., 2010; Lawrence et al., 2009) and Lake Baikal (Prokopenko et al., 2001). Low-amplitude precession changes during the MIS 11c led to relatively stable and moderate summer-insolation intensity, thus contributing to the long-term establishment of regional forests. When the obliquity increases and reaches a certain threshold, the precession and obliquity-controlled temperature rises and triggers the onset of interglaciation at *c.* 424 ka BP. When the obliquity moves to the trough, despite moderately low precession-related summer insolation intensity, the dominance of taiga is

replaced by tundra. More concisely, the Lake El'gygytgyn data suggest that obliquity perhaps plays a more significant role in triggering vegetation succession or biome type in the northern high latitudes, while both precession and obliquity rather impact the onset of interglaciation.

The onset of glacials/stadials (MIS 80, MIS 11b and MIS 5d) is characterized by minimized obliquity and simultaneously reduced precession-related summer insolation intensity. Short daylight and low temperature in the summer likely contributed to the ice-sheet formation and further limited the extent of shrub or herb tundra.

The early Pleistocene Mediterranean vegetation succession is largely controlled by precession-related summer-insolation intensity instead of obliquity change (Joannin et al., 2008). However, our results suggest that during the Pleistocene the role of precession on vegetation change at northern high latitudes possibly was not as significant as at low- to mid-latitudes (Joannin et al., 2007, 2008 and 2011). With regard to climatic forcing, global modeling results (e.g. Paillard, 1998; Khodri et al., 2001; Parrenin and Paillard, 2012) also show that precession and obliquity have a similar influence on the deglaciation, with obliquity playing a marginally more important role.

2.6 Conclusions

This study provides a detailed examination of the Lake El'gygytgyn pollen record in the interval ~2.150 to 2.100 Myr BP (late MIS 82 to MIS 79), which includes the Réunion Subchron polarity reversal event, and uses both qualitative interpretations of the pollen assemblages as well as biome and landscape openness reconstructions.

During late MIS 82, vegetation was characterized by drought- and cold-tolerant herbaceous communities reflecting an extremely dry and cold climate. Increases in shrub and *Larix* pollen and *Sphagnum* spores suggest climate amelioration at the beginning of MIS 81. Optimal climatic conditions were reached in the middle part of MIS 81, when the extent of larch-dominated deciduous forest and stone pine populations were at a maximum. A gradual increase of herbaceous taxa in late MIS 81 suggests a drying and cooling trend and greater openness to the landscape. During MIS 80 high percentages of herb-taxa imply cold and dry climatic conditions. Subsequent expansion of shrub birch, shrub alder, and *Sphagnum* during early MIS 79 reflects the onset of wetter and warmer conditions. After this period, the greater abundance of herb pollen and *Selaginella rupestris* spores suggests rather cold and dry

climates, while larch, shrub birch, and possibly shrub alder have survived in protected areas throughout MIS 79. A slightly wetter climate in the upper part of MIS 79 (*c.* 2.102-2.100 Myr BP), is indicated by increases in shrub pollen and *Sphagnum* spores with an accompanying decline in herb pollen.

From the comparison of the results from MIS 82 to MIS 79 with those from MIS 11 and MIS 5, it becomes evident that vegetation change at Lake El ́gygytgn clearly responded to the combined effects of the precession-related summer-insolation intensity and obliquity-related daylight duration. On the one hand, MIS 82 to MIS 79 have a similar vegetation succession and astronomical configuration as that for MIS 6 to 5c. Nearly simultaneous peaks of obliquity and precession trigger the onset of interglaciation and forest expansion, while minimal values of both correspond to increases in herbaceous components in the regional vegetation, marking the end of the interglacials. On the other hand, the super interglacial MIS 11c is warmer and longer compared to MIS 81 and MIS 5e, due to stable and moderate precession. Obliquity probably is more significant in triggering vegetation succession, while both precession and obliquity control the onset of the MIS 11c interglacial.

Acknowledgements. This study was funded by the China Scholarship Council (CSC) Ph.D. Scholarship to WWZ. Financial support for the palynological analyses was provided by the BMBF (grant 03G0642) and the German Research Foundation (DFG; grant ME 1169/24). The work of AA was also performed according to the Russian Government Program of Competitive Growth of Kazan Federal University. The work of PT was financed by the Heisenberg program of the DFG (grant TA 540/5). The contribution of AL to this study was supported by grants from the Russian Foundation for Basic Research (14-05-00573; 15-05-06420) and the Far East Branch of the Russian Academy of Sciences (15-I-2-067).

2.7 References

Andreev, A.A., Klimanov, V.A. and Sulerzhitsky, L.D., 2001. Vegetation and climate history of the Yana River lowland, Russia, during the last 6400 yr. Quaternary Science Reviews, 20, 259-266.

Andreev, A.A., Morozova, E., Fedorov, G., Schirrmeister, L., Bobrov, A.A., Kienast, F., Schwamborn, G., 2012. Vegetation history of central Chukotka deduced from permafrost paleoenvironmental records of the El'gygytgyn Impact Crater. Climate of the Past, 8, 1287-1300.

Andreev, A.A., Tarasov, P.E., Wennrich, V., Raschke, E., Herzschuh, U., Nowaczyk, N.R., Brigham-Grette, J., Melles, M., 2014. Late Pliocene and early Pleistocene environments of the north-eastern Russian Arctic inferred from the Lake El'gygytgyn pollen record. Climate of the Past, 9, 4599-4653.

Bar-Matthews, M., Ayalon, A., Gilmour, M., Matthews, A., Hawkesworth, C.J., 2003. Sea-land oxygen isotopic relationships from planktonic foraminifera and speleothems in the Eastern Mediterranean region and their implication for paleorainfall during interglacial intervals. Geochimica et Cosmochimica Acta, 67, 3181-3199.

Belikovich, A.V., 1994. Recreation sources of planned "El'gygytgyn Lake Park", FEB RAS, Vestnik, 3, 57-63.

Berger, A., Li, X., Loutre, M., 1999. Modeling northern hemisphere ice volume over the last 3 Ma. Quaternary Science Reviews, 18, 1-11.

Berger, A., Loutre, M.F., 2004. Astronomical theory of palaeoclimates, Comptes Rendus Geoscience, 336, 701-709.

Bobrov, A.E., Kupriyanova, L.A., Litvintseva, M.V., Tarasevich, V.F., 1983. Spores and pollen of gymnosperms from the flora of the European part of the USSR, Nauka, Leningrad.

Brigham-Grette, J., Melles, M., Minyuk, P., Andreev, A., Tarasov, P., DeConto, R., Koenig, S., Nowaczyk, N., Wennrich, V., Rosén, P., Haltia-Hovi, E., Cook, T., Gebhardt, C., Meyer-Jacob, C., Snyder, J., Herzschuh, U., 2013. Pliocene Warmth, extreme Polar Amplification, and Stepped Pleistocene Cooling recorded in NE Russia. Science, 340, 1421-1427.

Cremer, H., Wagner, B., 2003. The diatom flora in the ultra-oligotrophic Lake El'gygytgyn, Chukotka. Polar Biology, 26, 105-114.

Cremer, H., Wagner, B., Juschus, O., Melles, M., 2005. A microscopical study of diatom phytoplankton in deep Crater Lake El'gygytgyn, Northeast Siberia. Algological studies, 116, 147-169.

Fægri, K., Iversen, J., 1989. Textbook of Pollen Analysis, fourth ed. John Wiley and Sons, London, UK.

Fedorov, G., Nolan, M., Brigham-Grette, J., Bolshiyanov, D., Schwamborn, G., Juschus, O., 2013. Preliminary estimation of Lake El'gygytgyn water balance and sediment income. Climate of the Past, 9, 1455-1465.

Francke, A., Wennrich, V., Sauerbrey, M., Juschus, O., Melles, M., Brigham-Grette, J., 2013. Multivariate statistic and time series analysis of grain-size data in quaternary sediments of Lake El'gygytgyn, NE Russia. Climate of the Past, 9, 2459-2470.

Galanin, A.V., Belikovich, A.V., Galanin, A.A., Tregubov, O.D., 1997. Priroda i resursy Chukotki (Nature and sources of Chukotka), IBPS FEB RAS, Magadan.

Haltia, E.M., Nowaczyk, N.R., 2014. Magnetostratigraphy of sediments from Lake El'gygytgyn ICDP Site 5011-1: paleomagnetic age contraints for the longest paleoclimate record from the continental Arctic. Climate of the Past, 10, 623-642.

Hays, J.D., Imbrie, J., d Shackleton, N.J., 1976. Variations in the Earth's orbit: pacemarker of the ice ages. Science, 194, 1121-1132.

Joannin, S., Quillévéré, F., Suc, J.P., Lécuyer, C., Marzineau, F., 2007. Early Pleistocene climate changes in the central Mediterranean region as inferred from integrated pollen and planktonic foraminiferal stable isotope analyses. Quaternary Reviews, 67, 264-274.

Joannin, S., Ciaranfi, N., d Stefanelli, S., 2008. Vegetation changes during the late Early Pleistocene at Montalbano Jonico (Province of Matera, southern Italy) based on pollen analysis. Palaeogeography, Palaeoclimatology, Palaeoecology, 270, 92-101.

Joannin, S., Bassinot, F., Nebout, N.C., Pezron, O., Beaudouin, C., 2011. Vegetation response to obliquity and precession forcing during the Mid-Pleistocene Transition in Western Mediterranean region (ODP site 976). Quaternary Science Reviews, 30, 280-297.

Kataoka, H., Takahara, H., Krivonogov, S.K., Bezrukova, E.V., Orlova, L., Kropivina, S., Miyoshi, N. and Kawamuro, K., 2003. Pollen record from the Chivyrkui Bay Outcrop on the Eastern Shore of Lake Baikal since the Late Glacial, Long continental record from Lake Baikal (ed. By K. Kashiwaya), pp. 207-218. Springer-Verlag, Tokyo.

Khodri, M., Leclainche, Y., Ramstein, G., Braconnot, P., Marti, O., Cortijo, E., 2001. Simulating the amplification of orbital forcing by ocean feedbacks in the last glaciation. Nature, 410, 570-574.

Kunes, P., Pelankova, B., Chytry, M., Jankovska, V., Pokorny, P., Petr, L., 2008. Interpretation of the last-glacial vegetation of eastern-central Europe using modern analohues from southern Siberia. Journal of Biogeography, 35, 2223-2236.

Kupriyanova, L.A., Alyoshina, L.A., 1972. Pollen and spores of plants from the flora of European part of USSR, Vol. I., Academy of Sciences USSR, Komarov Botanical Institute, Leningrad.

Kupriyanova, L.A., Alyoshina, L.A., 1978. Pollen and spores of plants from the flora of European part of USSR, Academy of Sciences USSR, Komarov Botanical Institute, Leningrad.

Lawrence, K.T., Herbert, T.D., Brown, C. M., Raymo, M.E., Haywood, A.M., 2009. High amplitude variations in North Atlantic Sea surface temperature during the early Pliocene warm period. Paleoceanography, 24, PA2218.

Laskar, J., Robutel, R., Joutel, F., Gastineau, M., Correia, A.C.M., Levrand, B., 2004. A long term numerical solution for the insolation quantities of the Earth. Astron. Astrophys. 428, 261-285.

Layer, P., 2000. Argon-40/argon-39 age of the El'gygytgyn impact event, Chukotka, Russia, Meteor. Planet. Science, 35, 591-599.

Lisecki, L.E., Raymo M.E., 2005. A Pliocene-Pleistocene stack of 57 globally distributed benthic $\delta^{18}O$ records. Paleoceanography, 20, PA1003.

Liu, Z., Herbert, T.D., 2004. High-latitude influence on the eastern equatorial Pacific climate in the early Pleistocene epoch. Nature, 427, 720-723.

Lozhkin, A.V., Anderson, P.M., Vartanyan, S., Brown, T., Belaya, B., Kotov, A., 2001. Reconstructions of late Quaternary paleo-environments and modern pollen data from Wrangel Island (northern Chukotka). Quaternary Science Reviews, 20, 217-233.

Lozhkin, A.V., Anderson, P.M., Matrosova, T.V., Minyuk, P.S., 2007. The pollen record from El'gygytgyn Lake: implications for vegetation and climate histories of northern Chukotka since the late middle Pleistocene. Journal of Paleolimnology, 37, 135-153.

Lozhkin, A.V., Anderson, P.M., 2013. Vegetation responses to interglacial warming in the Arctic: examples from Lake El'gygytgyn, Far East Russian Arctic, Climate of the Past, 9, 1211-1219.

Maslin, M.A., Ridgwell, A.J., 2005. Mid-Pleistocene revolution and the 'eccentricity myth'. In: Head, M.J., Gibbard, P.L. (Eds.), Early-Middle Pleistocene Transitions: The Land-Ocean Evidence. Special Publication Geological Society of London, 247, pp. 19-34.

Matrosova, T., 2009. Reconstruction of vegetation and climate in northern Chukotka during the last 350 thousand years (according to palynological evidence from El'gygytgyn Lake), Vesnik, 1, 23-30. (in Russian)

Melles, M., Brigham-Grette, J., Minyuk, P., Koeberl, C., Andreev, A., Cook, T., Fedorov, G., Gebhardt, C., Haltia-Hovi, E., Kukkonen, M., Nowaczyk, N., Schwamborn, G., Wennrich, V. and El'gygytgyn Scientific Party, 2011. The El'gygytgyn Scientific Drilling Project – conquer-ing Arctic challenges through continental drilling. Scientific Drilling, 11, 29-40.

Melles, M., Brigham-Grette, J., Minyuk, P.S., Nowaczyk, N.R., Wennrich, V., DeConto, R.M., Anderson, P.M., Andreev, A., Coletti, A., Cook, T., Haltia-Hovi, E., Kukkonen, Lozhkin, A.V., Rosén, P., Tarasov, P., Vogel, H., Wagner, B., 2012. 2.8 Million Years of Arctic Climate Change from Lake El'gygytgyn, NE Russia. Science, 337, 315-320.

Milankovitch, M., 1941. Canon of insolation and ice-age problem. Royal Serbian Academy, Special publication No. 132.

Nolan, M., Liston, G., Prokein, P., Brigham-Grette, J., Sharpton, V.L., Huntzinger, R., 2003. Analysis of lake ice dynamics and morphology on the Lake El'gygytgyn, NE Siberia, using synthetic aperture rader (SAR) and Landsat, Journal of Geophysical Research, 108, NO. D2, 8162.

Nolan, M., Brigham-Grette, J., 2007. Basic hydrology, limnology, and meteorology of modern Lake El'gygytgyn, Siberia. Journal of Paleolimnology, 37, 17-35.

Nowaczyk, N.R., Haltia, E.M., Ulbricht, D., Wennrich, V., Sauerbrey, M.A., Rosén, P., Vogel, H., Francke, A., Meyer-Jacob, C., Andreev, A.A., Lozhkin, A.V., 2013. Chronology of Lake El'gygytgyn sediments - a combined magnetostratigraphic, palaeoclimatic and orbital tuning study based on multi-parameter analyses. Climate of the Past, 9, 2413-2432.

Parrenin, F., Paillard, D., 2012. Terminations VI and VIII (～530 and ～720 kyr BP) tell us the importance of obliquity and precession in the triggering of deglaciations. Climate of the Past, European Geoscience Union, 8, 2031-2037.

Paillard, D., 1998. The timing of Pleistocene glaciations from a simple multiple-state climate model, Nature, 391, 378-381.

Prentice, I.C., Guiot, J., Huntley, B., Jolly, D., Cheddadi, R., 1996. Reconstructing biomes from palaeoecological data: a general method and its application to European pollen data at 0 and 6 ka, Climate Dynamics, 12, 185-194.

Prokopenko, A.A., Hinnov, L.A., Williams, D.F., Kuzmin, M.I., 2006. Orbital forcing of continental climate during the Pleistocene: a complete astronomically tuned climatic record from Lake Baikal, SE Siberia. Quaternary Science Reviews, 25, 3431-3457.

Prokopenko, A.A., Karabanov, E.B., Willianms, D.F., Shackleton, N.J., Crowhurst, S.J., Peck, J.A., Gvozdkov, A.N., 2001. Biogenic silica record of the lake Baikal response to climatic forcing during the Brunhes. Quaternary Research, 55, 123-132.

Reille, M., 1992.Pollen et spores d'Europe et d'Afrique du nord, Laboratoire de Botanique Historique et Palynologie, Marseille.

Reille, M., 1995. Pollen et spores d'Europe et d'Afrique du nord, supplement 1, Laboratoire de Botanique Historique et Palynologie, Marseille.

Reille, M., 1998. Pollen et spores d'Europe et d'Afrique du nord, supplement 2, Laboratoire de Botanique Historique et Palynologie, Marseille.

Ruddiman, W.F., Mclntyre, A., 1984. Ice-age thermal response and climatic role of the surface North Atlantic Ocean. Geological Society of American bulletin 95, 381-396.

Ruddiman, W.F., 2003. Orbital forcing ice volume and greenhouse gases. Quaternary Science Reviews, 22, 1597-1629.

Shackleton, N.J., Crowhurst, S., Weedon, C., Laskar, J., 1999. Astronomical calibration of Oligocene-Miocene time. Proceedings of the Royal Society of London A 357, 1907-1929.

Schwamborn, G., Fedorov, G., Schirrmeister, H.M., Hubberten, H.W., 2008. Periglacial sediment variations controlled by late Quaternary climate and lake level change at El'gygytgyn Crater, Arctic Siberia. Boreas, 37, 55-65.

Stockmarr, J., 1971. Tablets with spores used in absolute pollen analysis. Pollen Spores, 13, 615-621.

Tarasov, P.E., Andreev, A.A., Anderson, P.M., Lozhkin, A.V., Leipe, C., Haltia, E., Nowaczyk, N.R., Wennrich, V., Brigham-Grette, J., Melles, M., 2013. A pollen-based biome reconstruction over the last 3.562 million years in the East Russia Arctic–new insights into climate – vegetation relationships at the regional scale. Climate of the Past, 9, 2759-2775.

Tzedakis, P.C., Andrieu, V., de Beaulieu, J.L., Crowhurst, S., Follieri, M., Hooghiemstra, H., Magri, D., Reille, M., Sadori, L., Shackleton, N.J., Wijmstra, T.A., 1997. Comparison of terrestrial and marine records of changing climate of the last 500,000 years. Earth and Planetary Science Letters, 150, 171-176.

van Geel, B., 2001. Non-pollen palynomorphs, in: Tracking environmental change using lake sediments. Volume 3: Terrestrial, algal and silicaceous indicators, edited by: Smol, J.P., Birks, H.J.B., Last, W.M., Bradley, R.S., and Alverson, K., Kluwer, Dordrecht, 99-119.

Voelker, A.H.L., Rodrigues, T., Billups, K., Oppo, D., McManus, J., Stein, R., Hefter, J., Grimalt, J.O., 2010. Variations in mid latitude North Altantic surface water properties during the midBrunhes (MIS 9-14) and their implications for the thermohaline circulation. Climate of the Past, 6, 531-552.

Wennrich, V., Francke, A., Dchnert, A., Juschus, O., Leipe, T., Vogt, C., Brigham-Grette, J., Minyuk, P.S., Melles, M., and El'gygytgyn Scienece Party, 2013. Modern sedimentation patterns in Lake El'gygytgyn, NE Russia, derived from surface sediment and inlet streams samples. Climate of the Past, 9, 135-148.

3 High-latitude vegetation and climate changes during the Mid-Pleistocene Transition inferred from a palynological record from Lake El'gygytgyn, NE Russian Arctic*

Abstract

A continuous pollen record from Lake El'gygytgyn (northeastern Russian Arctic) provides detailed information concerning the regional vegetation and climate history during the Mid-Pleistocene Transition (MPT), between 1091 ka (end of Marine Isotope Stage (MIS) 32) and 715 ka (end of MIS 18). Pollen-based qualitative vegetation reconstruction along with biome reconstruction indicates that the interglacial regional vegetation history during the MPT is characterized by a gradual replacement of forest and shrub vegetation by open herbaceous communities (i.e. tundra/cold steppe). The pollen spectra reveal seven vegetation successions that have clearly distinguishable glacial-interglacial cycles. These successions are represented by the intervals of CLDE biome scores changing from high to low, which are basically in phase with the variations of obliquity from maxima to minima. The dominating influence of obliquity forcing on vegetation successions contradicts with the stronger power of eccentricity, as demonstrated by the result of wavelet analysis based on landscape openness reconstruction. This discrepancy shows that a single index is insufficient for catching signals of all the impacting factors. Comparisons with vegetation and environmental changes in the Asian interior suggest that global cooling during the MPT was probably the key force driving long-term aridification in the Arctic region. The accelerated aridification after MIS 24-22 was probably caused by the additional effect of the Tibetan Plateau uplift, which played an important role on intensification of the Siberian High and Westerly jet systems.

Keywords: Lake El'gygytgyn, Mid-Pleistocene transition, Palynological record, ICDP, North-eastern Russian Arctic

* This chapter is based on Zhao, W.W., Tarasov, P.E., Lozhkin, A.V., Anderson, P., Andreev, A.A., Korzun, J.A., Melles, M., Nedorubova, E.Yu., 2017. High-latitude vegetation and climate changes during the Mid-Pleistocene Transition inferred from a palynological record from Lake El'gygytgyn, NE Russian Arctic. Boreas doi: 10. 1111/bor. 12262.

The MPT (Mid-Pleistocene Transition) marks a fundamental change in the Earth's climate system between 1250 and 700 ka, when the dominant climate cycles changed from 41 to 100 kry without substantial change in orbital configuration (Medina-Elizalde & Lea, 2005; Clark et al., 2006; Elderfield et al., 2012). High-resolution marine oxygen isotope records reveal a remarkable ice volume increase and deep-water temperature decrease during the MPT (e.g. Lisiecki & Raymo, 2005). The most conspicuous "900 ka event" (MIS 24-22) is indicated by a notable advance of continental ice masses (Maasch, 1988) and the sudden stagnation of deep-water circulation, as indicated by the minimal carbonate accumulation in the South Atlantic (Schmieder et al., 2000). Consequently, the MPT also witnessed profound variations in biota and environments in many localities around the globe (Raymo et al., 1997; Head & Gibbard, 2005; Li et al., 2008).

Pollen data from the eastern Mediterranean show that the floristic diversity significantly declined during the interglacial intervals following MIS 24-22 (Tzedakis et al., 2006). This decline was traced back to a response of the vegetation succession to obliquity and precession changes (Joannin et al., 2011). Palynological records from the South China Sea provide evidence for a strengthened winter monsoon after 900 ka (Sun et al., 2003). West African C4 plants (mainly grasses and sedges) gradually decreased in abundance with the tropical Atlantic Ocean warming because of precession-related high insolation values (Schefuβ et al., 2003). The regional vegetation history also shows well-pronounced glacial-interglacial cycles after MIS 24-22 (Dupont et al., 2001).

Most of the marine and ice core records indicate that orbital variations are responsible for global ice volume and deep-water temperature changes during the MPT. As continuous long-term terrestrial records are usually very rare and low in temporal resolution, we still lack understanding of how these changes have influenced the terrestrial environment, especially in the high latitudes. Previous studies imply that orbital parameters have different levels of forcing on climate change at different latitudes (e.g. Berger & Loutre, 2004; Maslin & Ridgwell, 2005). More specifically, the obliquity of the Earth's axis is more important in driving vegetation succession at higher latitudes, while precession has a more significant influence on climate change at lower latitudes, although it remains a key factor in amplifying feedback mechanisms in the high latitudes as well (Maslin & Ridgwell, 2005).

Lake El'gygytgyn has yielded a unique continuous terrestrial record of Arctic climate fluctuations back to the middle Pliocene. Three parallel holes drilled in 2009 at ICDP Site 5011-1 in the central part of Lake El'gygytgyn (Fig. 3.1) have resulted in a 318-m long

composite sediment core that comprises the entire lake sediment succession (Melles et al., 2011) above a suevite layer that was formed by a meteorite impact event 3.58±0.04 Ma ago (Layer, 2000).

High-resolution multi-proxy studies of this core have provided invaluable insights into regional and global climatic response to changes in orbital forcing (e.g. Melles et al., 2012; Brigham-Grette et al., 2013; Francke et al., 2013; Tarasov et al., 2013; Wennrich et al., 2014, 2016; Andreev et al., 2014). Amongst these studies, palynological analyses provide insights into the vegetation and climate history since the upper Pliocene (Lozhkin et al., 2007; Andreev et al., 2012, 2014, 2016; Lozhkin & Anderson, 2013; Tarasov et al., 2013; Zhao et al., 2015). In this study, we continue to explore the Lake El'gygytgyn sediments, adding new pollen data from the MPT interval. The aims of the current study are (i) to infer MPT vegetation succession in the northeastern Siberian Arctic based on biome reconstructions; (ii) to discover the response of Arctic vegetation to changes in orbital forcing; (iii) to detect the dominant orbital forcing that controls the cyclic pattern of vegetation change; (iv) to discuss possible mechanisms driving climatic variations in the high latitudes during the MPT.

3.1 Study site

Lake El'gygytgyn (67°30' N, 172°05' E; Fig. 3.1) is located at 492 m above sea level in the Far East Russian Arctic, 100 km to the north of the Arctic Circle. The modern lake has a diameter of ~12 km and a bowl-shaped morphology with a maximum water depth of 175 m. The catchment area of 293 km^2 is about three times the lake's surface area of 100 km^2, being fed by ~50 ephemeral streams, which form multiple alluvial fans, particularly in the west and north (Nolan & Brigham-Grette, 2007; Schwamborn et al., 2012). The inlets deliver ~350 t a^{-1} of sediment into the lake, with spring and early summer being the main seasons of sediment influx (Fedorov et al., 2013). Today, Lake El'gygytgyn is a cold-monomictic, ultra-oligotrophic lake with slightly acidic pH (Nolan & Brigham-Grette, 2007). However, phytoplankton growth significantly contributes to the sedimentation, taking place even beneath the ice cover in winter times (Cremer et al., 2005).

The climate in the region is dry and cold, with a mean annual air temperature (MAT) of about -10 ℃ and mean July and January temperatures of 8 and -35 ℃, respectively (Melles et al., 2012). Mean annual precipitation (MAP) is about 200 mm a^{-1}, consisting of ~90 mm summer

rainfalls (June-September) and ~110 mm water-equivalent snowfalls (Nolan & Brigham-Grette, 2007).

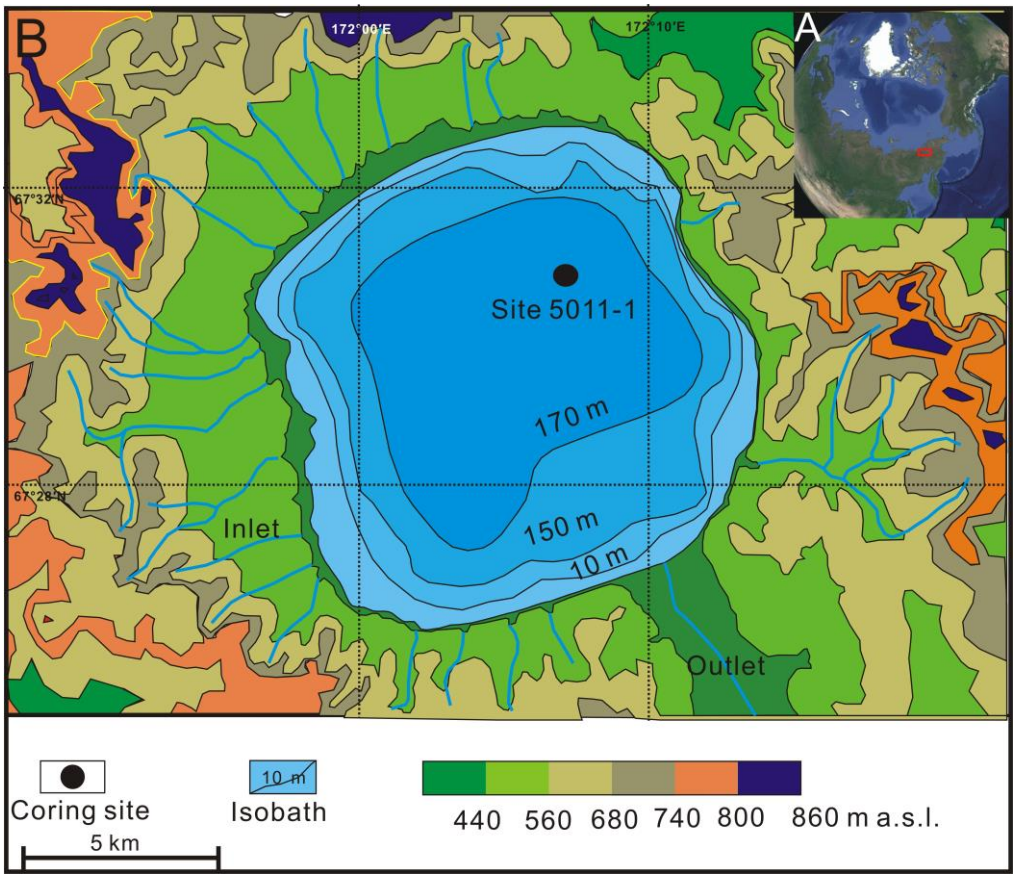

Fig. 3.1 A. Location of the study area marked with red rectangular (source: Google Earth). B. Bathymetric map of Lake El'gygytgyn and topography of its catchment (modified from Swann et al., 2010). The drilling site 5011-1 is marked with a black dot.

Due to the harsh climatic conditions as well as barren edaphic conditions caused by the meteorite impact, the catchment of Lake El'gygytgyn is generally sparsely vegetated, with patches of shrub willows (*Salix krylovii* and *S. alaxensis*) and dwarf birch (*Betula exilis*) limited to protected habitats in valleys and saddles (Lozhkin & Anderson, 2013). The surrounding uplands are populated by low-shrub and herb-dominated tundra communities, which are mainly composed of *Salix polaris, Cassiope tetragona, Carex tripartite, Phippsia algida, Koenigia islandica, Saxifraga hyperborean, Eritrichium villosum, Primula tschuktschorum, Hierochloe pauciflora,* together with small populations of *Pinus pumila* and *Alnus fruticosa* (for details see Belikovich, 1994; Andreev et al., 2012; Lozhkin & Anderson, 2013 and references therein). Scattered stands of *Larix gmelinii* appear ~150 km to the south and west of the lake and the continuous forest belt is located ~300 km south of the lake (Tarasov et al., 2013).

3.2 Material and methods

3.2.1 Pollen analysis

Palynological analyses were carried out on 250 samples from the depth interval between 43.55 and 29.62 m (~1091-715 ka, between the end of MIS 32 and MIS 18) of the composite core from ICDP Site 5011-1 in the central part of Lake El'gygytgyn. The temporal resolution of the samples varies between 1 and 4 ka. The samples of ~1.5 g dry weight were subject to successive chemical treatments with HCl, KOH, and HF, following acetolysis, as described in Fægri & Iversen (1989). A tablet of *Lycopodium* marker spores was added to each sample for calculating total pollen and spore concentrations following Stockmarr (1971). The concentrated pollen residues were preserved in glycerol for further identification and counting. About 400 terrestrial pollen grains were counted in most samples using a light microscope at 400× magnification. Identification of pollen, spore, and non-pollen-palynomorphs (NPPs) is in accordance with relevant regional keys and atlases (Kupriyanova & Alyoshina, 1972; Bobrov et al., 1983; Reille, 1992, 1995, 1998; Van Geel, 2001). Palynomorph percentages and concentrations are calculated in each sample (for details see Zhao et al., 2015).
Pollen data of 250 samples are involved in this study, comprising (i) 204 samples (696.0-1055.8 ka) analyzed by W.W. Zhao (this study), (ii) 18 samples (1057.2-1091.4 ka) published by Lozhkin & Anderson (2013), and (iii) 28 samples (720.2-917 ka) published by Lozhkin et al. (2016).

3.2.2 Biome and landscape openness reconstructions

Pollen-based 'biomization' is a quantitative approach, which was first designed and tested using a limited number of key pollen taxa digitalized from the 0 and 6 ka pollen spectra from Europe (Prentice et al., 1996). The method has been further adapted for reconstructing the main vegetation types (biomes) present in northern Eurasia (Tarasov et al., 1998, 2000, 2013). In recent years, it has been successfully applied to the modern and fossil pollen spectra from Lake El'gygytgyn, in order to reconstruct the vegetation and climate history of this Arctic region since the late Pliocene (Brigham-Grette et al., 2013; Tarasov et al., 2013; Andreev et al., 2014, 2016; Zhao et al., 2015). Pollen taxa found in the Lake El'gygytgyn record and their assignments to the respective biomes are presented in Table 3.1 (for further details see also Tarasov et al., 2013). By calculating the difference between the maximal forest biome score (MFBS) and the maximal open biome score (MOBS), a qualitative assessment of the

landscape openness can be achieved with a higher confidence compared to a more traditional approach using arboreal and non-arboreal pollen percentages (Tarasov et al., 2013).

Table 3.1 Terrestrial pollen taxa identified in the Lake El'gygytgyn sediments accumulated between 1091 and 715 ka and their corresponding biomes (following Tarasov et al., 2013). Taxa, whose percentages in the biome-taxon matrix are <0.5% (threshold suggested by Prentice et al., 1996), and which do not influence the results of the biome reconstruction, are marked with an asterisk.

Biome	Terrestrial pollen taxa
TUND/Tundra	*Alnus fruticosa*-type (shrub), *Betula* sect. *Albae*-type (tree)*, *B.sect. Nanae*-type (shrub), *B.* undif, Cyperaceae, Ericales, Poaceae, Polemoniaceae, Polygonaceae, *Rubus chamaemorus*, *Salix*, Saxifragaceae, Valerianaceae
CLDE/Cold deciduous forest	*Alnus fruticosa*-type (shrub), *Betula* sect. *Albae*-type (tree)*, *B.* sect. *Nanae*-type (shrub), *B.* undif, Ericales, *Larix/Pseudotsuga*, *Pinus subgenus Haploxylon*, Pinaceae undif, *Rubus chamaemorus*, *Salix*
TAIG/Taiga	*Alnus sp, Abies**, *Betula* sect. *Albae*-type (tree)*, *B.* sect. *Nanae*-type (shrub), *B.* undif, Ericales, *Larix/Pseudotsuga*, *Picea**, *Pinus* s/g *Haploxylon*, Pinaceae undif, *Rubus chamaemorus*, *Salix*
COCO/Cool conifer forest	*Alnus sp, Abies**, *Betula* sect. *Albae*-type (tree)*, *B.* sect. *Nanae*-type (shrub), *B.* undif, *Carpinus*-type*, *Corylus**, Ericales, *Larix/Pseudotsuga*, *Picea**, *Pinus subgenus Haploxylon*, Pinaceae undif, *Salix*, *Tilia**, *Tsuga**
STEP/Cold steppe	*Artemisia*, Asteraceae, Asteraceae Cichorioideae*, Caryophyllaceae, *Cannabis*-type, Chenopodiaceae, Fabaceae, Lamiaceae, Onagraceae, Papaveraceae, Poaceae, Polygonaceae, Ranunculaceae, Rosaceae*, *Thalictrum*, Valerianaceae

3.3 Results

3.3.1 Chronology and sedimentation rates

The age-depth model of the composite core at ICDP Site 5011-1 was developed based upon palaeomagnetic data and tuning of sediment proxies to the local summer insolation and a global marine isotope stack (for details see Melles et al., 2012; Nowaczyk et al., 2013). The model provides detailed information concerning the chronology and sedimentation rates for the time interval between ~1100 and 715 ka ago. The sedimentation rates generally show

rather strong fluctuations and a mean value of 0.04 m ka^{-1}. Within the studied time interval the highest sedimentation rates appear during MIS 24 (up to 0.2 m ka^{-1}; Fig. 3.3D).

3.3.2 Results of pollen and NPP analyses

A total of 69 pollen, spore, and NPP types have been identified in the 250 investigated samples. Among the 250 samples, pollen data of 47 samples, which contain only a few pollen grains, are not presented in the pollen diagram (Fig. 3.2). Major changes in pollen assemblages are described in Table 3.2. The pollen spectra are subdivided into 16 pollen assemblage zones (PAZs) based on the visual inspection of the major percentages and stratigraphically constrained cluster analysis (CONISS). *Alnus* and *Betula* are most important taxa in PAZ-II and PAZ-VII, where total pollen concentrations are particularly high. Major herbaceous taxa are Poaceae, Cyperaceae, and *Artemisia*. Herbaceous pollen taxa percentages reach high values in PAZ-III, PAZ-V, PAZ-VIII, PAZ-IX, PAZ-XI, and PAZ-XIV.

3.3.3 Biome reconstruction

A total of 86 samples with very low pollen counts of <50 terrestrial pollen grains (labeled in Table 3.2) were excluded from biome score calculations due to statistical uncertainties. The reconstruction performed for the remaining pollen spectra shows that five biomes, comprising tundra (TUND), cold steppe (STEP), cold deciduous forest (CLDE), taiga (TAIG) and cool conifer forest (COCO), appeared at least once as the dominant vegetation type during the studied interval between 1091 and 715 ka. Major changes in reconstructed biome scores are described in Table 3.2. TUND and STEP have the highest affinity scores, with the exception of PAZs II and VII, in which CLDE, COCO, and TAIG scores are relatively high.

The biome score calculations reveal that the landscape around Lake El'gygytgyn became gradually more open after 940 ka (PAZ-VIII), with the higher proportion of woods occurring in PAZ-II and PAZ-VII (Fig. 3.3C).

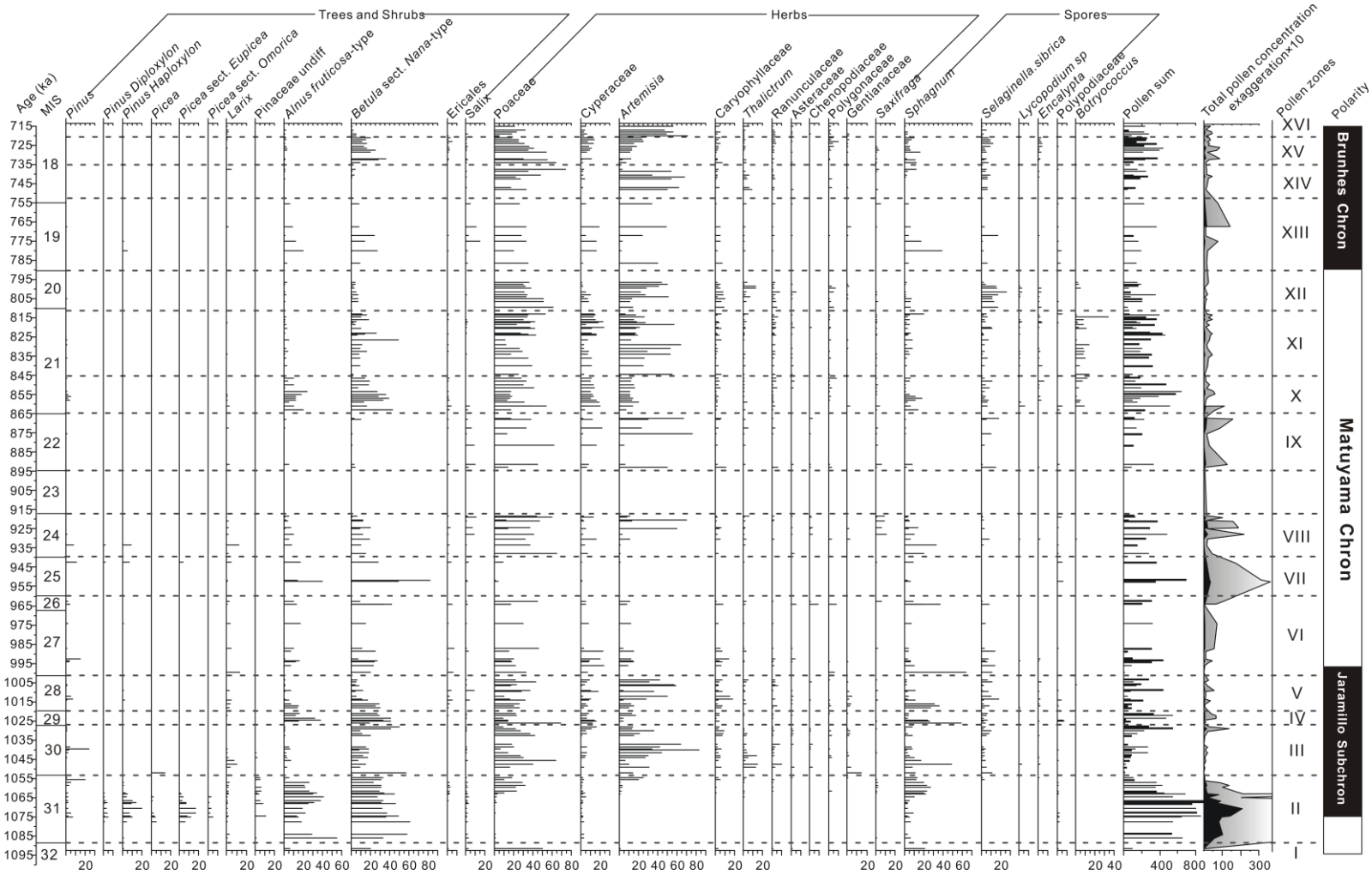

Fig. 3.2 Summary diagram showing percentages of major pollen, spore, fungal and algal taxa that accumulated between 1091 and 715 ka in the Lake El'gygytgyn sediments.

Table 3.2 Characteristic pollen assemblages and biomization results for the pollen assemblage zones (PAZ) revealed in the Lake El'gygytgyn sediments accumulated between 1091 and 715 ka.

PAZ	Age (ka)	Sample number (excluded samples)/ temporal resolution (ka)	Characteristic pollen assemblages	Biomization results
I	1091-1090	1 (0) /1	Low amount of tree pollen and high percentage of Poaceae	TUND is the dominant biome, STEP scores are higher than CLDE scores
II	1090-1055	17 (0) /2	Peaks of tree and shrub pollen percentages, highest pollen concentrations; high percentages of *Sphagnum* spores in the upper MIS 31	TAIG biome becomes dominant, COCO replaces TAIG biome within the optimum of super interglacial MIS 31
III	1055-1027	29 (14) /2	Drastic decrease in tree and shrub pollen percentages and increase in herb pollen; appearance of *Selaginella rupestris* spores	STEP becomes the dominant biome
IV	1027-1020	8 (3) /1.4	Increase in *Betula* and *Alnus* pollen percentages, larger amounts of *Sphagnum* spores	TUND becomes the dominant biome, CLDE scores are higher than STEP scores
V	1020-1000	11 (6) /4	Decrease in shrub pollen (particularly *Alnus*), small amount of *Salix* and *Ericales* pollen; increase in herb pollen	STEP replaces TUND biome, and CLDE scores are lowest in this zone
VI	1000-960	34 (17) /2.4	Increase in *Betula* and *Alnus* shrub pollen; *Artemisia* pollen significantly decreases	TUND biome is dominant and CLDE scores increase. At 965 ka, CLDE scores abruptly decrease
VII	960-940	12 (7) /4	High shrub pollen percentages (mainly *Alnus* and *Betula*)	CLDE expands and becomes the dominant biome, STEP scores have the lowest value
VIII	940-918	12 (3) /2.4	Remarkable increase in herb pollen; few *Salix* pollen	TUND and STEP scores increase
	918-895	10 (10) /2.3	No pollen	
IX	895-865	9 (1) /4	High percentages of herb pollen and relatively high content of *Selaginella rupestris* spores; tree and shrub pollen are almost absent, few *Salix* pollen	STEP becomes the dominant biome, CLDE scores drop markedly
X	865-845	17 (2) /1.3	Notable increase in *Betula* and *Alnus* pollen, small amounts of *Pinus* pollen and *Sphagnum* spore, occurrence of *Botryococcus*	CLDE scores increase and exceed STEP, but TUND remains dominant

PAZ	Age (ka)	Sample number (excluded samples)/ temporal resolution (ka)	Characteristic pollen assemblages	Biomization results
XI	845-810	23 (0) /1.5	Decrease in *Alnus* pollen percentages, increase in *Botryococcus*	CLDE and TUND scores decrease but TUND remains dominant
XII	810-790	15 (2) /1.5	Increase in herb pollen percentages, particularly *Artemisia*, decrease in *Betula*, significantly higher contents of *Selaginella rupestris*	STEP scores reach their peak for the entire study interval
XIII	790-755	16 (8) /4	Increase in *Alnus*, *Betula* and *Salix* pollen percentages, high contents of *Sphagnum* spores	CLDE and TUND scores increase and TUND becomes dominant
XIV	755-735	17 (10) /3	Disappearance of tree and shrub pollen, high percentages of herb pollen (mainly Poaceae and *Artemisia*)	STEP becomes dominant, CLDE and TUND scores decrease
XV	735-720	14 (2) /1.2	Increase in *Betula* pollen; small amount of *Alnus*, *Ericales* and *Salix*, high content of *Sphagnum* and *Selaginella. rupestris* spores	CLDE and TUND scores increase slightly, TUND is dominant
XVI	720-715	5 (1) /1.2	*Betula* pollen disappears again, while herb (particularly *Artemisia*) pollen percentages significantly increase	CLDE and TUND scores decrease, STEP is dominant biome

Table 3.2: Continued.

3.4 Discussion

3.4.1 Vegetation and environmental conditions during the MPT

The pollen assemblages from Lake El'gygytgyn document distinct changes of regional vegetation and climate during the MPT (Fig. 3.2 and 3.3). Shrub tundra and cold steppe communities dominated in the area between 1091 and 715 ka. During the colder (glacial) intervals, relatively low pollen concentrations and high percentages of herbaceous pollen taxa (mainly Poaceae, Cyperaceae, and *Artemisia*) suggest open (i.e. treeless and/or shrubless) vegetation as a result of severe (very cold and dry) climate conditions. High contents of *Selaginella rupestris* spores also indicate harsh climate (Lozhkin et al., 2007). In contrast,

interglacial intervals are characterized by increased amounts of tree and shrub pollen. Dwarf birch (*Betula*) is the most common shrub throughout the studied interval, usually accompanied by shrub alder (*Alnus*). These shrubs generally dominated the vegetation cover during interglacials, while trees are subordinate with sporadic occurrences of larch (*Larix*). Remains of green algae colonies (mainly *Botryococcus*), which are most frequent in the sediments accumulated between 865 and 810 ka, suggest the widespread occurrence of shallow-water habitats during this interval (Andreev et al., 2014).

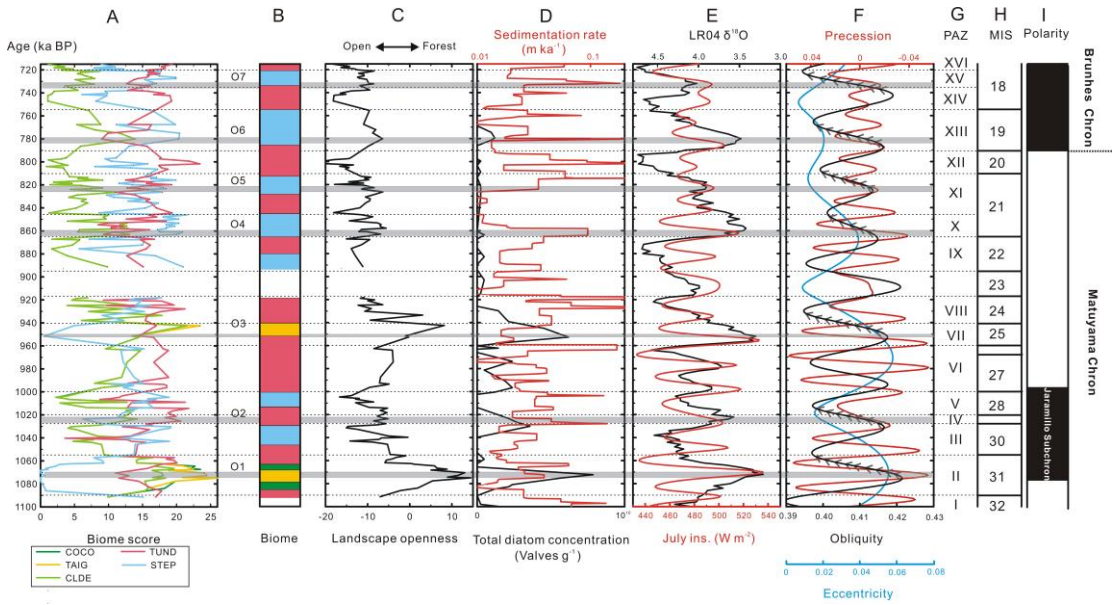

Fig. 3.3 Summary figure. A. Time series of individual biomes. B. Dominant biomes (the blank zone denotes the period without available information from pollen). C. Qualitative characteristic of landscape openness, reflected by the difference between the maximum score of forest biomes (MSFB) and the maximum score of open biomes (MSOB) at each level. D. Total diatom concentration (black line, according to Snyder et al., 2013) and sedimentation rate (red line, according to Nowaczyk et al., 2013). E. LR04 global marine isotope stack (black line, according to Lisiecki & Raymo 2005) and mean July insolation for 67.5 °N (red line, according to Laskar *et al.* 2004). F. precession curve (red line), obliquity curve (black line) and eccentricity curve (blue line, according to Laskar et al., 2004). G. pollen zones according to Fig. 3.2. H. Marine Isotope Stages (MIS) according to Lisiecki & Raymo (2005). I. Paleomagnetic chrons and subchrons according to Nowaczyk et al. (2013). The onset of each vegetation succession is marked with grey horizontal bars and labeled from O1 to O7. The arrows on obliquity line correlated with successions O1-O7 (between A and B) indicate the obliquity shift from maxima to minima. Biome names are abbreviated as follows: COCO - Cool conifer forest, TAIG - Taiga, CLDE - Cold deciduous forest, TUND - Tundra, STEP - Cold steppe.

PAZs I and II (~1091-1055 ka) encompass late MIS 32 and MIS 31 and are described in detail by Lozhkin & Anderson (2013). Vegetation responses are initially marked by the spread of *Betula-Alnus* shrub tundra, which is accompanied by small amounts of larch and subsequently followed by the evergreen conifers. MIS 31 is reported to be one of the warmest interglacials during the entire Quaternary and the optimum of the so-called 'superinterglacial' corresponds to the onset of the palaeomagnetic polarity event Jaramillo Subchron (Melles et

al., 2012, Fig. 3.2). Biome reconstructions show that the decline of STEP and TUND scores marks the transition from MIS 32 to MIS 31, when TAIG replaced TUND as the dominant biome (Tarasov et al., 2013). During MIS 31, between 1078 and 1066 ka, the COCO biome, which requires warmest conditions among the here reconstructed biomes (Prentice et al., 1992; Kaplan, 2001), appeared in the region closest to the lake. Towards the late MIS 31, increasing contents of herbaceous pollen and *Sphagnum* spores suggest cooler, though still wet conditions. This trend culminates at the end of MIS 31, when the TUND biome regained dominance, implying that the climate became colder.

Between 1055 and 1027 ka (PAZ-III, MIS 30) cold steppe and meadow plant communities became common in the region, as indicated by significantly increased herbaceous pollen (*Artemisia*, Poaceae, Cyperaceae, Caryophyllaceae, and *Thalictrum*) and *Selaginella rupestris* spore contents, as well as a much lower pollen concentration. STEP scores remarkably increase at the onset of MIS 30 and later exceed TUND scores. This suggests the presence of a steppe-tundra in the area, being indicative of a severe climatic deterioration. The cold and dry climate conditions resulted in open vegetation, as reflected by increased abundance of *Artemisia* pollen and *Selaginella rupestris* spores. However, the continued presence of a few *Larix* and *Pinus* pollen suggests the existence of scattered woodland (or krummholz) stands, probably limited to protected areas in the lake vicinity.

In the sediments accumulated between 1027 and 1020 ka (PAZ-IV, MIS 29), the percentages of *Alnus* and *Betula* pollen are significantly higher than those in MIS 30, suggesting that shrub alder and dwarf birch became more widespread in the area. High contents of Cyperaceae pollen and *Sphagnum* spores indicate the presence of locally mesic habitats. Increased CLDE scores and increased forestation of the landscape provide further evidence for climate conditions warmer than during MIS 30.

Between 1020 and 1000 ka (PAZ-V, MIS 28), shrubby vegetation (dwarf birch and shrub alder) decreased in the region again, while larch probably still grew in the lake vicinity. Simultaneous increases in *Artemisia* and Caryophyllaceae pollen percentages as well as *Selaginella rupestris* spores suggest an expansion of open steppe habitats and cold and dry climate conditions. This interpretation is supported by increased STEP scores.

Environmental conditions ameliorated between 1000 and 960 ka (PAZ-VI, MIS 27 and 26), as reflected by a further increase of larch, dwarf birch, and alder percentages and presence in the local vegetation, although herb communities were still common in the region. Biomization

results show a slight increase in the CLDE scores and a reduction in the STEP scores, indicating warmer and wetter conditions. An abrupt increase in the STEP scores at ~975 ka points to a climatic deterioration at the onset of the short MIS 26 glacial.

Between 960 and 940 ka (PAZ-VII, MIS 25) *Betula* and *Alnus* pollen percentages increased significantly, accompanied by minor contents of *Pinus* and *Larix* pollen, as well as the occasional occurrence of *Picea* pollen. The absolute predominance of *Betula* and *Alnus* in the pollen spectra is indicative of vegetation dominated by relatively dense tree-sized shrubs. This conclusion is supported by the high-affinity scores of CLDE, TAIG, and COCO biomes, and correspondingly low STEP scores. These data evidence that Arctic climate experienced short-term moist and warm conditions during MIS 25, which is coeval with the frequent presence of thermophilic diatoms in Lake Baikal sediments (Khursevich et al., 2005).

During MIS 24 (940-918 ka, PAZ-VIII) the vegetation was dominated by gradually expanding xeric Poaceae-*Artemisia* habitats with some *Betula-Alnus-Salix* shrubby communities, suggesting significantly regional cooling. Other woody plants are stone pine shrubs, which might have benefited from insulating effects of sufficiently deeper winter snow cover due to increased moisture availability (Lozhkin et al., 2007) during early MIS 24. Similar conditions are also inferred from the coevally decreased frequencies of planktonic diatoms showing that Lake El'gygytgyn was covered by permanent ice with a thick blanketing snow cover during summertimes (Snyder et al., 2013). Furthermore, maximum sedimentation rates during late MIS 24 probably reflect larger exposed areas in the catchment due to declined vegetation cover in consequence of increased aridity. Particularly high sedimentation rates interpreted to reflect severe climatic deterioration also occurred in Lake Baikal during MIS 24 (Prokopenko et al., 2006).

It is elusive why pollen is absent in the sediments accumulated between 918 and 895 ka (MIS 23) despite high values in total organic carbon concentrations, Si/Ti ratios and biogenic silica (BSi) percentages (Nowaczyk et al., 2013). We speculate that the following two scenarios might account for the absence of pollen. Firstly, a prominent feature in the respective sediments is the 6.9-cm thick T3 tephra at ~918 ka (van den Bogaard et al., 2013). Contemporaneous tephra layers are also observed in the Alaska interior (Westgate et al., 1990) and in the State of Washington, USA (Easterbrook et al., 1981). All these tephra layers were deposited after the well-defined normal polarity event Jaramillo Subchron. Hence, the T3 tephra obviously represented a large-scale volcanic eruption event. Tephra layers were indicated to have buried former vegetation and they may even have contributed to the

formation of permafrost in Alaska (Matheus et al., 2003). Therefore, we speculate that the T3 tephra partly may have led to particularly sparse vegetation during MIS 23, although this tephra layer probably is too thin to have prohibited plant growth for more than 20 ka. Secondly, an alternative explanation is related to pollen delivery. Previous studies have shown that MIS 23 in the Lake El'gygytgyn sediment record was characterized by low diatom concentrations (Snyder et al., 2013) and low BSi contents (Nowaczyk et al., 2013). These data imply that permanent lake ice has covered the lake, thereby potentially limiting the supply of allochthonous material to the lake, including pollen grains, and thus ultimately leading to relatively low pollen loads (Fig. 3.3D).

During MIS 22 (895-865 ka, PAZ-IX) open steppe communities dominated the landscape. However, dwarf birch and willow grew in more protected areas, while conifer and shrub alder stands probably completely disappeared from the lake vicinity. Dry and cold climate conditions are also suggested by an increase in *Selaginella rupestris* spore content.

The pollen assemblages that accumulated between 865 and 810 ka (MIS 21) can be subdivided into 2 subzones. In the lower subzone (PAZ-X, 865-845 ka) *Betula* and *Alnus* pollen are abundant and small amounts of *Pinus* and *Larix* pollen occur. Such pollen spectra reflect that shrubby communities (stone pine, birch, and alder) returned to the lake vicinity. An increase in *Sphagnum* spore contents points to the presence of wet swampy habitats around the lake (Kozhevnikov, 1993). Generally, the revealed pollen assemblages indicate relatively warm and probably wet climate conditions. However, relatively high amounts of *Artemisia* pollen and *Selaginella rupestris* spores point to the presence of open tundra-steppe-like communities around the lake as well. In the lower subzone (PAZ-XI, 845 and 810 ka) larch and shrub alder stands were rather limited, probably related to decreased summer insolation (Fig. 3.3E). The broadly distributed open steppe communities in this period indicate colder climate conditions.

Between 810 and 790 ka (PAZ-XII, MIS 20) a further decline of *Betula* pollen, together with an increase in herb pollen, suggest climate conditions harsher than during the previous interval. Cold and dry conditions are also indicated by the highest affinity scores of the STEP biome in the entire record. Significantly drier environmental conditions are also confirmed by a remarkable increase of *Selaginella rupestris* contents.

The PAZ-XIII (790-755 ka, MIS 19) pollen assemblages indicate that the local vegetation was codominant by herb and shrub communities, sharing characteristics with pollen spectra of

MIS 24, although percentages of shrubby taxa are higher during MIS 19. This indicates that climatic amelioration during this interglacial was moderate. The relatively open landscape also suggests that shrubs were scattered and restricted to protected habitats (e.g. river valleys). Increased contents of *Sphagnum* spores provide evidence for moister soil conditions. The lower boundary of PAZ-XIII is coeval with the palaeomagnetic Matuyama-Brunhes polarity change at ~780 ka (Fig. 3.2), as identified in the sediment record by magnetostratigraphic studies (Melles et al., 2012; Nowaczyk et al., 2013).

Shrub alders were nearly absent in the study region between 755 and 715 ka (PAZ-XIV to PAZ-XVI, MIS 18), while herb communities with Poaceae, Cyperaceae, and Caryophyllaceae significantly increased. The occurrence of *Selaginella rupestris* spores suggests that soils around the lake were relatively dry. Among the three pollen zones, relatively high amounts of dwarf birch pollen are characteristic of PAZ-XV. At the same time, the minor presence of Cyperaceae pollen and *Sphagnum* spores imply that relatively mesic habitats existed during mid-MIS 18. A small peak in spores of *Encalypta* points to the occurrence of disturbed soils around the lake (van Geel, 2001).

3.4.2 MPT vegetation succession and astronomical configuration

Vegetation succession is an ecological term referring to progressive vegetation development over time. Long-term ecosystem evolution is mainly controlled by ecological development with increasing productivity and nutrient availability (Wardle et al., 2004). This process is most obvious at the onset of interglacials and reflected by the improvement of soil fertility (Birks & Birks, 2004).

The vegetation successions and the corresponding astronomical configurations during three interglacials (MIS 81/79, MIS 11c/11b, and MIS 5e/5c) have been investigated based on the Lake El'gygytgyn pollen record by Zhao et al. (2015). It was concluded that obliquity has a more significant influence on vegetation successions in the Arctic than precession, while the onset of interglacials is rather triggered by both effects. More specifically, when obliquity moves from peak to trough, an increased difference in the seasonal daylight duration could eventually drive the replacement of forest and shrub vegetation by open steppe and tundra communities. Precession, in contrast, affects climate variations through its control on the intensity of summer insolation at high latitudes. Simultaneous maxima in obliquity and precession are characteristic of an interglacial onset.

During the MPT, seven complete vegetation successions (marked as O1-O7 in Fig. 3.3) are recognized and characterized by the replacement of trees and shrubs by herbs, which presumably responded to climatic changes from relatively warm-humid boreal towards cold-arid arctic conditions. The onset of each vegetation succession is marked by maximized CLDE scores coinciding with peak precession and obliquity, which led to high insolation and triggered the onset of interglacials. Conversely, minimal CLDE scores, indicating the ends of the successions, are in line with obliquity minima. Hence, the vegetation successions are generally in phase with obliquity cycles.

PAZ-VI (MIS 27) shows relatively subtle changes in biome scores. With the predominance of the TUND biome, CLDE scores gradually increase, exceed STEP scores at 980 ka, and abruptly decline at 965 ka. Other proxies, showing low diatom concentrations, low BSi percentages, and low Si/Ti ratios, also suggest rather interstadial conditions around 985 ka. Hence, we assume that vegetation dynamics in PAZ-VI was influenced by the antiphase relationship between precession and obliquity, which have offset their effects on the summer insolation and impeded vegetation development (Fig. 3.3A). Consequently, this orbital setting probably excluded the development of full interglacial conditions within MIS 27. Such a vegetation change implies that the high-amplitude precession forcing may have remained the dominant factor at high latitude.

STEP biome scores significantly increased since ~890 ka, suggesting increasing aridification of the northeastern Russian Arctic. Changes in landscape openness are also closely correlated with changes in global ice volume, as inferred from the LR04 records (Fig. 3.3C, E). The time interval around ~890 ka as a turning point reveals a more open vegetation in the regional landscape and climatic deterioration during the MPT. After 890 ka, the increasingly open landscape and low diatom concentrations correspond to low-amplitude changes in the three orbital parameters. Glacial-interglacial cycles also became longer than before.

Although the existing pollen record is still not highly resolved enough to reveal eccentricity's modulation of the climate throughout the whole Quaternary, the existing data clearly show the crucial role of eccentricity in forcing long-term vegetation changes in the high latitudes through the synchronous changes in landscape openness and the 100 ka eccentricity cycle. According to Maslin & Ridgwell (2005), a higher eccentricity makes a more elliptical orbit that exaggerates the difference of season length between northern and southern hemispheres despite the weaker performance of eccentricity on insolation change as compared to other orbital parameters.

3.4.3 Spectral analysis of the landscape openness

Spectral and wavelet analysis is applied to landscape openness data from the time interval between 1091 and 900 ka (Fig. 3.4). The results reveal a long eccentricity (400 ka) signal, which, due to the limited length of our record, cannot be interpreted. The secondary power is the 100-ka modulation, which clearly shows up between 1080 and 960 ka. Precession and obliquity, in contrast, do not exhibit strong power throughout the entire studied interval.

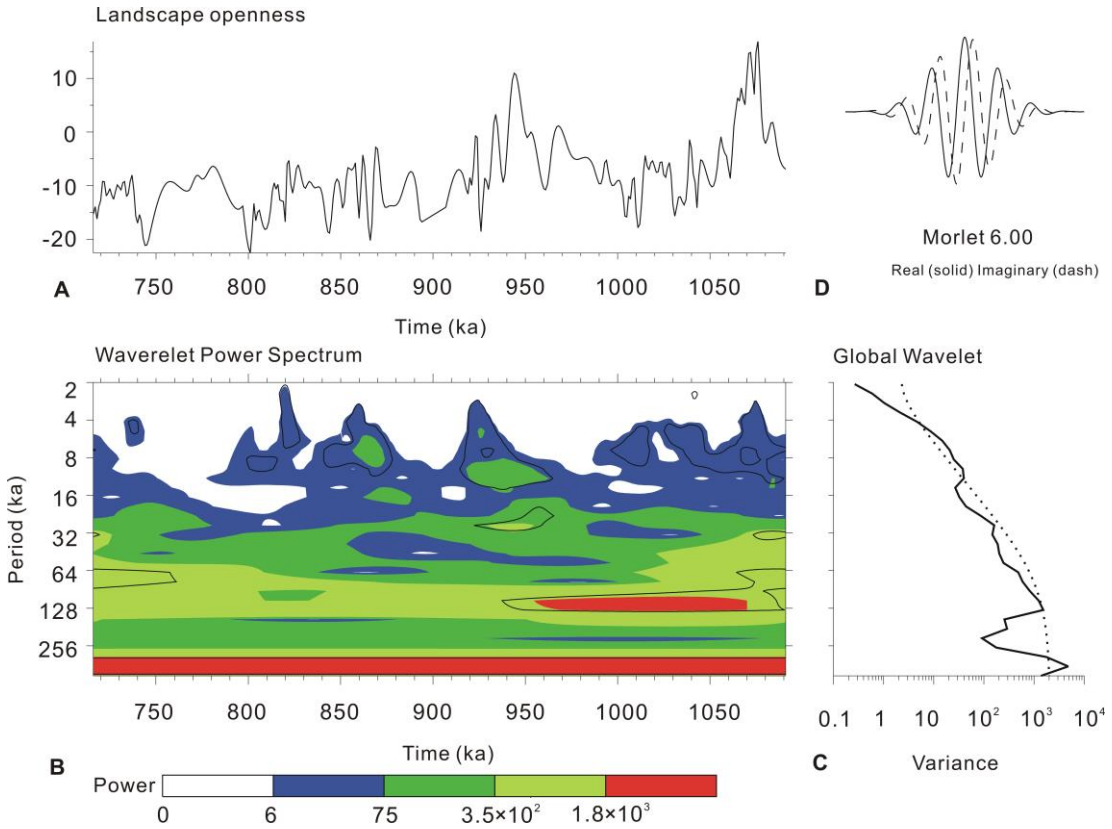

Fig. 3.4 A. Landscape openness time series created by IDL wavelet software. B. The wavelet power spectrum, computed by Torrence & Compo (1998). The color represents the amplitude of the signal at a given time and spectral period (red equals the highest power, white equals the lowest). The black contour is the 10% significance level, using a red-noise (autoregressive lag 1) background spectrum. C. The global wavelet power spectrum (black line). The dashed line is the significance for the global wavelet spectrum, assuming the same significance level and background spectrum as in (B). D. "Morlet" wavelet used for (B).

Time series analysis on PC1 values of grain-size data from the same core has shown different results in the relative dominance of orbital cycles (Francke et al., 2013). According to these data, a 98.5 ka cycle became initiated about 1250 ka ago. After 1000 ka, the eccentricity modulation weakens, while the obliquity signal strengthens. At *c.* 670 ka, obliquity oscillation decreased its relative power, thereby marking the end of the MPT. The differences reflected in the analysis of grain-size and landscape-openness data might be due to different signals of

superimposed climate dynamics caught by these two proxies. Grain-size changes reflect the duration of lake-ice cover and thickness of the active layer in the summertime (Francke et al., 2013), while changes in landscape openness point to variations in the regional vegetation cover. Local responses of the lake surface and regional vegetation cover to orbitally-controlled climate change might exhibit diverse patterns.

Spectral analysis of arboreal pollen percentages from the Tenaghi Philippon record, Greece, has shown strong response during the MPT only to eccentricity modulation on eastern Mediterranean climate (Tzedakis et al., 2006). However, combing wavelet analysis on arboreal pollen percentages and sea surface temperatures (Lourens et al., 1992), Tzedakis et al. (2006) underline the pervasive influence of precession and obliquity on Mediterranean climates. Joannin et al. (2011) applied modern analogues techniques based on western Mediterranean pollen data to reconstruct a climate index for the first half of the MPT. Analysis of further time series displays discontinuous and weak signals of precession and obliquity (Joannin et al., 2011). Analysis of the Lake El'gygytgyn record also reveals that precession and obliquity played an important role in regulating vegetation and climate changes, whereas wavelet analysis only captures the power of the eccentricity cycle. Hence, we support the interpretation proposed by Joannin et al. (2011) that a single parameter is insufficient for revealing the full complexity of superimposed forcing.

3.4.4 Regional environmental implications

The MPT is a prominent interval in the Quaternary. According to marine oxygen isotope records, the MPT is marked by a gradual increase in average global ice volume and a decrease in deep-water temperature (Rial, 2004). Global cooling and the expansion of Arctic ice sheets presumably caused the strengthening of the Siberian high-pressure cell, leading to significantly intensified aridity in the Asian interior (Ruddiman & Kutzbach, 1989; Guo et al., 2002; Han et al., 2014). On this basis, we compare the reconstructed vegetation and environmental changes in the northeastern Russian Arctic (Lake El'gygytgyn) with proxy data reflecting developments in the interior of Asia (soil organic matter $\delta^{13}C$ and *Pinus* contents in China) and globally (marine benthic $\delta^{18}O$), in order to reveal possible driving mechanisms for climatic variations during the MPT (Fig. 3.5).

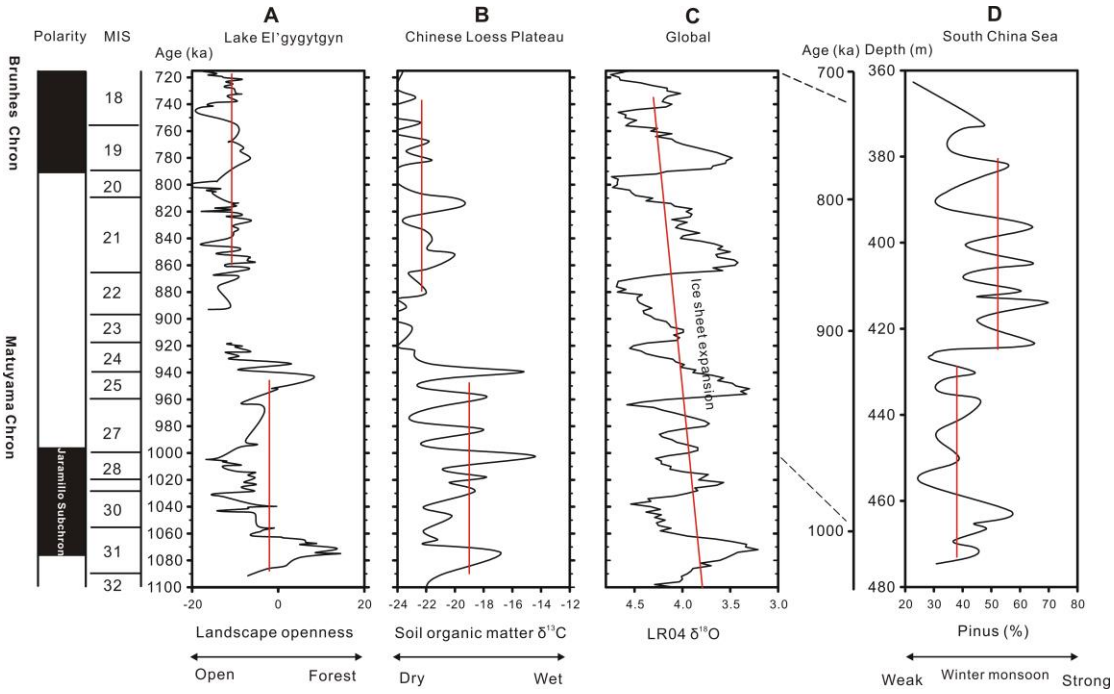

Fig. 3.5 Correlation of records in different latitudes. A. Landscape openness (indicative of vegetation cover in Lake El'gygytgyn vicinity). B. Soil organic matter $\delta^{13}C$ from Lantian, China (An et al., 2005). C. LR04 global marine isotope stack (Lisiecki & Raymo, 2005). D. *Pinus* percentage from ODP Site 1144 (Sun et al., 2003), red lines illustrate the base-line level drop during the MPT.

Zonation and biomization of the pollen data presented in our study show three main vegetation phases during the MPT (Fig. 3.2 and 3.3). The first phase (~1091-930 ka) was characterized by a gradual opening of the vegetation cover (Fig. 3.5A), with decreasing trees and shrubs, being replaced by increasing herbs. This suggests that the high latitudinal study region experienced cooler and dryer conditions, which well agrees with the aridification of the Chinese Loess Plateau that is indicated by decreasing A/C ratios of pollen spectra (Cai et al., 2013).

The next phase comprises MIS 24-MIS 22 (*c.* 930-865 ka). Globally, this is a remarkable interval during the MPT, because it represents the first large glaciation, extreme SST cooling, and a decline in thermohaline circulation (Schmieder et al., 2000; Clark et al., 2006). In the Lake El'gygytgyn sediments, the absence of pollen during MIS 23 (Fig. 3.2) prohibits to analyze the mechanisms behind the vegetation change in high northern latitudes. Nevertheless, low diatom concentrations indicate that the time interval between 930 and 715 ka was characterized by rather cold conditions (Snyder et al., 2013). Coevally, on the Chinese Loess Plateau, soil organic matter experience a shift previously high $\delta^{13}C$ values to notably depleted $\delta^{13}C$ (Fig. 3.5B). This suggests the virtual absence of C4 plants in the vegetation, which indicates extremely cold and dry conditions (An et al., 2005). This interval also coincides

with the prevalence of the coarse-grained L9 loess unit in the Chinese Loess Plateau, which is a cold event indicative of severe climatic deterioration (Kukla & An, 1989).

The third vegetation phase (865-715 ka), marked by maximum affinity scores of the STEP biome (Fig. 3.3), is characterized by high abundances of drought-enduring herbs (e.g. *Artemisia*), thus suggesting that a dry climate prevailed during this interval. The Chinese Loess Plateau records during this interval show generally low soil $\delta^{13}C$ values (Fig. 3.5B), suggesting moderate amounts of C4 plants in the local vegetation, indicative of dry climate conditions (An et al., 2005). Similar conditions are also inferred from a pollen record of Chinese Loess Plateau, which shows that steppe dominated the vegetation landscape, replacing forest-steppe that existed before 0.95 Ma (Wu et al., 2007).

The long-term drying and cooling trend during the MPT corresponded with a global ice sheet expansion (Lisiecki & Raymo, 2005; Fig. 3.5C). This led to a significant sea-level lowering, exposure of continental shelves and enhancement of the westerly jet. The consequent enhancement of sinking winter cold-dry airmass intensified the Siberian High (Ruddiman & Kutzbach, 1989). As a result, the Siberian High and the Polar Front shifted southward, and thus significantly strengthened the Asian winter monsoon circulation (Yoshino, 1978) as demonstrated by notably increased pine pollen contents in the northern South China Sea (Sun et al., 2003; Fig. 3.5D).

The persistent and pronounced dry conditions in the high latitudes and the Asian interior after 865 ka may be explained by a significant intensification of the westerly jet and the Siberian High. This was probably facilitated at least to some extent by the concomitant uplift of the northeastern Tibetan Plateau since ~0.9-0.8 Ma (Ruddiman & Kutzbach, 1989; Li, 1995; Fang et al., 2005, 2007).

3.5 Conclusions

The millennial-scale resolution pollen record from Lake El'gygytgyn documents in details the history of vegetation and climate changes in the high Arctic during the MPT (1091-715 ka). It provides the basis for qualitative analysis of the pollen assemblages and for the calculation of biome scores and landscape openness.

Seven vegetation successions following glacial-interglacial oscillations occurred between 1091 and 715 ka. The glacials are characterized by a predominance of open herbaceous communities, and the interglacials by a predominance of boreal trees and shrubs. The long-term vegetation history shows a gradual replacement of shrubby vegetation, dominated by *Pinus, Alnus,* and *Betula*, by herbaceous communities, dominated by Poaceae, Cyperaceae, and *Artemisia*. This reflects a general cooling and drying trend throughout the entire MPT.

From MIS 24-22, CLDE biome scores significantly declined, indicating that the initially forested landscape became more open. Afterwards, the study area became mostly dominated by open herbaceous communities. Nevertheless, during the interglacials, the presence of trees and shrubs in the regional vegetation increased.

The vegetation successions in the northeastern Russian Arctic clearly responded to obliquity cycles, with both CLDE scores and the corresponding obliquity signal shifts from maximum to minimum values. However, wavelet analysis of landscape openness change does not reveal a strong obliquity signal. Instead, eccentricity exhibits a stronger power in regulating landscape openness. This suggests that time-series analysis of a single parameter may not catch the full complexity of its superimposed controls.

Global cooling, especially in the high latitudes of the Northern Hemisphere, is probably the driving force of long-term vegetation deterioration trend during the MPT. The accelerated increase in aridification that occurred after MIS 24-22 was possibly associated with the tectonic uplift of Tibetan Plateau, which forced intensification of cold-dry flow of the Siberian High and the westerly jet systems.

Acknowledgments. The work of W.W. Zhao was financed by the China Scholarship Council Ph.D. Scholarship. Financial support for palynological analyses was also provided by the German Ministry for Education and Research (BMBF, grant 03G0642) and the German Research Foundation (grant ME 1169/24). The work of J.A. Korzun, A. V. Lozhkin and E.Y. Nedorubova was supported by the Russian Foundation for Fundamental Research (grant 15-05-06420) and the Russian Academy of Sciences (grant 15-I-2-067). The work of A.A. Andreev was also partly performed under the Russian Government Program of Competitive Growth of Kazan Federal University. Two anonymous reviewers are sincerely acknowledged for their invaluable comments, which improve the manuscript.

3.6 References

An, Z., Huang, Y., Liu, W., Guo, Z. Clemens, S., Li, L., Prell, W., Ning, Y., Cai, Y., Zhou, W., Lin, B., Zhang, Q., Cao, Y., Qiang, X., Chang, H. & Wu, Z. 2005: Multiple expansions of C4 plant biomass in East Asia since 7 Ma coupled with strengthened monsoon circulation. *Geology 33*, 705-708.

Andreev, A. A., Morozova, E., Fedorov, G., Schirrmeister, L., Bobrov, A. A., Kienast, F. & Schwamborn, G. 2012: Vegetation history of central Chukotka deduced from permafrost paleoenvironmental records of the El'gygytgyn Impact Crater. *Climate of the Past 8*, 1287-1300.

Andreev, A. A., Tarasov, P. E., Wennrich, V., Raschke, E., Herzschuh, U., Nowaczyk, N. R., Brigham-Grette, J. & Melles, M. 2014: Late Pliocene and early Pleistocene environments of the northeastern Russian Arctic inferred from the Lake El'gygytgyn pollen record. *Climate of the Past 9*, 4599-4653.

Andreev, A. A., Tarasov, P. E., Wennrich, V. & Melles, M. 2016: Millennial-scale vegetation changes in the north-eastern Russian Arctic during the Pliocene/Pleistocene transition (2.7-2.5 Ma) inferred from the pollen record of Lake El'gygytgyn. *Quaternary Scienece Reviews 147*, 245-258.

Belikovich, A. V. 1994: Recreation sources of planned "El'gygytgyn Lake Park". *FEB RAS Vestnik 3*, 57-63.

Berger, A. & Loutre, M. F. 2004: Astronomical theory of palaeoclimates. *Comptes Rendus Geoscience 336*, 701-709.

Bobrov, A. E., Kupriyanova, L. A., Litvintseva, M. V. & Tarasevich, V. F. 1983: *Spores and Pollen of Gymnosperms from the Flora of the European Part of the USSR, 208 pp*. Nauka, Leningrad.

Brigham-Grette, J., Melles, M., Minyuk, P., Andreev, A., Tarasov, P., DeConto, R., Koenig, S., Nowaczyk, N., Wennrich, V., Rosén, P., Haltia-Hovi, E., Cook, T., Gebhardt, C., Meyer-Jacob, C., Snyder, J. & Herzschuh, U. 2013: Pliocene warmth, extreme polar amplification, and stepped Pleistocene cooling recorded in NE Russia. *Science 340*, 1421-1427.

Birks, H. H. & Birks, H. J. B. 2004: The rise and fall of forests. *Science 305*, 484-485.

Cai, M. T., Fang, X. M., Wu, F. L., Miao, Y. F. & Appel, E. 2012: Pliocene-Pleistence stepwise drying of central Asia: Evidence from paleomagnetism and sporopollen record of the deep borehole SG-3 in the western Qaidam Basin, NE Tibetan Plateau. *Global and Planetary Change 94-95*, 72-81.

Clark, P. U., Archer, D., Pollard, D., Blum, J. D., Rial, J.A., Brovkin, V., Mix, A. C., Pisias, N. G. & Roy, M. 2006: The middle Pleistocene transition: characteristics, mechanisms, and implications for long-term changes in atmospheric pCO_2. *Quaternary Science Reviews 25*, 3150-3184.

Cremer, H., Wagner, B., Juschus, O. & Melles, M. 2005: A microscopical study of diatom phytoplankton in deep Crater Lake El'gygytgyn, Northeast Siberia. *Algological studies 116*, 147-169.

Dupont, L. M., Donner, B., Schneider, R. & Wefer, G. 2001: Mid-Pleistocene environmental change in tropical Africa began as early as 1.05 Ma. *Geology 29*, 195-198.

Easterbrook, D. J., Briggs, N. D., Westgate, J. A. & Gorton, M. P. 1981: Age of the Salmon Springs Glaciation in Washington. *Geology 9*, 87-93.

Elderfield, H., Ferretti, P., Greaves, M., Crowhurst, S., McCave, I. N., Hodell, D. & Piotrowski, A. M. 2012: Evolution of ocean temperature and ice volume through the Mid-Pleistocene Climate Transition. *Science 337*, 704-709.

Fang, X. M., Yan, M. D., Van der Voo, R., Rea, D. K., Song, C. H., Pares, J. M., Gao, J. P., Nie, J. S. & Dai, S. 2005: Late Cenozoic deformation and uplift of the NE Tibetan plateau: evidence from high-resolution magneto stratigraphy of the Guide Basin, Qinghai Province, China. *Geological Society of America Bulletin 117*, 1208-1225.

Fang, X. M., Zhang, W. L., Meng, Q. Q., Gao, J. P., Wang, X. M., King, J., Song, C. H., Dai, S. & Miao, Y. F. 2007: High-resolution magnetostratigraphy of the Neogene Huaitoutala section in the eastern Qaidam Basin on the NE Tibetan Plateau, Qinghai Province, China and its implication on tectonic uplift of the NE Tibetan Plateau. *Earth Planetary Science Letters 258*, 293-306.

Fægri, K. & Iversen, J. 1989: *Textbook of Pollen Analysis, 328 pp*. John Wiley &Sons, New York.

Fedorov, G., Nolan, M., Brigham-Grette, J., Bolshiyanov, D., Schwamborn, G. & Juschus, O. 2013: Preliminary estimation of Lake El'gygytgyn water balance and sediment income. *Climate of the Past 9*, 1455-1465.

Francke, A., Wennrich, V., Sauerbrey, M., Juschus, O., Melles, M. & Brigham-Grette, J. 2013: Multivariate statistic and time series analysis of grain-size data in quaternary sediments of Lake El'gygytgyn, NE Russia. *Climate of the Past 9*, 2459-2470.

Guo, Z. T., Ruddiman, M. F., Hao, Q. Z., Wu, H. B., Qiao, Y. S., Zhu, R. X., Peng, S. Z., Wei, J. J., Yuan, B. Y. & Liu, T. S. 2002: Onset of Asian desertification by 22 Myr ago inferred from loess deposits in China. *Nature 416*, 159-163.

Han, W. X., Fang, X. M., Ye, C. C., Teng, X. H. & Zhang, T. 2014: Tibet forcing Quaternary stepwise enhancement of westerly jet and central Asian aridification: carbonate isotope records from deep drilling in the Qaidam salt playa, NE Tibet. *Global and Planetary Change 116*, 68-75.

Head, M. J. & Gibbard, P. L. 2005: Early-Middle Pleistocene transitions: the land-ocean evidence. Geological Society of London, Special Publication 247, 326 pp.

Joannin, S., Bassinot, F., Nebout, N. C., Pezron, O. & Beaudouin, C. 2011: Vegetation response to obliquity and precession forcing during the Mid-Pleistocene Transition in western Mediterranean region (ODP site 976). *Quaternary Science Reviews 30*, 280-297.

Kaplan, J. O. 2001: *Geophysical Applications of Vegetation Modelling, 113 pp.* Ph.D. dissertation, Lund University, Lund.

Khursevich, G. K., Prokopenko, A. A., Fedenya, S. A., Tkachenko, L. I. & Williams, D. F. 2005: Diatom biostratigraphy of Lake Baikal during the past 1.25 Ma: new results from BDP-96-2 and BDP-99 drill cores. *Quaternary International 136*, 95-104.

Kozhevnikov, Y. P. 1993: Vascular plants near El'gygytgyn Lake. In Belyi, V. F. & Chereshnev, I. A. (eds): *Natural Depression El'gygytgyn Lake (problems of study and protection), 62-82 pp*. NERSRI FEB RAS, Magadan (in Russian).

Kukla, G. & An, Z. S. 1989: Loess stratigraphy in central China. *Palaeogeography, Palaeoclimatology, Palaeoecology 72*, 203-225.

Kupriyanova, L. A. & Alyoshina, L. A. 1972: *Pollen and Spores of Plants from the Flora of European Part of USSR, vol. I., I-171 pp.* Academy of Sciences USSR, Komarov Botanical Institute, Leningrad.

Laskar, J., Robutel, R., Joutel, F., Gastineau, M., Correia, A. C. M. & Levrand, B. 2004: A long term numerical solution for the insolation quantities of the Earth. *Astronomy and Astrophysics 428*, 261-285.

Layer, P. 2000: Argon-40/argon-39 age of the El'gygytgyn impact event, Chukotka, Russia. *Meteoritics & Planetary Science 35*, 591-599.

Li, Q., Wang, P., Zhao, Q., Tian, J., Chen, X. & Jian, Z. 2008: Paleoceanography of the mid-Pleistocene South China Sea. *Quaternary Science Reviews 27*, 1217-1233.

Li, J. J. 1995: *Uplift of Qinghai–Xizang (Tibet) Plateau and Global Change, 207 pp*. Lanzhou University Press, Lanzhou.

Lisiecki, L. E. & Raymo M. E. 2005: A Pliocene-Pleistocene stack of 57 globally distributed benthic $\delta^{18}O$ records. *Paleoceanography 20*, PA1003, doi/10.1029/2004PA001071.

Lourens, L. J., Hilgen, F. J., Gudjonsson, L. & Zachariasse, W. J. 1992: Late Pliocene to Early Pleistocene astronomically forced sea surface productivity and temperature variations in the Mediterranean. *Marine Micropaleontology 19*, 49-78.

Lozhkin, A. V., Anderson, P. M., Matrosova, T. V. & Minyuk, P. S. 2007: The pollen record from El'gygytgyn Lake: implications for vegetation and climate histories of northern Chukotka since the late middle Pleistocene. *Journal of Paleolimnology 37*, 135-153.

Lozhkin, A. V. & Anderson, P. M. 2013: Vegetation responses to interglacial warming in the Arctic: examples from Lake El'gygytgyn, Far East Russian Arctic. *Climate of the Past 9*, 1211-1219.

Lozhkin, A. V., Anderson, P. M., Minyuk, P. S. & Nedorubova. E. Yu. 2016: Changes in biocenoses in the eastern Arctic 374-917 thousand years BP (palynological data from Lake El'gygytgyn). *Vestnik SVNTs DVO RAN 2*, 3-9 (in Russian).

Maasch, K. 1988: Statistical detection of the mid-Pleistocene transition. *Climate Dynamics 2*, 133-143.

Maslin, M. A. & Ridgwell, A. J. 2005: Mid-Pleistocene revolution and the 'eccentricity myth'. In Head, M. J. & Gibbard, P. L. (eds.), *Early-Middle Pleistocene Transitions: The Land-Ocean Evidence, 19-34 pp.* Geological Society of London Special Publication 247.

Matheus, P., Begét, J., Mason, O. & Gelvin-Reymiller, C. 2003: Late Pliocene to Late Pleistocene environments preserved at the Palisades Site, central Yukon River, Alaska. *Quaternary Research 60*, 33-43.

Medina-Elizalde, M. & Lea, D. W. 2005: The mid-Pleistocene transition in the tropical Pacific. *Science 310*, 1009-1012.

Melles, M., Brigham-Grette, J., Minyuk, P., Koeberl, C., Andreev, A., Cook, T., Fedorov, G., Gebhardt, C., Haltia-Hovi, E., Kukkonen, M., Nowaczyk, N., Schwamborn, G., Wennrich, V. & El'gygytgyn

Scientific Party 2011: The El'gygytgyn Scientific Drilling Project - conquering Arctic challenges through continental drilling. *Scientific Drilling 11*, 29-40.

Melles, M., Brigham-Grette, J., Minyuk, P.S., Nowaczyk, N.R., Wennrich, V., DeConto, R.M., Anderson, P.M., Andreev, A., Coletti, A., Cook, T., Haltia-Hovi, E., Kukkonen, M., Lozhkin, A.V., Rosén, P., Tarasov, P., Vogel, H. & Wagner, B. 2012: 2.8 Million Years of Arctic Climate Change from Lake El'gygytgyn, NE Russia. *Science 337*, 315-320.

Nolan, M. & Brigham-Grette, J. 2007: Basic hydrology, limnology, and meteorology of modern Lake El'gygytgyn, Siberia. *Journal of Paleolimnology 37*, 17-35.

Nowaczyk, N. R., Haltia, E. M., Ulbricht, D., Wennrich, V., Sauerbrey, M. A., Rosén, P., Vogel, H., Francke, A., Meyer-Jacob, C., Andreev, A. A. & Lozhkin, A. V. 2013: Chronology of Lake El'gygytgyn sediments-a combined magnetostratigraphic, palaeoclimatic and orbital tuning study based on multi-parameter analyses. *Climate of the Past 9*, 2413-2432.

Prentice, I. C., Cramer, W., Harrison, S. P., Leemans, R., Monserud, R. A. & Solomon, A. M. 1992: A global biome model based on plant physiology and dominance, soil properties and climate. *Journal of Biogeography 19*, 117-134.

Prentice, I. C., Guiot, J., Huntley, B., Jolly, D. & Cheddadi, R. 1996: Reconstructing biomes from palaeoecological data: a general method and its application to European pollen data at 0 and 6 ka. *Climate Dynamics 12*, 185-194.

Prokopenko, A. A., Hinnov, L. A., Williams, D. F. & Kuzmin, M. I. 2006: Orbital forcing of continental climate during the Pleistocene: a complete astronomically tuned climatic record from Lake Baikal, SE Siberia. *Quaternary Science Reviews 25*, 3431-3457.

Raymo, M. E., Oppo, D. W. & Curry, W. 1997: The mid-Pleistocene climate transition: a deep sea carbon isotopic perspective. *Paleoceanography 12*, 546-559.

Reille, M. 1992: *Pollen et Spores d'Europe et d'Afrique du Nord,1-543 pp*. Laboratoire de Botanique Historique et Palynologie, Marseille.

Reille, M. 1995: *Pollen et Spores d'Europe et d'Afrique du Nord, supplement 1, 1-331 pp*. Laboratoire de Botanique Historique et Palynologie, Marseille.

Reille, M. 1998: *Pollen et Spores d'Europe et d'Afrique du Nord, supplement 2, 1-327 pp*. Laboratoire de Botanique Historique et Palynologie, Marseille.

Rial, J. A. 2004: Earth's orbital eccentricity and the rhythm of the Pleistocene ice ages: the concealed pacemaker. *Global and Planetary Change 41*, 81-93.

Ruddiman, W. F. & Kutzbach, J. E., 1989: Forcing of the late Cenozoic uplift northern hemisphere climate by plateau uplift in the Southern Asia and American West. *Journal of Geophysical Research 94*, 18409-18427.

Schefuβ, E., Schouten, S., Jansen, J. H. F. & Sinninghe Damsté, J. S. 2003: African vegetation controlled by tropical sea surface temperatures in the mid-Pleistocene period. *Nature 422*, 418-421.

Schmieder, F., von Dobeneck, T. & Bleil, U. 2000: The Mid-Pleistocene climate transition as documented in the deep South Atlantic Ocean: initiation, interim state and terminal event. *Earth and Planetary Science Letters 179*, 539-549.

Schwamborn, G., Fedorov, G., Ostanin, N., Schirrmeister, L., Andreev, A. & the El'gygytgyn Scientific Party 2012: Depositional dynamics in the El'gygytgyn Crater margin: implications for the 3.6 Ma old sediment archive. *Climate of the Past 8*, 1897-1911.

Snyder, J. A., Cherepanova, M. V. & Bryan, A. 2013: Dynamic diatom response to changing climate 0-1.2 Ma at Lake El'gygytgyn, Far East Russian Arctic. *Climate of the Past 9*, 1309-1319.

Stockmarr, J. 1971: Tablets with spores used in absolute pollen analysis. *Pollen Spores 13*, 615-621.

Sun, X., Luo, Y., Huang, F., Tian, J. & Wang, P. 2003: Deep-sea pollen from the South China Sea: Pleistocene indicators of East Asian monsoon. *Marine Geology 201*, 97-118.

Swann, G. E. A., Leng, M. J., Juschus, O., Melles, M., Brigham-Grette, J. & Sloane, H. j. 2010: A combined oxygen and silicon diatom isotope record of Late Quaternary change in Lake El'gygytgyn, North East Siberia. *Quaternary Science Reviews 29*, 774-786.

Tarasov, P. E., Webb III, T., Andreev, A. A., Afanas'eva, N. B., Berezina, N. A., Bezusko, L. G., Blyakharchuk, T. A., Bolikhovskaya, N. S., Cheddadi, R., Chernavskaya, M. M., Chernova, G. M., Dorofeyuk, N. I., Dirksen, V. G., Elina, G. A., Filimonova, L. V., Glebov, F. Z., Guiot, J., Gunova, V. S., Harrison, S. P., Jolly, D., Khomutova, V. I., Kvavadze, E. V., Osipova, I. M., Panova, N. K., Prentice, I. C., Saarse, L., Sevastyanov, D. V., Volkova, V. S. & Zernitskaya, V. P. 1998: Present-day and mid-Holocene biomes reconstructed from pollen and plant macrofossil data from the former Soviet Union and Mongolia. *Journal of Biogeography 25*, 1029-1053.

Tarasov, P. E., Volkova, V. S., Webb III, T., Guiot, J., Andreev, A. A., Bezusko, L. G., Bezusko, T. V., Bykova, G. V., Dorofeyuk, N. I., Kvavadze, E. V., Osipova, I. M., Panova, N. K. & Sevastyanov, D.V. 2000: Last Glacial Maximum biomes reconstructed from pollen and plant macrofossil data from Northern Eurasia. *Journal of Biogeography 27*, 609-620.

Tarasov, P. E., Andreev, A. A., Anderson, P. M., Lozhkin, A. ., Leipe, C., Haltia, E., Nowaczyk, N. R., Wennrich, V., Brigham-Grette, J. & Melles, M. 2013: A pollen-based biome reconstruction over the last 3.562 million years in the East Russia Arctic–new insights into climate – vegetation relationships at the regional scale. *Climate of the Past 9*, 2759-2775.

Torrence, C. & Compo, G. P. 1998: A practical guide to wavelet analysis. *Bulletin of the American Meteorological Society 7*9, 61-78.

Tzedakis, P. C., Hooghiemstra, H. & Pälike, H. 2006: The last 1.35 million years at Tenaghi Philippon: revised chronostratigraphy and long-term vegetation trends. *Quaternary Science Reviews 25*, 3416-3430.

Van den Bogaard, C., Jensen, B. J. L., Pearce, N. J. G., Froese, D. G., Portnyagin, M. V., Ponomareva, V. V. & Wennrich, V. 2014: Volcanic ash layers in Lake El'gygytgyn: eight new regionally significant chronostratigraphic markers for western Beringia. *Climate of the Past 10*, 1041-1062.

Van Geel, B. 2001: Non-pollen palynomorphs, in Smol, J. P., Birks, H. J. B., Last, W. M., Bradley, R. S., & Alverson, K., Kluwer (eds): *Tracking environmental change using lake sediments. Volume 3: Terrestrial, algal and silicaceous indicators 99-119 pp*. Kluwer, Dordrecht.

Wardle, D. A., Walker, L. R. & Bardgett, R. D. 2004: Ecosystem properties and forest decline in contrasting long-term chronosequences. *Science 305*, 509-513.

Wennrich, V., Minyuk, P. S., Borkhodoev, V., Francke, A., Ritter, B., Nowaczyk, N. R., Sauerbrey, M. A., Brigham-Grette, J. & Melles, M. 2014: Pliocene to Pleistocene climate and environmental history of Lake El'gygytgyn, Far East Russian Arctic, based on high-resolution inorganic geochemistry data. *Climate of the Past 10*, 1381-1399.

Wennrich, V., Andreev, A. A., Tarasov, P. E., Fedorov, G., Zhao, W. W., Gebhardt, C. A., Meyer-Jacob, C., Snyder, J. A., Nowaczyk, N. R., Chapligin, B., Anderson, P. M., Lozhkin, A. V., Minyuk, P. S., Koeberl, C. & Melles, M. 2016: Impact processes, permafrost dynamics, and climate and environmental variability in the terrestrial Arctic as inferred from the unique 3.6 Myr record of Lake El'gygytgyn, Far East Russia - a review. *Quaternary Science Reviews 147*, 221-244.

Westgate, J. A., Stemper, B. A. & Pewe, T. L. 1990: A 3 m.y. record of Pliocene-Pleistocene loess in interior Alaska. *Geology 18*, 858-861.

Wu, F. L., Fang, X. M., Ma, Y. Z., Mark, H., Volker, M., An, Z. S. & Miao, Y. F. 2007: Plio-Quaternary stepwise drying of Asia: evidence from a 3-Ma pollen record from the Chinese Loess Plateau. *Earth Planetary Science Letters 257*, 160-169.

Yoshino, M. M. 1978: *Climate Change and Food Production, 331 pp*. University of Tokyo, Tokyo.

Zhao, W. W., Andreev, A. A., Wennrich, V., Tarasov, P. E., Anderson, P., Lozhkin, A. V. & Melles, M. 2015: The Réunion Subchron vegetation and climate history of the northeastern Russian Arctic inferred from the Lake El'gygytgyn pollen record. *Palaeogeography, Palaeoclimatology, Palaeoecology 436*, 167-177.

4 The penultimate interglacial vegetation and climate of the northeastern Russian Arctic inferred from the Lake El'gygytgyn pollen record

Abstract

We present a high-resolution pollen record from Lake El'gygytgyn, Northeast Siberia and analyze the dynamics of vegetation and climate between 240.5 and 181.5 ka (Marine Isotope Stage (MIS) 7.5-6.6). The penultimate interglacial vegetation was characterized by mixed herb and shrub (mainly alder and birch) dominated plant communities. Pollen-based biome reconstruction shows that the vegetation landscape was generally open due to the high affinity scores of the TUND (tundra) biome. The warm intervals (MIS 7.5, 7.3, and 7.1) were marked by an increase in the CLDE (cold deciduous forest) biome scores and a synchronous decrease in the STEP (cold steppe) biome scores. The climatic optimum occurred during MIS 7.1. It was marked by the highest CLDE biome scores and lasted ~10 ka, possibly favored by the high precession-related summer insolation and a legacy of the preceding mild stadial. In contrast, MIS 7.5 and 7.3 were characterized by shorter durations (~4 ka) and lower summer temperatures. The preceding cold glacial/stadial might have led to an extensive distribution of permafrost that further hindered subsequent vegetation development during warm intervals. The MIS 7.4 and 6.6 were cold and wet, triggered by low obliquity values and coevally low precession-related summer insolation. As a result, these periods were marked by a significantly reduced summer temperature and an enhanced snow-ice albedo feedback. This study provides potential scenarios for future climate pattern and allows a better understanding of the relationship between vegetation, climate, and external/internal forcings in the high latitudes.

Key words: Lake El'gygytgyn, Penultimate interglacial, MIS 7.4, MIS 6.6, pollen, ICDP, Northeast Russian Arctic

4.1 Introduction

The warm interglacial periods during the late Quaternary are considered potential analogs for the present climate conditions. Therefore, understanding the climate variabilities during past interglacials can provide valuable insights into the future. Despite the extensive studies on the last and present interglacial, the timing, duration, magnitude, and climatic mechanisms of the penultimate interglacial received much less attention (e.g. Kukla et al., 1997; Winograd et al., 1997; Tzedakis et al., 2004). Pollen data from terrestrial records (Tzedakis et al., 1997; de Beaulieu et al., 2001; Tzedakis et al., 2004), marine records (Desprat et al., 2006), and sea-level records (Dutton et al., 2009) show that the Marine Isotope Stage (MIS) 7 was marked by an alternation of five warm and cold periods. So far, ongoing debates are focused on the timing of the climatic optimum during MIS 7. On one hand, MIS 7.5 is considered as a climatic optimum as warm as the Holocene (de Beaulieu et al., 2001). On the other hand, the climate state of substage MIS 7.3 is argued to be similar as the MIS 7.5 (Tzedakis et al., 1997, 2004).

Compared to the warm substages of MIS 7, climate information concerning the cold intervals is inadequate. In Siberia, calculations of energy balance suggest that the maximum summer temperature reductions during the past 500 ka occurred during the MIS 7.4 and MIS 6.6, and the decrease was greater than MIS 4 and MIS 2 (Short et al., 1991). At Lake El'gygytgyn, multi-proxy analyses of lithology, biogeochemistry, inorganic geochemistry, and diatoms indicate the intervals of MIS 7.4 and MIS 6.6 were relatively cold and wet (Melles et al., 2007; Minyuk et al., 2014; Snyder et al., 2013).

Despite the ongoing discussions on the relationship between the climate and limnological conditions at Lake El'gygytgyn, little is known about the detailed history of regional vegetation between MIS 7.5 and MIS 6.6. Existing palynological records based on the cores PG 1351 and LZ 1024 from Lake El'gygytgyn cover the past 300 ka (Lozhkin et al., 2007). However, the temporal resolutions of these records were low and the characteristics of different warm/cold intervals were not sufficiently analyzed. In this study, high-resolution pollen data of the deep-drilled core 5011-1 from Lake El'gygytgyn are analyzed aiming: i) to reconstruct a detailed vegetation and environmental history of the Lake El'gygytgyn region between 240.5 and 181.5 ka, and ii) to discuss the possible mechanisms behind the climatic pattern and the influence of orbital and/or internal forcings in the Arctic region.

4.2 Regional setting

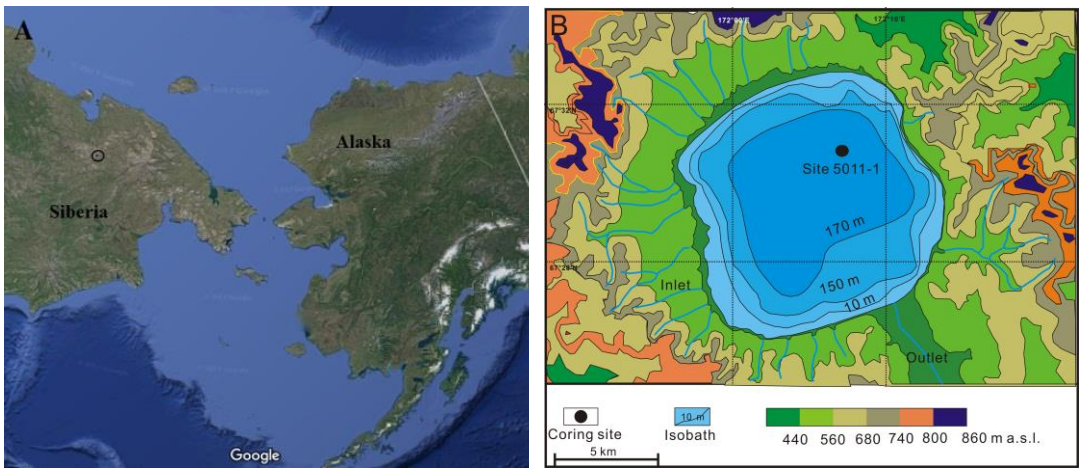

Fig. 4.1 Map of the study region. (A) Location of Lake El'gygytgyn marked by a circle. (B) Bathymetric map of Lake El'gygytgyn and topography of its catchment, after Swann et al. (2010). The drilling site 5011-1 is indicated as a black dot.

Lake El'gygytgyn is located ~100 km to the north of the Arctic Circle in Northeast Siberia (*c.* 67 °30'N, 172 °05'E; 492 m above sea level; Fig. 4.1). The 170-m deep and 12-km diametric lake currently covers an area of 110 km^2 within a 293-km^2 large catchment that is defined by the meteorite impact crater rim. The area is characterized by extremely harsh climate with a mean July temperature of 8 °C and a mean annual precipitation of 200 mm (Nolan and Brigham-Grette, 2007). As a result, the local vegetation is dominated by herb tundra. In protected habitats with more favorable climatic conditions, patches of dwarf shrubs occur (Andreev et al., 2012; Lozhkin and Anderson, 2013 and references therein). The surrounding upland vegetation is dominated by shrub-tundra with dwarf birch (*Betula exilis*), shrub alder (*Alnus fruticosa*), stone pine (*Pinus Haploxylon*), and different species of willow (*Salix*) and Ericales.

4.3 Material and methods

In spring 2009, the sediment cores retrieved at site 5011-1 in central Lake El'gygytgyn yielded a composite core of 318 m. The age/depth model applied in this study is according to Melles et al. (2012) and Nowaczyk et al. (2013).

Pollen subsamples of ~1.5 g were investigated between 8.13-12.41 m (181.5-240.5 ka) of the composite depth below the lake floor. The average temporal resolution is *c.* 1 ka. The samples

were processed following the standard HF technique (Fægri and Iversen, 1989) and by ultrasonic sieving to remove clay-sized particles. Generally, around 300 terrestrial pollen grains were counted for each sample. In the case of samples with extremely low pollen concentration, less than 50 terrestrial pollen grains were counted.

For biome reconstruction, the assignments of pollen taxa to respective biomes were made in accordance with the criteria presented by Tarasov et al. (2013; Table 4.1). Biome affinity scores (Fig. 4.3A) were calculated for each sample following the equation of Prentice et al. (1996). Landscape openness, which provides a qualitative assessment of changes in vegetation cover, was calculated by evaluating the difference between maximum forest biome scores and maximum open biome scores (for details see Tarasov et al., 2013).

Table 4.1 Terrestrial pollen taxa identified in the Lake El'gygytgyn sediments accumulated between 240.5 and 181.5 ka and their corresponding biomes (following Tarasov et al., 2013). Taxa, whose percentages in the biome-taxon matrix are <0.5% (threshold suggested by Prentice et al., 1996), and which do not influence the results of the biome reconstruction, are marked with an asterisk.

Biome	**Terrestrial pollen taxa**
TUND/Tundra	*Alnus fruticosa*-type (shrub), *Betula* sect. *Albae*-type (tree)*, *B.sect. Nanae*-type (shrub), *B.* undif, Cyperaceae, Ericales, Poaceae, Polemoniaceae, Polygonaceae, *Rubus chamaemorus*, *Salix*, Saxifragaceae, Valerianaceae
CLDE/Cold deciduous forest	*Alnus fruticosa*-type (shrub), *Betula* sect. *Albae*-type (tree)*, *B.* sect. *Nanae*-type (shrub), *B.* undif, Ericales, *Larix/Pseudotsuga*, *Pinus Haploxylon*, Pinaceae undif, *Rubus chamaemorus*, *Salix*
STEP/Cold steppe	*Artemisia*, Asteraceae, Asteraceae Cichorioideae*, Caryophyllaceae, *Cannabis*-type, Chenopodiaceae, Fabaceae, Lamiaceae, Onagraceae, Papaveraceae, Poaceae, Polygonaceae, Ranunculaceae, Rosaceae*, *Thalictrum*, Valerianaceae

4.4 Results

A total of 69 pollen, spore, and non-pollen-palynomorph types were identified in 65 samples. Eight of these samples were excluded from further analysis because they have extremely low pollen concentration. The most abundant pollen types are presented in Fig. 4.2. Pollen assemblage zones (PAZs) were subdivided by visual inspections of major changes in pollen assemblages and the presence/absence of indicator taxa.

Corresponding MIS boundaries according to Liesecki and Raymo (2005) are also shown in the pollen diagram. The investigated sediments of the composite core 5011-1 encompass the penultimate interglacial MIS 7 as well as MIS 6.6. The pollen assemblages are generally characterized by two vegetation types: (i) mixed shrub- and herb-dominated (PAZs-I, III, V, VII, and VIII) and (ii) herb-dominated (PAZs-II, IV, VI and IX). Besides, moderate amounts of *Pinus Haploxylon* pollen occur in PAZs-III, VII, and IX. The investigated interval is marked by three biome types including the CLDE, TUND and STEP biome. Characteristics of the pollen assemblage zones and reconstructed biomes are described in Table 4.2.

Table 4.2 Description of the pollen assemblage zones (PAZs) and the biomization result from sediments of Lake El'gygytgyn accumulated between 240.5-181.5 ka.

PAZs	Age (ka)	Characteristic pollen assemblage	Reconstructed biome
I	240.5-236.5	High *Betula* and Poaceae pollen contents; high amounts of *Sphagnum* and *Selaginella rupestris* spores	Lowest affinity scores of STEP biome; Predominance of TUND biome
II	236.5-230.5	A significant decrease in *Betula* pollen contents and an increase in herb pollen (particularly *Artemisia*); *Sphagnum* spore almost disappears	STEP scores abruptly increase; TUND remained the dominate biome type
III	230.5-225	A significant increase in *Betula* pollen and moderate amounts of *Pinus Haploxylon* and *Alnus* pollen; appearance of *Sordaria* fungi spores and the decrease in *Selaginella rupestris* spores	CLDE scores significantly increase but remain lower than STEP and TUND scores
IV	225-213.5	*Betula* pollen drastically decreases and *Pinus Haploxylon* pollen is almost absent, while Poaceae and *Artemisia* pollen increase; the presence of *Salix* and *Thalictrum* pollen in the upper part	STEP biome became the dominate type
V	213.5-209.5	An increase in *Betula*, *Alnus* and Ericales pollen contents and *Sphagnum* spores	CLDE scores gradually increase
VI	209.5-203	The disappearance of *Alnus* pollen and an increase in herb pollen contents	STEP became the dominate biome; CLDE scores drop markedly
VII	203-193	A remarkable increase in *Betula* and *Alnus* pollen percentages; high contents of *Sphagnum* spores occur in the part	CLD scores increase and exceed STEP, while TUND remains dominant
VIII	193-188	A gradual decrease in *Alnus* pollen and an increase in Poaceae, *Artemisia*, and Polygonaceae pollen as well as *Selaginella rupestris* spore contents.	CLDE and TUND scores gradually decrease, while STEP scores increase
IX	188-181.5	*Pinus Haploxylon* and *Alnus* pollen and *Sphagnum* spores are in small quantities.	STEP biome was the dominate type

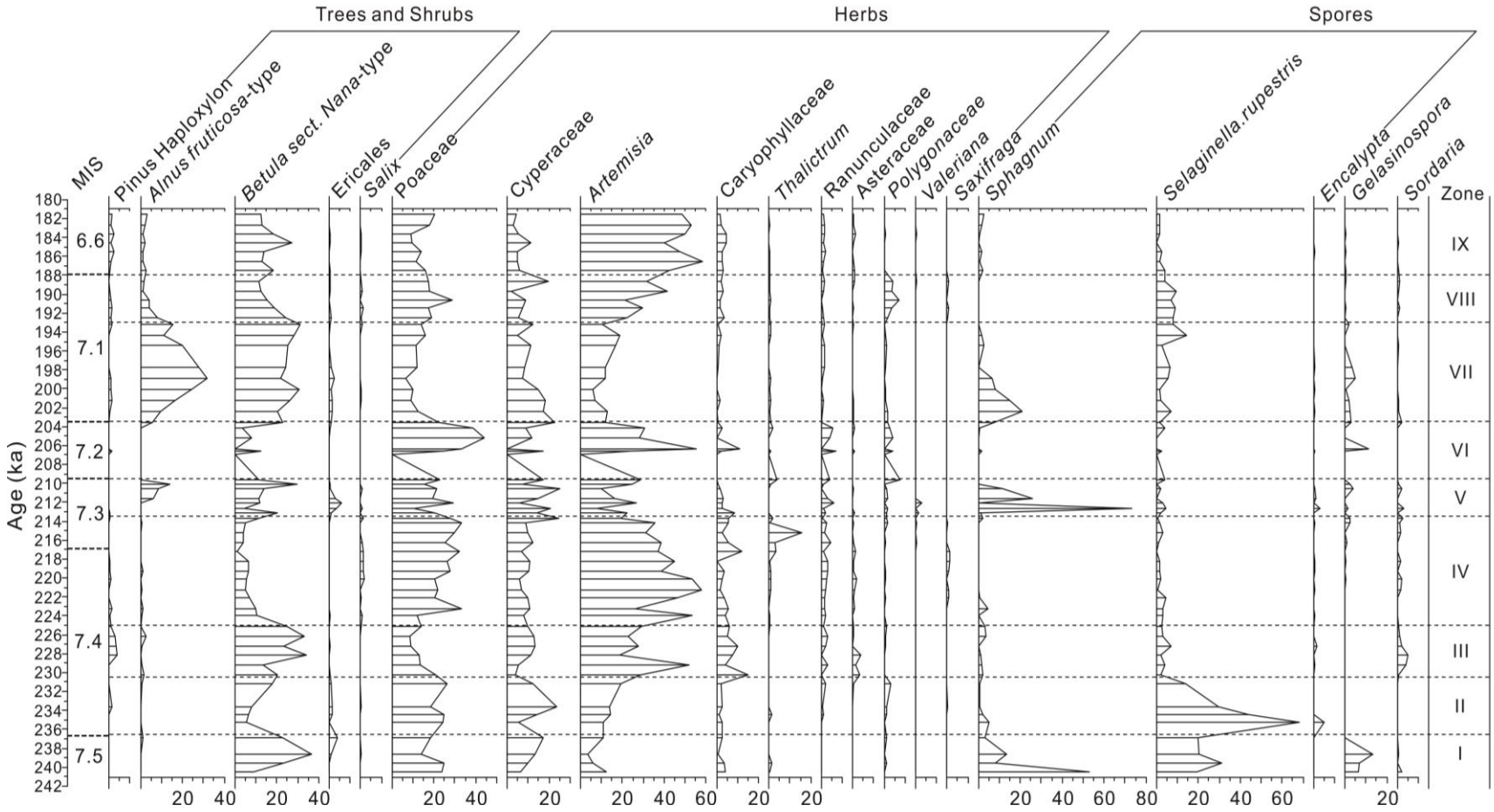

Fig. 4.2 Summary diagram showing percentages of major pollen, spore, fungal and algal taxa that accumulated between 240.5 and 181.5 ka in the Lake El'gygytgyn sediments.

4.5 Discussion and conclusion

4.5.1 Vegetational and climatic variability

The high percentages of *Betula* and Poaceae pollen in PAZ-I suggested that low shrub dwarf birch-herb tundra dominated the Lake El'gygytgyn area between 240.5 and 236.5 ka (Fig. 4.2). This period represents the entire MIS 7.5, because PAZ-I is parallel to the pollen zone E2 of the Lake El'gygytgyn PG 1351 record, which is dated back to 300 ka (back to MIS 8.4; Lozhkin et al., 2007). The low affinity scores of the STEP biome implied that generally moderate climatic conditions prevailed in the region (Fig. 4.3A). However, the decreasing amounts of *Sphagnum* spores and increasing *Selaginella rupestris* spores suggest a drying trend in the local habitats.

Between 236.5 and 230.5 ka (PAZ-II, lower MIS 7.4), the pollen spectra showed some decrease in dwarf birches and an expansion of graminoid communities, suggesting cold and dry climatic conditions. This interpretation is also supported by the biome reconstruction, which shows an increase in STEP scores and a decrease in CLDE and TUND scores. Peak percentages of *Selaginella* spores in this PAZ pointed to drier local conditions than the previous interval (Lozhkin et al., 2007). Hence, the shift between MIS 7.5/7.4 was characterized by a gradual climatic deterioration.

The notable increase of *Betula* pollen in PAZ-III (mid-MIS 7.4) as well as the slightly increased *Pinus Haploxylon* pollen suggested the expansion of shrubby communities in the lake vicinity, mirroring slightly ameliorated climatic conditions between 230.5 and 225 ka. In terms of biomization, the CLDE scores slightly increased but STEP biome remained dominant. The stone pines might have benefited from the insulating effects of sufficiently deep snow cover in the winter (Lozhkin et al., 2007). In addition, the plankton rareness (Snyder et al., 2013) and the absence of coarse material (Minyuk et al., 2014) of the El'gygytgyn Lake sediments indicated a significantly reduced light penetration and a declined delivery of materials into the lake. This is related to the snowcover blanketing the permanent lake ice, implying generally humid conditions in the area. High contents of coprophilous *Sordaria* fungal spores indirectly pointed to the presence of herbivores around the lake (Baker et al., 2013) and thus confirmed the occurrence of open habitats.

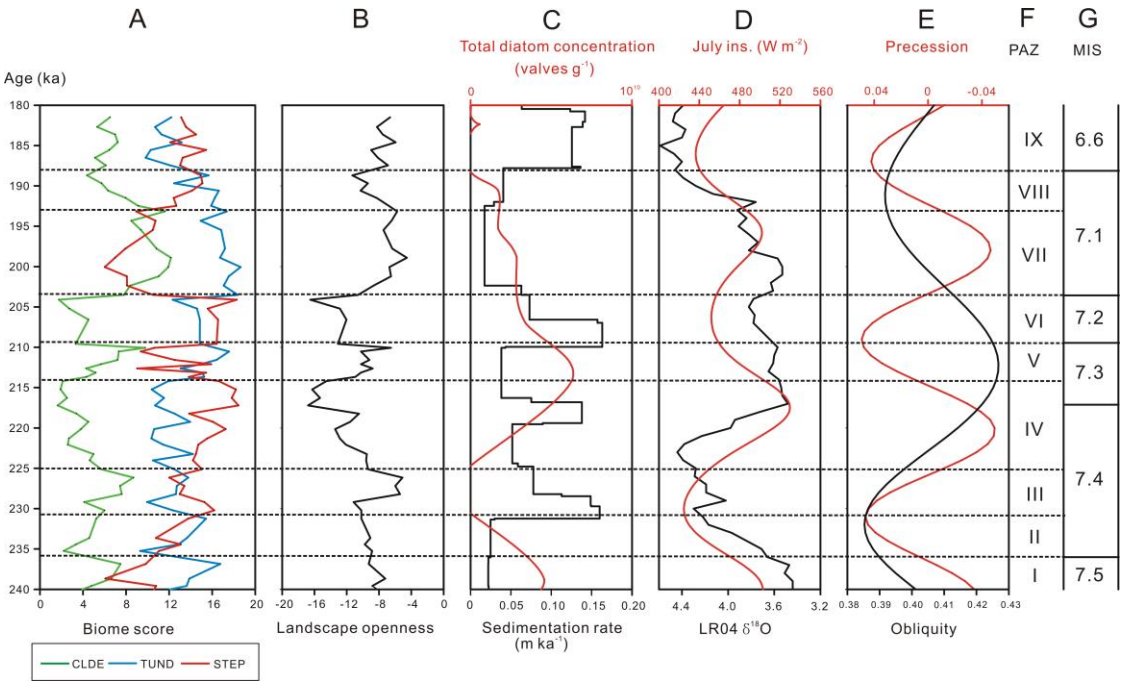

Fig. 4.3 Summary figure. A. Time series of individual biomes (biome names are abbreviated as follows: CLDE = cold deciduous forest; TUND = tundra; STEP = cold steppe). B. Qualitative characteristic of landscape openness reflected by the difference between the maximum score of forest biomes (MSFB) and the maximum score of open biomes (MSOB) at each level. C. Total diatom concentration (red line, Snyder et al., 2013) and sedimentation rate (black line). D. LR04 global marine isotope stacks (black line, Lisiecki & Raymo 2005) and mean July insolation for 67.5 ° N (red line, Laskar et al., 2004). E. Precession curve (red line) and obliquity curve (black line), after Laskar et al. (2004). F. pollen assemblage zones (PAZs) according to Fig. 4.2. G. Marine Isotope Stages (MIS) according to Lisiecki & Raymo (2005).

In PAZ-IV (upper MIS 7.4, 225-213.5 ka), the pollen spectra suggested that vegetation near Lake El'gygytgyn was predominantly herb tundra, with some patches of dwarf birches and shrub willows growing in protected habitats (e.g. creeks and river valleys). The reduced affinity scores of CLDE biome also indicated that effective moisture was lacking for the growth of woody taxa. The concomitant numerous diatom shells (Snyder et al., 2013) in Lake El'gygytgyn implied the decline of permanent snow cover in summer.

Between 213.5 and 209.5 ka (PAZ-V, upper MIS 7.3), the environmental condition ameliorated as reflected by the high percentages of *Alnus*, *Betula* and Ericales pollen representing the expansion of shrub components. The increased CLDE scores and decreased STEP scores further suggested a climatic amelioration. The remarkable increase in *Sphagnum* spores pointed to the presence of wet swampy habitats around the Lake (Kozhevnikov, 1993).

Between 209.5 and 203 ka (PAZ-VI, MIS 7.2), dwarf shrubs (birches and alder) decreased in the region, while simultaneous increases in herb pollen suggested an expansion of open

steppe vegetation and cold and dry climate conditions. The abrupt decrease in the CLDE scores and landscape openness provide further evidence to a climatic deterioration.

High contents of *Betula* and *Alnus* pollen accumulated in the sediments between 203 and 196 ka (PAZ-VII). It suggested the presence of dwarf birches and shrub alder in the region and favorable climatic conditions during MIS 7.1. The TUND biome was in predominance but CLDE biome had high affinity scores as well. The comparatively dense vegetation cover led to less soil erosion and mud flows, probably resulting in the low sedimentation rate (*c.* 2.5 cm yr^{-1}) during this time interval.

Since the late MIS 7 (196-188 ka, PAZ-VIII), a tendency of climatic deterioration was evident as indicated by the decreasing significance of shrubby components in the landscape and corresponding increases in herb pollen. This shift is also obvious in the biomization results which show a decrease in CLDE and TUND affinity scores. These changes implied a gradual cooling towards the MIS 6. *Artemisia* pollen and *Selaginella rupestris* spores notably increased reflecting a broader distribution of dry habitats in the lake vicinity. The transition from the penultimate interglacial to the penultimate glacial was also marked by the start of an increase in sedimentation rate in Lake El'gygytgyn (Fig. 4.3C). It was probably due to aggravated soil erosion induced by a vegetation cover decline (Zhao et al., 2015).

Between 188 and 181.5 ka (PAZ-IX, MIS 6.6), the pollen spectra were similar to that of PAZ-III (mid-MIS 7.4) showing graminoid tundra dominated the landscape, although slightly higher *Artemisia* pollen percentages in PAZ-IX indicated marginally drier conditions. The STEP biome had the highest affinity scores and was the dominant vegetation type. Small amounts of *Pinus Haploxylon* pollen suggested the presence of a thick snow cover in the winter that protected pines from desiccation. The similarity between MIS 7.4 and MIS 6.6 also lies in the remarkably low diatom concentration in lake sediments, reflecting the coverage of thick snow over permanent lake ice in the summertime (Snyder et al., 2013).

4.5.2 Climate variability and astronomical configurations

Previous studies show that vegetation successions in the Arctic were unambiguously linked to the astronomical configurations (Zhao et al., 2015, 2017). The evidence show that nearly simultaneous highs of obliquity and precession-related summer insolation triggered the onset of interglaciation and forest expansions (e.g. MIS 5.5 and MIS 31). In contrast, inverse orbital

configurations corresponded to the increases of herbaceous components in the regional vegetation, marking the end of an interglaciation (e.g. MIS 5.4). For the period between MIS 7.5 and MIS 6.6, a close association between vegetation successions and the orbital parameters can be observed as well (Fig. 4.3).

4.5.2.1 The warm intervals of MIS 7

The vegetation landscape in the Northeast Siberia was consistently open between MIS 7.5 and MIS 6.6 (240.5-181.5 ka), due to the stable and high affinity scores of the TUND biome. The warm stages (MIS 7.5, 7.3 and 7.1) were generally marked by increased CLDE biome scores and synchronously decreased STEP biome scores. Nevertheless, the CLDE biome scores were consistently lower than that of the MIS 5.5 and the postglacial thermal maximum (PGTM; Tarasov et al., 2013). It suggests that the climate conditions of MIS 7 warm intervals were comparatively harsh, which agrees with the result of the Lake El'gygytgyn PG 1351 pollen record (Lozhkin et al., 2007).

All the MIS 7 warm intervals coincided with the periods when the obliquity showed a decreasing trend. However, different conditions of precession-related summer insolation marked each interval. The MIS 7.5 was characterized by the synchronous decreasing trend of obliquity and precession-related summer insolation. The MIS 7.3 (~4 ka duration) was coincident with the interval of high obliquity values and low precession-relation summer insolation. The MIS 7.1 had a similar orbital configuration as the MIS 7.5 (~4 ka duration), but lasted much longer (~10 ka) and involved a long period of high precession-relation summer insolation. The orbital configurations of these warm stages were reflected by the differences in vegetation and climate dynamics.

The MIS 7.1 is the most prominent in terms of its long duration and relatively high CLDE biome scores (8.39-12.18), as compared to the MIS 7.3 (4.29-9.78) and MIS 7.5 (4.79-7.49). This feature is also expressed by remarkably high contents of alder pollen, suggesting the MIS 7 climatic optimum in the northern Siberia occurred at the stage MIS 7.1. This conclusion disagrees with the pollen results from southern Europe indicating that MIS 7.5 and MIS 7.3 were the most climatically favorable intervals as marked by the pronounced spread of tree populations (Tzedakis et al., 2004). Moreover, a recent palynological study in the Near East suggests that the highest proportions of temperate trees occurred during MIS 7.3 (Pickarski and Litt, 2017; Fig. 4.4B).

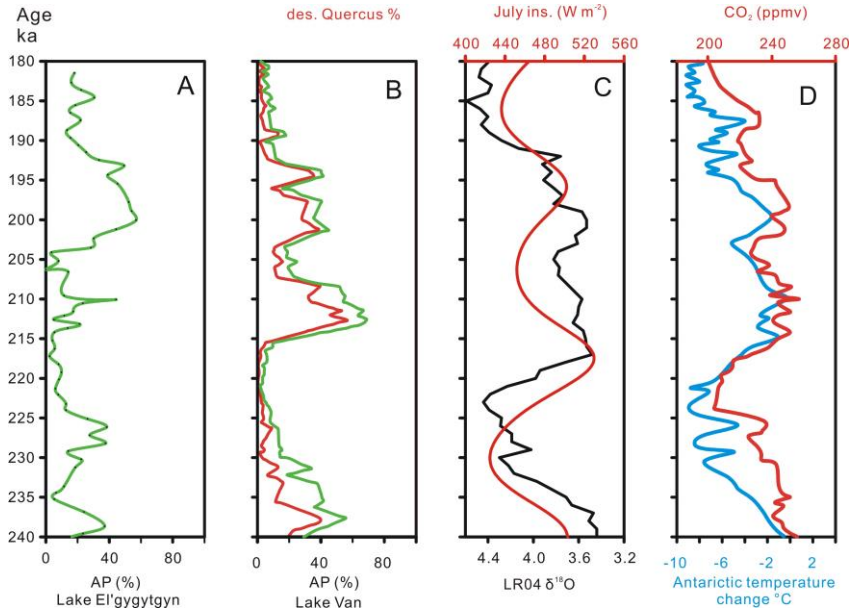

Fig. 4.4 Summary figure. A. Arboreal pollen percentages (AP) from Lake El'gygytgyn 5011-1 sediments. B. Percentages of AP (green line) and deciduous *Quercus* (red line) from Lake Van pollen record (Pickarski and Litt, 2017). C. LR04 global marine isotope stacks (black line, Lisiecki & Raymo, 2005) and mean July insolation for 67.5 ° N (red line, Laskar et al., 2004). D. Compiled Antarctic ice-core CO_2 (red line, Lüthi et al., 2008) and EPICA Dome C temperature record (blue line, Jouzel et al., 2007).

In the Northeast Siberia, the presence of climatic optimum at stage MIS 7.1 can be alternatively explained by the legacies of glacials/stadials on subsequent warm intervals. Based on multivariate analyses of pollen data from Lake El'gygytgyn 5011-1 sediments, Herzschuh et al. (2016) indicate that mild glacials led to the proximity of arboreal refugia to the investigated site as well as labilization of the permafrost. Indeed, the MIS 7.2 was short-lived and mild according to the record of sea level (Dutton et al., 2009) and the marine isotope stack LR04 (Lisecki and Raymo, 2005; Fig. 4.4C). Consequently, the subsequent MIS 7.1 was exceptionally long and warm under favorable orbital configurations.

The MIS 7.5 and 7.3 share strong similarities in terms of pollen spectra and biome distributions, as well as a preceding long and cold glacial/stadial (MIS 8 and MIS 7.4, respectively; Lozhkin et al., 2007) imposing on the development of trees and shrubs. In particular, the MIS 7.4 stadial was dinstinctive by the large magnitude of ice-sheet that approached the extent of a glacial period (Huybers and Wunsch, 2005). As a result, the widespread and deep permafrost was stabilized and required millennia for the active layer to respond to summer insolation maxima (Herzschuh et al., 2016). This might explain the late onset of increases in CLDE biome scores (~213.5 ka) during MIS 7.3 (~216-209.5 ka), which is in line with the lag of peak CO_2 concentrations (Lüthi et al., 2008) and peak Antarctic temperatures (Jouzel et al., 2007) following the onset of deglaciation (Fig. 4.4C, D).

4.5.2.2 The cold but wet MIS 7.4 and MIS 6.6

Multi-proxy analyses of lithology, biogeochemistry (Melles et al., 2007), inorganic geochemistry (Minyuk et al., 2014), and diatoms (Cherepanova et al., 2007; Snyder et al., 2013) based on the Lake El'gygytgyn 5011-1 sediments indicate pronouncedly cold and wet conditions during MIS 7.4 and 6.6. This climate regime pointed to a temperature reduction and a source of sustainable atmospheric moisture.

In the Northeast Siberia, the moisture is mainly brought by the westerlies from the warm surface of the North Altantic. During cold and wet glacial intervals, however, the westerlies was probably not the moisture source due to a >3000 km distance of Lake El'gygytgyn to the eastern margin of the Eurasian Ice Sheet (Melles et al., 2007). At the onset of mid-MIS 7.4 (PAZ-II) and MIS 6.6, the extent of ice-sheet rapidly reached maximum when minimum precession-related summer insolation nearly coincided with the lowest obliquity values (Fig. 4.3D, E), resulting in extremely low summer temperatures. Hence, a possible explanation might be that the cold airs in the East Siberia acted as a "cryogenic pump" drawing moisture from coastal Arctic seas to Northeast Siberia, so that large glaciations initiated. This mechanism was first proposed based on a Lake Baikal sedimentary record and was suggested to have existed throughout the late Pleistocene (Karabanov et al., 1998). In turn, the increased snowfall and continuously augmented snowfields would lead to a stronger snow- and ice-albedo feedback that can cause further summer termperature reductions (Milankovitch, 1941). The deep snowcover and its insulating effects during mid-MIS 7.4 and MIS 6.6 probably accounted for the survival of *Pinus Haploxylon* (Fig. 4.2).

***Acknowledgements*.** This study was funded by the China Scholarship Council (CSC) Ph.D. Scholarship to WWZ. Financial support for the palynological analyses was provided by the BMBF (grant 03G0642) and the German Research Foundation (DFG; grant ME 1169/24). The work of AA was performed also under the auspice of the Russian Government Program of Competitive Growth of Kazan Federal University.

4.6 References

Andreev, A.A., Morozova, E., Fedorov, G., Schirrmeister, L., Bobrov, A.A., Kienast, F., Schwamborn, G., 2012. Vegetation history of central Chukotka deduced from permafrost paleoenvironmental records of the El'gygytgyn Impact Crater. Climate of the past 8, 1287-1300.

Andreev, A.A., Tarasov, P.E., Wennrich, V., Melles, M., 2016. Millennial-scale vegetation changes in the north-eastern Russian Arctic during the Pliocene/Pleistocene transition (2.7–2.5 Ma) inferred from the pollen record of Lake El'gygytgyn. Quaternary Science Reviews 147, 245-268.

Baker, A.G., Bhagwar, S., Willis, K.J., 2013. Do dung fungal spores make a good proxy for past distribution of large herbivores? Quaternary Science Reviews 62, 21-31.

Cherapanova, M.V., Snyder, J.A., Brigham-Grette, J., 2007. Diatom stratigraphy of the last 250 ka at Lake El'gygytgyn, northeast Siberia. Journal of Paleolimnology 37, 155-162.

de Beaulieu, J.L., Andrieu-Ponel, V., Reille, M., Grüger, E., Tzedakis, P.C., Svobodova, H., 2001. An attempt at correlation between the Velay pollen sequence and the Middle Pleistocene stratigraphy from central Europe. Quaternary Science Reviews 20, 1593-1602.

Desprat, S., Goni, S.M.F., Turon, J.L., Duprat, J., Malaize, B., Peypouquet, J.P., 2006. Climatic variability of Marine Isotope Stage 7: direct land-sea-ice correlation from a multiproxy analysis of a north-western Iberian margin deep-sea core. Quaternary Science Reviews 25, 1010-1026.

Dutton, A., Bard, E., Antonioli, F., Esat, T. M., Lambeck, K., McCulloch, M. T., May 2009. Phasing and amplitude of sea-level and climate change during the penultimate interglacial. Nature Geoscience 2, 355-359.

Fægri, K., Iversen, J., 1989. Textbook of Pollen Analysis. fourth ed. John Wiley and Sons, London, UK.

Herzschuh, U., Birks, H.J.B., Laepple, T., Andreev, A.A., Melles, M., Brigham-Grette, J., 2016. Glacial legacies on interglacial vegetation at the Pliocene-Pleistocene transition in NE Asia. Nature DOI: 10.1038/ncomms11967.

Laskar, J., Robutel, R., Joutel, F., Gastineau, M., Correia, A.C.M., Levrand, B., 2004. A long term numerical solution for the insolation quantities of the Earth. Astron. Astrophys 428, 261-285.

Lisecki, L.E., Raymo M.E., 2005. A Pliocene-Pleistocene stack of 57 globally distributed benthic δ18O records. Paleoceanography 20, PA1003.

Lüthi, D., Le Floch, M., Bereiter, B., Blunier, T., Barnola, J.M., Siegenthaler, U., Raynaud, D., Jouzel, J., Fischer, H., Kawamura, K., Stocker, T.F., 2008. High-resolution carbon dioxide concentration record 650, 000-800, 000 years before present. Nature 453, 379-382.

Lozhkin, A.V., Anderson, P.M., Matrosova, T.V., Minyuk, P.S., 2007. The pollen record from El'gygytgyn Lake: implications for vegetation and climate histories of northern Chukotka since the late middle Pleistocene. Journal of Paleolimnology 37, 135-153.

Lozhkin, A.V., Anderson, P.M., 2013. Vegetation responses to interglacial warming in the Arctic: examples from Lake El'gygytgyn, Far East Russian Arctic, Climate of the Past 9, 1211-1219.

Jouzel, J., Masson-Delmotte, V., Cattani, O., Dreyfus, G., Falourd, S., Hoffmann, G., Minster, B., Nouet, J., Barnola, J. M., Chappellaz, J., Fischer, H., Gallet, J. C., Johnsen, S., Leuenberger, M., Loulergue, L., Luethi, D., Oerter, H., Parrenin, F., Raisbeck, G., Raynaud, D., Schilt, A., Schwander, J., Selmo, E., Souchez, R., Spahni, R., Stauffer, B.,

Steffensen, J. P., Stenni, B., Stocker, T. F., Tison, J. L., Werner, M., Wolff, E. W., 2007. Orbital and millennial antarctic climate variability over the past 800,000 years. Science 317, 793-796.

Karabanov, E.B., Prokopenko, A.A., Williams, D.F., Colman, S.M., 1998. Evidence from Lake Baikal for Siberian Glaciation during Oxygen-Isotope Substage 5d. Quaternary Research 50, 46-55.

Kozhevnikov, Y.P. 1993: Vascular plants near El'gygytgyn Lake. In Belyi, V.F. & Chereshnev, I.A. (eds.): *Natural Depression El'gygytgyn Lake (Problems of Study and Protection)*, 62-82. NERSRI FEBRAS, Magadan (in Russian).

Kukla, G., McManus, J.F., Rousseau, D.D., Chuine, I., 1997. How long and how stable was the last interglacial? Quaternary Scienece Review 16, 605-612.

Melles, M., Brigham-Grette, J., Glushkova, O.Y., Minyuk, P.S., Nowaczyk, N.R, Hubberten, H.W., 2007. Sedimentary geochemistry of core PG1351 from Lake El'gygytgyn-a sensitive record of climate variability in the East Siberian Arctic during the past three glacial-interglacial cycles. Journal of Paleolimnology 37, 89-104.

Melles, M., Brigham-Grette, J., Minyuk, P.S., Nowaczyk, N.R., Wennrich, V., DeConto, R.M., Anderson, P.M., Andreev, A., Coletti, A., Cook, T., Haltia-Hovi, E., Kukkonen, Lozhkin, A.V., Rosén, P., Tarasov, P., Vogel, H., Wagner, B., 2012. 2.8 Million Years of Arctic Climate Change from Lake El'gygytgyn, NE Russia. Science 337, 315-320.

Milankovitch, M., 1941. Canon of insolation and the ice-age problem. Royal Serbian Academy, Special Publication NO. 1321941.

Minyuk, P.S., Borkhodoev, V.Y., Wennrich, V., 2014. Inorganic geochemistry data from Lake El'gygytgyn sediments: marine isotope stages 6-11. Climate of the Past 10, 467-485.

Nolan, M., Brigham-Grette, J., 2007. Basic hydrology, limnology, and meteorology of modern Lake El'gygytgyn, Siberia. Journal of Paleolimnology 37, 17-35.

Nowaczyk, N.R., Haltia, E.M., Ulbricht, D., Wennrich, V., Sauerbrey, M.A., Rosén, P., Vogel, H., Francke, A., Meyer-Jacob, C., Andreev, A.A., Lozhkin, A.V., 2013. Chronology of Lake El'gygytgyn sediments-a combined magnetostratigraphic, palaeoclimatic and orbital tuning study based on multi-parameter analyses. Climate of the Past 9, 2413-2432.

Pickarski, N., Litt, T., 2017. A new high-resolution pollen sequence at Lake Van, Turkey: insights into penultimate interglacial-glacial climate change on vegetation history. Climate of the Past 13, 689-710.

Prentice, I.C., Guiot, J., Huntley, B., Jolly, D., Cheddadi, R., 1996. Reconstructing biomes from palaeoecological data: a general method and its application to European pollen data at 0 and 6 ka, Climate Dynamics 12, 185-194.

Snyder, J.A., Cherepanova, M.V., Bryan, A., 2013. Dynamic diatom response to changing climate 0-1.2 Ma at Lake El'gygytgyn, Far East Russian Arctic. Climate of the Past 9, 1309-1319.

Short, D.A., Mengel, J.G., Crowley, T.J., Hyde, W.T., North, G.R., 1991. Filtering of Milankovitch cycles by Earth's Geography. Quaternary Research 35, 157-173.

Swann. G.E.A., Leng, M.J., Juschus, O., Melles, M., Brigham-Grette, J., Sloane, H.J., 2010. A combined oxygen and silicon diatom isotope record of Late Quaternary change in Lake El'gygytgyn, North East Siberia. Quaternary Science Reviews 29, 774-786.

Tarasov, P.E., Andreev, A.A., Anderson, P.M., Lozhkin, A.V., Leipe, C., Haltia, E., Nowaczyk, N.R., Wennrich, V., Brigham-Grette, J., Melles, M., 2013. A pollen-based biome reconstruction over the last 3.562 million years in the East Russia Arctic–new insights into climate – vegetation relationships at the regional scale. Climate of the Past 9, 2759-2775.

Tzedakis, P.C., Andrieu, V., de Beaulieu, J.L., Crowhurst, S., Follieri, M., Hooghiemstra, H., Magri, D., Reille, M., Sadori, L., Shackleton, N.J., Wijmstra, T.A., 1997. Comparison of terrestrial and marine records of changing climate of the last 500,000 years. Earth and Planetary Science Letters 150, 171-176.

Tzedakis, P.C., Roucoux, K.H., de Abreu, L., Shackleton, N.J., 2004. The Duration of Forest Stages in Southern Europe and Interglacial Climate Variability. Science 306, 2231-2235.

Winograd, I.J., Landwehr, J.M., Ludwig, K.P., Coplen, T.B., Riggs, A.C., 1997. Duration and structure of past four interglaciations. Quaternary Research 48, 141-154.

Zhao, W.W., Andreev, A.A., Wennrich, V., Tarasov, P.E., Anderson, P., Lozhkin, A.V., Melles, M., 2015. The Réunion Subchron vegetation and climate history of the northeastern Russian Arctic inferred from the Lake El'gygytgyn pollen record. Palaeogeography, Palaeoclimatology, Palaeoecology 436, 167-177.

Zhao, W.W., Tarasov, P.E., Lozhkin, A.V., Anderson, P., Andreev, A.A., Korzun, J.A., Melles, M., Nedorubova, E.Yu., 2017. High-latitude vegetation and climate changes during the Mid-Pleistocene Transition inferred from a palynological record from Lake El'gygytgyn, NE Russian Arctic. Boreas doi: 10. 1111/bor. 12262.

5 Synthesis and Discussion

5.1 Main results and conclusions

5.1.1 Arctic vegetation successions of glacial-interglacial cycles during the Quaternary

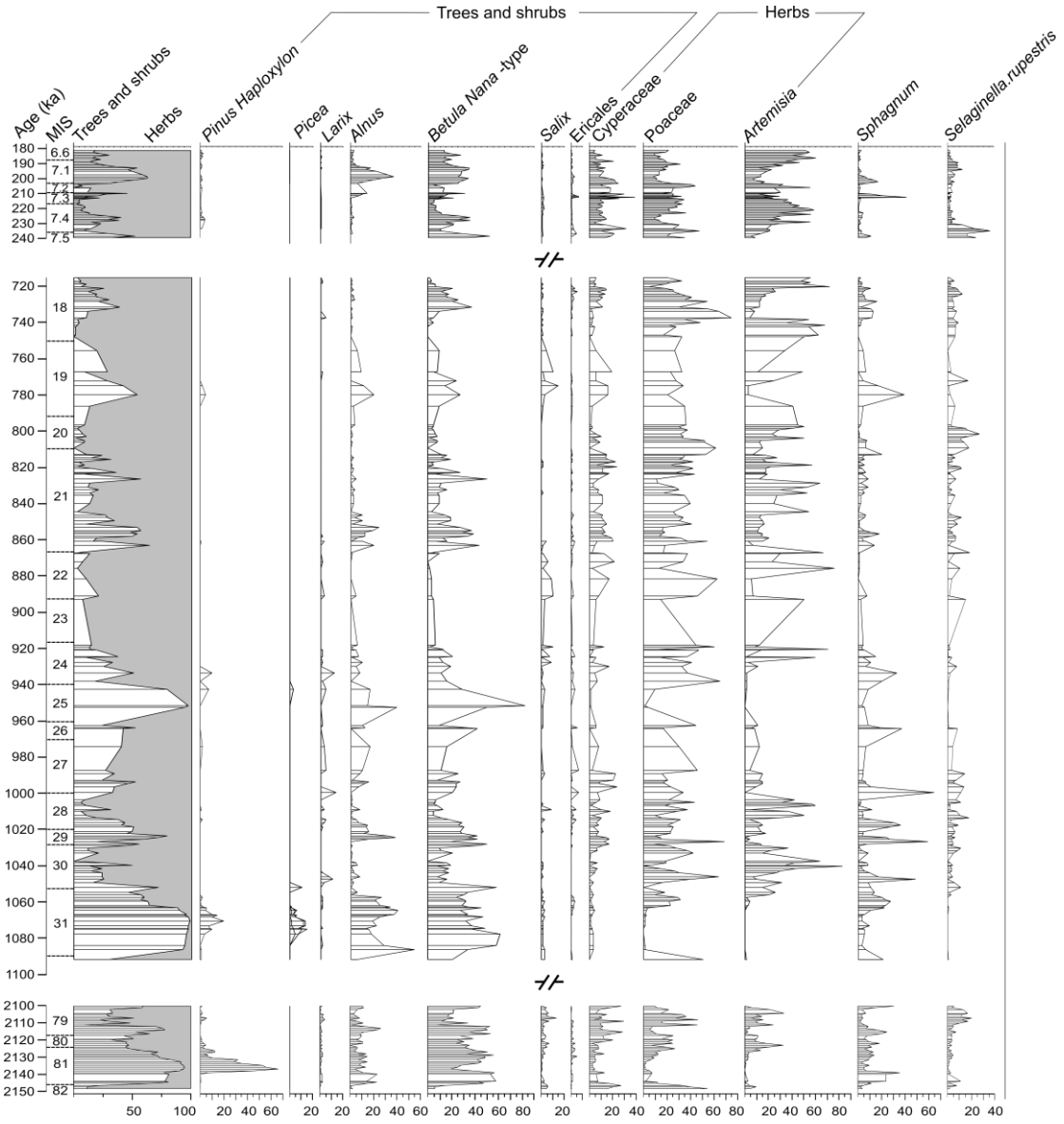

Fig. 5.1 Summary diagram showing percentages of major pollen and spore taxa of the Lake El'gygytgyn 5011-1 core sediments for the intervals of 2150-2100 ka (MIS 82-79), 1091-715 ka (MIS 31-18), and 240.5-181.5 ka (MIS 7.5-6.6). Note the breaks in temporal scale.

In the previous chapters (2, 3, and 4), the investigated pollen assemblages from Lake El'gygytgyn 5011-1 core sediments document regional vegetation and climate history during

the intervals of ~2150 to 2100 ka (MIS 82-79), ~1091 to 715 ka (MIS 31-18), and ~240.5 to 181.5 ka (MIS 7.5-6.6). In this section, all the pollen data are synthesized (Fig. 5.1) and the features of glacial and interglacial vegetation successions during different stages of the Quaternary are described.

5.1.1.1 Glacials

In general, the pollen and palynomorph assemblages during the glacials are marked by i) high contents of Poaceae and *Artemisia* pollen from the herb tundra dominated local and regional vegetation; ii) moderate percentages of regional shrubby taxa of *Salix* (in prostrate form) or *Betula*, *Alnus* and *Pinus Haploxylon* pollen that were wind-blown from a further distance; iii) some *Larix* pollen from trees in the lake basin or sheltered sites; and iv) the presence of Ranunculaceae pollen and *Selaginella repestris* spore that were found in specific microhabitats (e.g., xeric and/or rocky sites).

Despite the similarities, the features of glacial vegetation during different stages of the Quaternary are distinctive. During the early Pleistocene, the MIS 80 was marked by high contents of *Betula* and *Alnus* pollen (mean of 30.1% and 7.4%, respectively) and low amounts of *Artemisia* and Poaceae pollen (mean of 15.1% and 19.7%, respectively). During the mid-Pleistocene, the glacial pollen spectra before the first large glaciation (MIS 24-22) were composed of relatively high Poaceae and *Artemisia* pollen percentages (mean of 28.7% and 27.5%, respectively). Shortly after the first large glaciation, the glacial vegetation cover became lower, as indicated by very low shrub pollen contents (mean of <6.2%) and abundant *Artemisia* and Poaceae pollen (mean of 38.5% and 35.9%, respectively). During the late Pleistocene, the shrub pollen nearly disappeared during MIS 6 and MIS 2 (Lozhkin et al., 2007).

It can be indicated that the glacials during the early Pleistocene were comparatively warm. Towards the late Pleistocene, the xeric herb communities gradually increased at the expense of the declined diversity and populations of shrubs. As a result, the vegetation landscape became more open and a long-term cooling and drying trend can be inferred for the regional climate.

In addition, some of the cold intervals (glacials/stadials) were relatively wet, including MIS 80, MIS 30, MIS 28, MIS 26, MIS 24, MIS 7.4 and MIS 6.6. These periods were

characterized by the presence of some *Pinus Haploxylon* (stone pine) pollen, suggesting the presence of a sufficient snow cover protecting the evergreen shrub from winter desiccation.

5.1.1.2 Interglacials

As compared to the glacials, interglacials can be distinguished by the predominance of shrub components (*Betula-Alnus-Salix*) in the regional vegetation. The pollen spectra resemble Holocene pollen assemblages of Lake El'gygytgyn PG1351 core sediments, demonstrating a similarly warm climate setting (Lozhkin et al., 2007). Nevertheless, differences between the interglacials are also evident in terms of tree and shrub compositions.

Firstly, as a major pollen taxon of MIS 81 optimum (mean of 44.8%; ranging from 28.4% to 65.8%), MIS 5 and the Holocene (Lozhkin and Anderson, 2013), *Pinus Haploxylon* of MIS 79, MIS 27, MIS 25 and MIS 21 had very low pollen proportions (*c.* <5%). Secondly, the "super" interglacials (MIS 31 and MIS 11; Melles et al., 2012) were marked by the establishment of dark conifers (mainly *Picea* and *Pinus*) and deciduous forests (mainly *Larix*) accompanied by tree/high-shrub *Betula* and *Alnus* locally and regionally (Lozhkin and Anderson, 2013).

In terms of vegetation succession patterns, the interglacials preceding and following the first large glaciation show distinct shifts. Before MIS 24-22, the onset of interglacials was characterized by a progressive increase in tree/shrub components. In contrast, the subsequent interglacials were initiated by a rapid expansion of trees/shrubs followed by a gradual return to full glacial conditions.

5.1.2 Arctic biome variations during the Quaternary and the orbital forcings

The biome reconstruction provides a quantitative evaluation of vegetation changes that allows an explicit comparison with other paleoclimatic records (Tarasov et al., 2013). As shown in Fig. 5.2A, the biomization results derived from the Lake El'gygytgyn 5011-1 pollen records show distinct Arctic biome variations for the intervals of 2150-2100 ka (MIS 82-79), 1091-715 ka (MIS 31-18), and 240.5-181.5 ka (MIS 7.5-6.6; this study) and for the periods of 90-140 ka (MIS 5), 380-430 ka (MIS 11), and 1091-1060 ka (MIS 31; Tarasov et al., 2013).

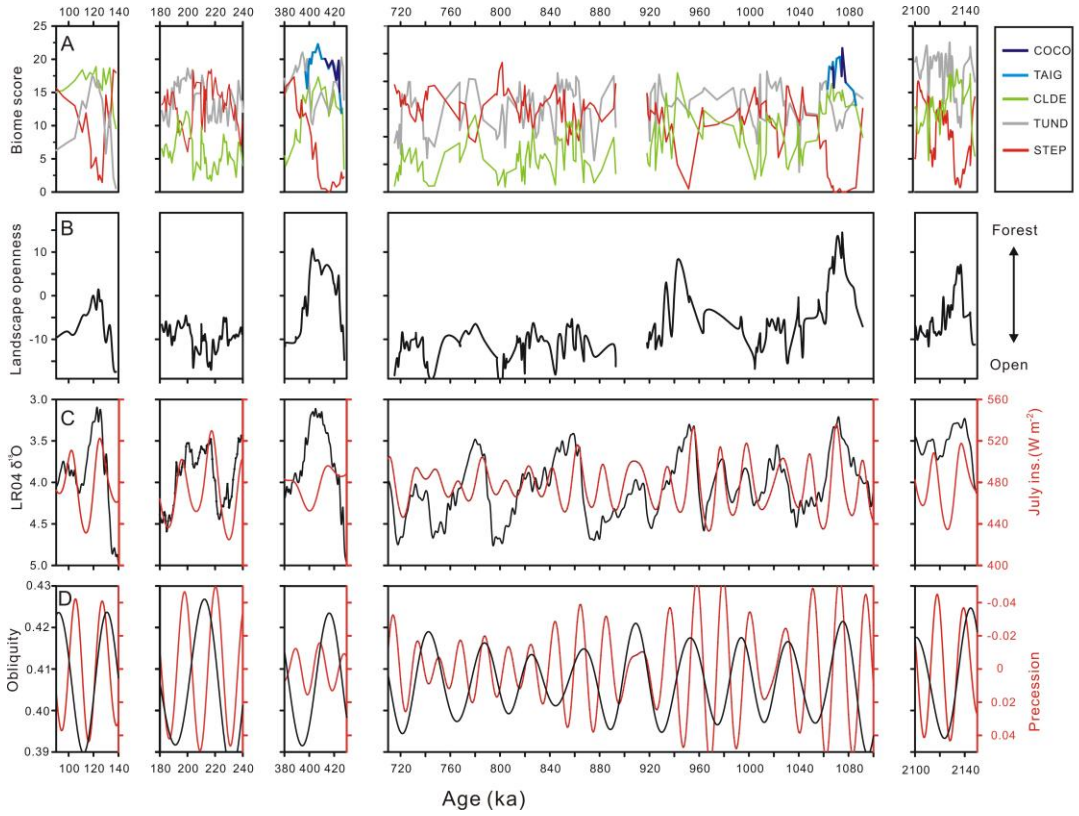

Fig. 5.2 Summary diagrams showing: (A) biome reconstructions of Lake El'gygytgyn 5011-1 core sediments for the intervals of 2150-2100 ka (MIS 82-79), 1091-715 ka (MIS 31-18), and 240.5-181.5 ka (MIS 7.5-6.6; this study) and previous biomization results for the periods of 90-140 ka (MIS 5), 380-430 ka (MIS 11), and 1091-1060 ka (MIS 31; Tarasov et al., 2013), (B) landscape openness calculated as the different between MSFB and MSOB, (C) LR04 global marine stack (black line, Liesecki and Raymo, 2005) and mean July insolation for 67.5 ℕ (red line, Laskar et al., 2004), and (D) precession curve (red line) and obliquity curve (black line), after Laskar et al. (2004).

A total of five biomes existed during the investigated periods, comprising tundra (TUND), cold steppe (STEP), cold deciduous forest (CLDE), taiga (TAIG), and cool conifer forest (COCO). The increases in CLDE biome affinity scores and simultaneous decreases in STEP biome scores characterized the interglacials and vice verse for the glacials. The "super" interglacials (MIS 31 and 11) were marked by the high scores of two additional biomes, the TAIG and COCO (Tarasov et al., 2013).

The cyclic pattern of glacial-interglacial climates was primarily forced by the variations in the earth's orbital parameters: the precession (23-ka cycle), eccentricity (100-ka cycle), and obliquity (41-ka cycle; Hays et al., 1976). According to Maslin and Ridewell (2005), obliquity and precession are the dominant influences on the glacial-interglacial cycles, whereas eccentricity "paces" rather than "drives" climatic change due to the very minor variations. The Lake El'gygytgyn biomization results show close associations with the changes in obliquity and precession (Fig. 5.2). The major control of these orbital parameters

is expressed as a combined effect of daylight duration and summer insolation intensity, respectively, which are vital for vegetation successions in the high latitudes.

During the early stage of most interglacials (i.e., MIS 81, 31, 29, 25, 21.1, 21.3 19,18.2, and 5.5), the onset of relatively high CLDE and/or TAIG and COCO biome scores corresponded with the nearly simultaneous peaks of obliquity and precession-related summer insolation (Fig. 5.2). Hence, this mode of orbital configuration probably triggered the onset of most interglacials. However, the onset of MIS 27 and 7 was coincident with high obliquity values and synchronously low precession-related summer insolation (Fig. 5.2D). During these interglacials, the increases in CLDE biome scores were minor, which might be explained by a weaker snow melt during springs/summers and a relatively stabilized permafrost due to the offset in orbital parameters.

The interglacial periods of high CLDE and/or TAIG and COCO biome scores were basically in phase with the intervals of obliquity values shifting from maxima to minima. It highlights the key role of obliquity cycle driving Arctic vegetation successions during the Quaternary.

5.1.3 Arctic vegetation and climate in response to internal forcings

In addition to the dominant influence of orbital forcings, the internal forcings of the earth system further modulated the regional vegetation and climate through snow- and ice-albedo feedbacks, as inferred from the Lake El'gygytgyn pollen records.

During the Mid-Pleistocene Transition, the pronounced ice-sheet expansion led to a significant sea-level lowering and an exposure of continental shelves. The consequently enhanced Siberian High and the westerly jet may have caused the long-term drying in the high latitudes following the first large glaciation. Moreover, the climate pattern might have been intensified by the concomitant uplift of the northeastern Tibetan Plateau since ~0.9-0.8 Ma. The prominent cooling probably resulted in a subdued snow melt and an expanded ice sheet that aggravated the earth-albedo feedback (Calov et al., 2005). As a consequence, deep permafrost was widely distributed in the Arctic region and the growth of trees/shrubs was hampered.

The duration and state of each warm stages (interglacial/interstadial) differs between one another, as reflected by the pollen spectra and biome reconstructions of Lake El'gygytgyn

sediments. Apart from the differential orbital configurations, the proposal of Herzschuh et al. (2016) provides additional explanations. That is, the climate conditions of preceding glacial/stadials had strong imprints on the subsequent warm intervals in the high altitudes at the Pliocene-Pleistocene transition. In this study, the phenomenon is also observed from the Lake El'gygytgyn pollen records for the warm intervals of MIS 21, 19, and 7.

As the most prominent example, the MIS 7 involves three warm intervals (MIS 7.5, 7.3, and 7.1) and two cold intervals (MIS 7.4 and 7.2). The climatic optimum occurred at the substage MIS 7.1 (~10 ka duration), as identified by the highest CLDE biome affinity scores and maximum arboreal pollen contents. In addition to the persistently high precession-related summer insolation, the MIS 7.1 was preceded by the mild short-lived MIS 7.2 stadial. As a result, the arboreal refugia were probably close to the Lake El'gygytgyn area and the permafrost was moderately distributed.

In contrast, the MIS 7.5 and 7.3 were short (~4 ka duration) and were characterized by much fewer trees and shrubs in the relatively disadvantageous orbital settings. Both intervals were preceded by a long and cold glacial/stadial (MIS 8 and MIS 7.4, respectively). In particular, the MIS 7.4 stadial was marked by a large glaciation, which was triggered by coevally low values of obliquity and precession-related summer insolation. The significantly reduced summer temperatures in the high latitudes resulted in a strong snow- and ice-albedo feedback. Consequently, the permafrost was extensive and stabilized preventing vegetation development.

5.2 Future perspective

The Lake El'gygytgyn 5011-1 sediments and pollen data allow a further analysis beyond the topics of chapters 2, 3, and 4. The ongoing work addresses:

5.2.1 Comparisons with mid- and low- latitude climate records during the Mid-Pleistocene Transition

The MPT is a prominent climate event in the entire Quaternary. According to the marine oxygen isotope records, the MPT is reflected by a gradual increase in average global ice volume and a decrease in deep-water temperature (Rial, 2004). Vegetation in the high, mid,

and low latitudes demonstrates various sensitivities to these changes under different climate systems (e.g. Singarayer and Valdes, 2010; Maslin and Ridgwell, 2005), because each of these climate systems has a different dominant effect of feedback mechanisms, which primarily include the feedback of snow-ice, thermohaline circulation and tropical SST (Clark et al., 2009). Tenaghi Philippon pollen data from the eastern Mediterranean (Tzedakis et al., 2006) and Angola Basin alkenone data from the eastern tropical Atlantic (Schefuβ et al., 2003) reflect vegetation changes throughout the entire MPT in the mid and low latitudes, respectively (Fig. 5.3B, C).

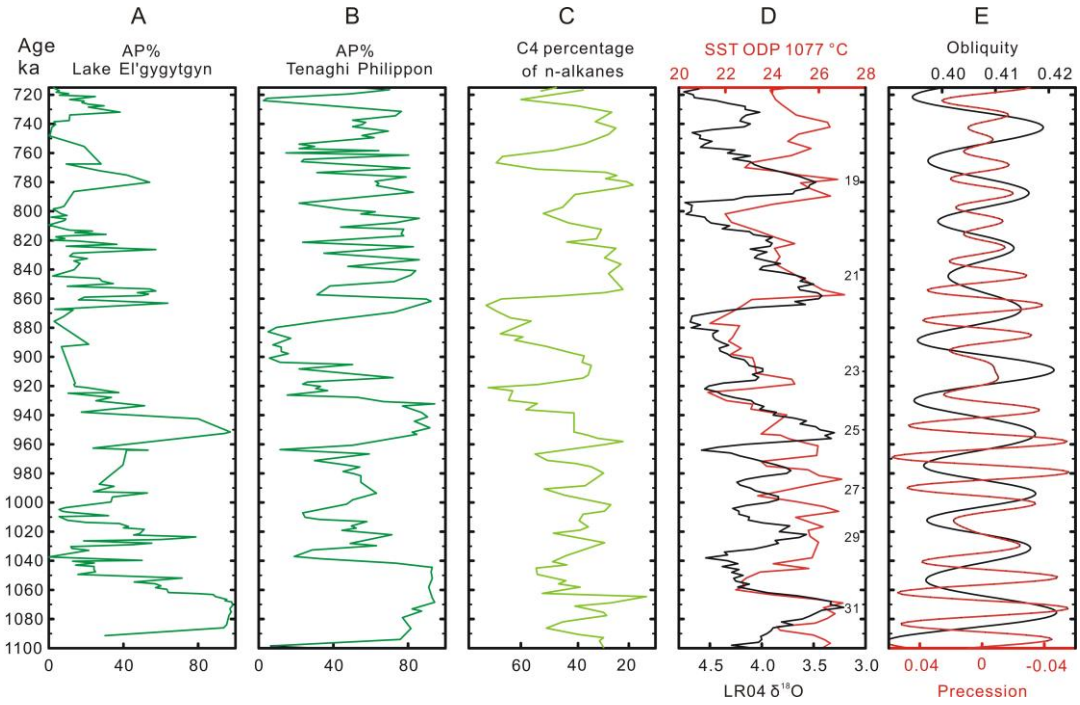

Fig. 5.3 Correlation of paleorecords in different latitudes for the Mid-Pleistocene Transition. (A) Trees and shrubs pollen (AP%) in Lake El'gygytgyn 5011-1 sediments. (B) AP percentages from Tenaghi Philippon record (Tzedakis et al., 2006). (C) C4 plant fraction of the plant wax n-alkanes using $\delta^{13}C$ values of the n-C31 alkane (Schefuβ et al., 2003). (D) Tropical alkenone-derived SST (℃) record at ODP Site 1077 (red line, Schefuβ et al., 2004) and LR04 global marine isotope stack marked with numbers of marine isotope stages (black line, Lisiecki and Raymo, 2005). (E) Precession curve (red line) and obliquity curve (black line), after Laskar et al. (2004).

In the initial stage of the MPT, synchronous peaks of precession and obliquity may have triggered the onset of the MIS 31 super interglacial (Melles et al., 2012) with high summer insolation intensity and long daylight in the high latitudes, which also had led to strikingly limited global ice volume, as reflected by the lowest oxygen isotope values in the benthic LR04 stack (Lisiecki and Raymo, 2005; Fig. 5.3F). With analogous orbital configuration, MIS 25 in both high and mid-latitudes was characterized by forested landscape regionally (Fig. 5.3A, B). These two interglacials were separated by the weak MIS 27 and 29 interglacials as a result of relatively low precession and obliquity values. In the low latitudes,

the gradual cooling of the tropical Atlantic did not follow the saw-tooth-like pattern as observed in the LR04 record. Instead, glacials appeared relatively rapid and are reflected by sharp drops in SSTs (Fig. 5.3E). Tropical SST declines resulted in large-scale aridification and favored the establishment and expansion of C4 grassland (Schefuβ et al., 2004). Thus, low-latitude vegetation dynamics are more closely linked with tropical SSTs changes and do not show a clear pattern of glacial-interglacial oscillations during the initial stage of the MPT.

MIS 24-22 is a remarkable interval during the MPT because it represents the first large glaciation, extreme SST cooling, and thermohaline circulation decline (Schmieder et al., 2000; Clark et al., 2006). Extremely low pollen concentrations in Lake El'gygytgyn within MIS 23 make it impossible to analyze the mechanisms behind the vegetation change in the high northern latitudes during this period. Comparing with other interglacials, trees and shrubs were much less floristically diversified in the eastern Mediterranean, while herbaceous taxa remained important components in the vegetation during MIS 23 (Tzedakis et al., 2006). African C4 plants also significantly expanded as a result of a cooling Atlantic and a reduced thermohaline circulation (Schefuβ et al., 2003).

Since *c.* 930 ka, the changes in the mean state and frequency of ice volume variations have an increasingly important impact on the variability of global vegetation. The LR04 benthic $\delta^{18}O$ record shows that global ice volume significantly increased after MIS 24-22 (Lisiecki and Raymo, 2005), suggesting a prominent cooling trend. Consequently, the relatively more open landscape persisted in the high latitudes with an orbital configuration similar to that during the MIS 29-27. The limited summer insolation intensity and daylight duration may have prevented snow from melting and led to an extended ice volume which in turn has caused strong earth-albedo feedback effect that aggravated glacial conditions in accordance with climate modeling studies (Calov et al., 2005).

In the mid-latitudes, forest expansions/contractions in the eastern Mediterranean region were closely linked to the global ice volume extent (Tzedakis et al., 2006). In the low latitudes, the C4 plant expansion was suppressed by the prominently strengthened thermohaline circulation and a long-term warming of the tropical Atlantic Ocean that was likely generated by extremely northward displaced Southern Ocean Fronts (Schefuβ et al., 2004). The tropical climate variability was also increasingly influenced by the glacial-interglacial variations of continental ice sheets. According to the tropical Atlantic palynological records (Dupont et al., 2001), warm-dry interglacial and cool-humid glacial environmental conditions prevailed in Africa after the first large glaciation.

During the MPT, the vegetation changes in the high latitudes exhibit a much higher amplitude in response to the external and internal forcings. Thus, a sensitive feedback of the Arctic ecosystems to future climate variations can be expected. It further underscores the potential and importance of Arctic paleoenvironmental researches.

5.2.2 A more continuous and detailed Arctic vegetation history over the Quaternary

The investigated intervals of the Lake El'gygytgyn pollen records covered the most characteristic periods of the Quaternary. Relevant studies of more time intervals would provide a more complete and continuous record of the Arctic vegetation and climate history, deepening the understanding of regional climate mechanisms.

As one of the most characteristic interglacial, MIS 25 is intriguing for a more detailed vegetation reconstruction due to the exceptionally high contents of *Betula* and *Alnus* pollen indicating the presence of dense tree-sized shrubs in the region. Given the mild and short preceding glacial, MIS 25 was probably marked by more favorable environmental settings as compared to other interglacials. However, herb pollen were almost absent while other arboreal pollen were not found as well, which is different from the pollen spectra of a "super" interglacial (e.g., MIS 31). However, a higher-resolution pollen analysis for MIS 25 is challenging because most samples are of extremely low pollen concentration.

Information of the vegetation conditions for the MIS 23 is missing due to the nearly absence of pollen grains in the Lake El'gygytgyn sediments. As the interglacial within the first large glaciation, MIS 23 is interesting considering the high values in total organic carbon concentrations, Si/Ti ratios and biogenic silica (BSi) percentages of Lake El'gygytgyn sediments (Nowaczyk et al. 2013).

In this case, increasing the sample volume may yield enough pollen counts. Otherwise, a parallel sedimentary record in the vicinity of Lake El'gygytgyn (e.g., in Alaska) possibly would fill the gaps.

References (chapter 1 and 5)

Andreev, A.A., Morozova, E., Fedorov, G., Schirrmeister, L., Bobrov, A.A., Kienast, F., Schwamborn, G., 2012. Vegetation history of central Chukotka deduced from permafrost paleoenvironmental records of the El'gygytgyn Impact Crater. Climate of the Past, 8, 1287-1300.

Andreev, A.A., Tarasov, P.E., Wennrich, V., Raschke, E., Herzschuh, U., Nowaczyk, N.R., Brigham-Grette, J., Melles, M., 2014. Late Pliocene and early Pleistocene environments of the north-eastern Russian Arctic inferred from the Lake El'gygytgyn pollen record. Climate of the Past, 9, 4599-4653.

Andreev, A. A., Tarasov, P. E., Wennrich, V., Melles, M., 2016. Millennial-scale vegetation changes in the north-eastern Russian Arctic during the Pliocene/Pleistocene transition (2.7-2.5 Ma) inferred from the pollen record of Lake El'gygytgyn. Quaternary Scienece Reviews, 147, 245-258.

Anderson, P.M., Brubaker, L.B., 1993. Holocene vegetation and climate histories of Alaska. In: Wright Jr HE, Kutzbach JE, Webb III, T., Ruddiman WF, Street-Perrot FA, Bartlein PJ (eds) Global climates since the last glacial maximum. University of Minnesota Press Minneapolis, pp: 386-400.

Anderson, P.M., Lozhkin, A.V., Belaya, B.V., Stetsenko, T.V., 2002a. Modern spore–pollen spectra from the mountain regions of the Kolyma and Indigirka rivers from lacustrine sediments. In: Simakov KV (ed) Quaternary paleogeography of Beringia. NEISRI FEB RAS Magadan, pp: 28-39 (in Russian).

Anderson, P.M., Lozhkin, A.V., Belaya, B.V., Stetsenko, T.V., 2002b. Modern spore–pollen spectra of northern Priokhot'ye from lacustrine sediments. In: Simakov KV (ed) Quaternary paleogeography of Beringia. NEISRI FEB RAS Magadan, pp: 51-61 (in Russian).

Belikovich, A.V., 1994. Recreation sources of planned "El'gygytgyn Lake Park", FEB RAS, Vestnik, 3, 57-63.

Berger, A., Loutre, M.F., 2004. Astronomical theory of palaeoclimates, Comptes Rendus Geoscience, 336, 701-709.

Brigham-Grette, J., Melles, M., Minyuk, P., Andreev, A., Tarasov, P., DeConto, R., Koenig, S., Nowaczyk, N., Wennrich, V., Rosen, P., Haltia-Hovi, E., Cook, T., Gebhardt, C., Meyer-Jacob, C., Snyder, J., Herzschuh, U., 2013. Pliocene warmth, extreme polar amplification, and stepped pleistocene cooling recorded in NE Russia. Science, 340, 1421-1427.

Calov, R., Ganopolski, A., Claussen, M., Petouhov, V., Greve, R., 2005. Transient simulation of the last glacial inception. Part I: glacial inception as a bifurcation in the climate system. Climate Dynamics, 24, 545-561.

Clark, P.U., Archer, D., Pollard, D., Blum, J.D., Rial, J.A., Brovkin, V., Mix, A.C., Pisias, N.G., Roy, M., 2006. The middle Pleistocene transition: characteristics, mechanisms, and implications for long-term changes in atmospheric pCO_2. Quaternary Science Review, 25, 3150-3184.

Clark, P.U., Dyke, A.S., Shakun, J.D., Carlson, A.E., Clark, J., Wohlfarth, B., Mitrovica, J.X., Hostetler, S.W., McCabe, A.M., 2009. The last glacial maximum. Science, 325, 710-713.

Cronin, T.M., Kitamura, A., Ikeya, N., Watanabe, M., Kamiya, T., 1994. Late Pliocene climate change 3.4-2.3 Ma: paleoceanographic record from the Yabuta Formation, Sea of Japan. Palaeogeography, Palaeoclimatology, Palaeoecology, 108, 437-455.

Ding, Z.L., Derbyshire, E., Yang, S.L., Yu, Z.W., Xiong, S.F., Liu, T.S., 2002. Stacked 2.6-Ma grain size record from the Chinese loess based on five sections and correlation withth e deep-sea $\delta^{18}O$ record. Paleoceanography, 17, doi:10.1029/2001PA00725.

Dupont, L.M., Donner, B., Schneider, R., Wefer, G., 2001. Mid-Pleistocene environmental change in tropical Africa began as early as 1.05 Ma. Geology, 29, 195-198.

Fedorov, G., Nolan, M., Brigham-Grette, J., Bolshiyanov, D., Schwamborn, G., Juschus, O., 2013. Preliminary estimation of Lake El'gygytgyn water balance and sediment income. Climate of the Past, 9, 1455-1465.

Forman, S.L., Pierson, J., Gomez, J., Brigham-Grette, J., Nowaczyk, N.R., Melles, M., 2007. Luminescence geochronology for sediments from Lake El'gygytgyn, northeast Siberia, Russia: constraining the timing of paleoenvironmental events for the past 200 ka. Journal of Paleolimnology, 37, 77-88.

Francke, A., Wennrich, V., Sauerbrey, M., Juschus, O., Melles, M., Brigham-Grette, J., 2013. Multivariate statistic and time series analysis of grain-size data in quaternary sediments of Lake El'gygytgyn, NE Russia. Climate of the Past, 9, 2459-2470.

Haltia, E.M., Nowaczyk, N.R., 2014. Magnetostratigraphy of sediments from Lake El'gygytgyn ICDP Site 5011-1: paleomagnetic age contraints for the longest paleoclimate record from the continental Arctic. Climate of the Past, 10, 623-642.

Hays, J.D., Imbrie, J., d Shackleton, N.J., 1976. Variations in the Earth's orbit: pacemarker of the ice ages. Science, 194, 1121-1132.

Herzschuh, U., Birks, H.J.B., Laepple, T., Andreev, A.A., Melles, M., Brigham-Grette, J., 2016. Glacial legacies on interglacial vegetation at the Pliocene-Pleistocene transition in NE Asia. Nature, doi: 10.1038/ncomms11967.

Juschus, O., Melles, M., Gebhardt, A.C., Niessen, F., 2009. Late quaternary mass movement events in Lake El'gygytgyn, north-eastern Siberia. Sedimentology, 56, 2155-2174.

Kalnay, E.M., Kanamitsu, M., Kistler, R., Collin, W., Deaven, D., Gandin, L., Iredell, M., Saha, S., White, G., Woollen, J., Zhu, Y., Chelliah, M., Ebisuzaki, W., Higgins, W., Janowlak, J., Mo, K.C., Ropelewski, C., Wang, J., Leetmaa, A., Reynolds, R., Jenne, R., Joseph, D., 1996. The NCEP/NCAR 40 year reanalysis project. Bull Am Meteorol Soc, 77, 437-471.

Kozhevnikov, Y. P., 1993. Vascular plants near El'gygytgyn Lake. In Belyi, V. F. & Chereshnev, I. A. (eds): Natural Depression El'gygytgyn Lake (problems of study and protection), NERSRI FEB RAS, Magadan, pp: 62-82 (in Russian).

Layer, P., 2000. Argon-40/argon-39 age of the El'gygytgyn impact event, Chukotka, Russia, Meteor. Planet. Science, 35, 591-599.

Laskar, J., Robutel, R., Joutel, F., Gastineau, M., Correia, A.C.M., Levrand, B., 2004. A long term numerical solution for the insolation quantities of the Earth. Astron. Astrophys, 428, 261-285.

Lisecki, L.E., Raymo M.E., 2005. A Pliocene-Pleistocene stack of 57 globally distributed benthic δ18O records. Paleoceanography, 20, PA1003.

Lozhkin, A.V., Anderson, P.M., Vartanyan, S.L., Brown, T.A., Belaya, B.V., Kotov, A.N., 2001. Reconstructions of late Quaternary paleo-environments and modern pollen data from Wrangel Island (northern Chukotka). Quaternary Science Reviews, 20, 217-233.

Lozhkin, A.V., Anderson, P.M., Belaya, B.V., Stetsenko, T.V., 2002. Reflections on modern pollen rain of Chukotka from bottom lake sediments. In: Simakov KV (ed) Quaternary paleogeography of Beringia. NEISRI FEB RAS Magadan, pp: 40-50 (in Russian)

Lozhkin, A.V., Anderson, P.M., Matrosova, T.V., Minyuk, P.S., 2007. The pollen record from El'gygytgyn Lake: implications for vegetation and climate histories of northern Chukotka since the late middle Pleistocene. Journal of Paleolimnology, 37, 135-153.

Lozhkin, A.V., Anderson, P.M., 2013. Vegetation responses to interglacial warming in the Arctic: examples from Lake El'gygytgyn, Far East Russian Arctic, Climate of the Past, 9, 1211-1219.

Lozhkin, A.V., Minyuk, P.S., Anderson, P.M., Nedorubova, E.Yu., Korzun, .J.V., 2017. Variability in landscape and lake systemresponses to glacial and interglacial climates during the Middle Pleistocene based on palynological and geochemical data from Lake El'gygytgyn, Eastern Arctic. Review of Palaeobotany and Palynology, 246, 1-13.

Maharaj, D., Elbra, T., Pesonen, L. J., 2013. Physical properties of the El'gygytgyn impact structure, NE Russia, Meteoritics & Planetary Science, 48, 1130-1142.

Maslin, M.A., Ridgwell, A.J., 2005. Mid-Pleistocene revolution and the 'eccentricity myth'. In: Head, M.J., Gibbard, P.L. (Eds.), Early-Middle Pleistocene Transitions: The Land-Ocean Evidence. Special Publication Geological Society of London, 247, 19-34.

Matrosova, T.V., 2009. Klimat i rastitel'nost' Anadyrskogo ploskogor'ya za poslednie 350 tys. let (palinologicheskaya kharakteristika os-adkov oz. El'gygytgyn), unpublished PhD Thesis, Magadan, p: 197.

Melles, M., Brigham-Grette, J., Minyuk, P., Koeberl, C., Andreev, A., Cook, T., Fedorov, G., Gebhardt, C., Haltia-Hovi, E., Kukkonen, M., Nowaczyk, N., Schwamborn, G., Wennrich, V. and El'gygytgyn Scientific Party, 2011. The El'gygytgyn Scientific Drilling Project – conquer-ing Arctic challenges through continental drilling. Scientific Drilling, 11, 29-40.

Melles, M., Brigham-Grette, J., Minyuk, P.S., Nowaczyk, N.R., Wennrich, V., DeConto, R.M., Anderson, P.M., Andreev, A., Coletti, A., Cook, T., Haltia-Hovi, E., Kukkonen, Lozhkin, A.V., Rosén, P., Tarasov, P., Vogel, H., Wagner, B., 2012. 2.8 Million Years of Arctic Climate Change from Lake El'gygytgyn, NE Russia. Science, 337, 315-320.

Müller, S., Tarasov, P.E., Andreev, A.A., Tütken, T., Gartz, S., Diekmann, B., 2010. Late Quaternary vegetation and environments in theVerkhoyansk Mountains region (NE Asia) reconstructed from a 50-kyr fossil pollen record from Lake Billyakh. Quaternary Science Reviews, 29, 2071-2086.

Naish, T., Kamp, P.J.J., Pillans, B., 1997. Recurring global sea-level changes recorded in shelf deposits near the G/M polarity transition, Wanganui Basin, New Zealand: implications for redefining the Pliocene-Pleistocene boundary. Quaternary International, 40, 61-71.

Naish, T.R., Abbott, S.T., Alloway, B.V., Beu, A.G., Carter, R.M., Edwards, A.R., Journeaux, T.D., Kamp, P.J.J., Pillans, B.J., Saul, G., Woolfe, K.J., 1998. Astronomical calibration of a Southern Hemisphere Plio-Pleistocene reference section, Wanganui Basin, New Zealand. Quaternary Science Reviews, 17, 695-710.

Nolan, M., Liston, G., Prokein, P., Huntzinger, R., Brigham-Grette, J., Sharpton, V., 2002. Analysis of Lake Ice dynamics and morphology on Lake El'gygytgyn, Siberia, using SAR and Landsat. Journal of Geophysical Research, 108(D2), 8162-8174.

Nolan, M. & Brigham-Grette, J. 2007: Basic hydrology, limnology, and meteorology of modern Lake El'gygytgyn, Siberia. Journal of Paleolimnology, 37, 17-35.

Nowaczyk, N.R., Melles, M., Minyuk, P., 2007. A revised age model for core PG1351 from Lake El'gygytgyn, Chukotka, based on magnetic susceptibility variations tuned to northern hemisphere insolation variations. Journal of Paleolimnology, 37, 89-104.

Nowaczyk, N.R., Haltia, E.M., Ulbricht, D., Wennrich, V., Sauerbrey, M.A., Rosén, P., Vogel, H., Francke, A., Meyer-Jacob, C., Andreev, A.A., Lozhkin, A.V., 2013. Chronology of Lake El'gygytgyn sediments – a combined magnetostratigraphic, palaeoclimatic and orbital tuning study based on multi-parameter analyses. Climate of the Past, 9, 2413-2432.

Prentice, I.C., Guiot, J., Huntley, B., Jolly, D., Cheddadi, R., 1996. Reconstructing biomes from palaeoecological data: a general method and its application to European pollen data at 0 and 6 ka, Climate Dynamics, 12, 185-194.

Prentice, I.C., Webb III, T., 1998. BIOME 6000: reconstructing global mid-Holocene vegetation patterns from palaeoecological records, Journal of Biogeography, 25, 997-1005.

Prokopenko, A.A., Hinnov, L.A., Williams, D.F., Kuzmin, M.I., 2006. Orbital forcing of continental climate during the Pleistocene: a complete astronomically tuned climatic record from Lake Baikal, SE Siberia. Quaternary Science Reviews, 25, 3431-3457.

Rial, J.A., 2004. Earth's obital eccentricity and the rhythm of the Pleistocene ice ages: the concealed pacemaker. Global and Planetary Change, 41, 81-93.

Rudaya, N., Tarasov, P.E., Dorofeyuk, N., Solovieva, N., Kalugin, I., Andreev, A., Daryin, A., Diekmann, B., Riedel, F., Tserendash, N., Wagner, M., 2009. Holocene environments and climate in the Mongolian Altai reconstructed from the Hoton-Nur pollen and diatom records: a step towards better understanding climate dynamics in Central Asia. Quaternary Science Reviews, 28, 540-554.

Schefuβ, E., Schouten, S., Jansen, J.H.F., Sinninghe Damsté, J.S., 2003. African vegetation controlled by tropical sea surface temperatures in the mid-Pleistocene period. Nature, 422, 418-421.

Schefuβ, E., Sinninghe Damste, J.S.S., Jansen, J.H.F., 2004. Forcing of tropical Atlantic sea surface temperatures during the mid-Pleistocene transition. Paleoceanography, 19, PA4029.

Schmieder, F., von Dobeneck, T., Bleil, U., 2000. The Mid-Pleistocene climate transition as documented in the deep South Atlantic Ocean: initiation, interim state and terminal event. Earth and Planetary Science Letters, 179, 539-549.

Shackleton, N.J., Opdyke, N.D., 1976. Oxygen-isotope and paleomagnetic stratigraphy of pacific core V28-239 late Pliocene to latest Pleistocene, in: Investigations of Late Quaternary Paleoceanography and Paleoclimatology, R. Cline and J. Hays, eds., Geological Society of America, 145, 449-464.

Shackleton, N.J., Hall, M.A., Pate, D., 1995. Pliocene stable isotope stratigraphy of ODP Site 846. In: Pisias, N.G., Mayer, L.A., Janacek, T.R., Palmer-Judson, A., van Andel, T.H. (Eds.), Proceedings of the Ocean Drilling Program, Scientific Results, vol. 138. Ocean Drilling Program, College Station, TX, 337-355.

Shahgedanova, M., Perov, V., Mudrov, Y., 2002. The Mountains of northern Russia. In: The Physical Geography of Northern Eurasia, Shahgedanova M (ed.). Oxford University Press: Oxford; 284-313

Shilo, N. A., Lozhkin, A. V., Anderson, P. M., Belaya, B. V., Stetsenko, T. V., Glushkova, O. Yu., Brigham-Grette, J., Melles, M., Minyuk, P. S., Nowaczyk, N., Forman, S., 2001. First continuous pollen record of vegetation and climate change in Beringia during the last 300 thousand years, Dokl. Akad. Nauk, 376, 231-234.

Singarayer, J.S., Valdes, P.J., 2010. High-latitude climate sensitivity to ice-sheet forcing over the last 120 kyr. Quaternary Science Reviews, 29, 43-55.

Singh, G., Opdyke, N.D., Bowler, J.M., 1981. Late Cainozoic stratigraphy, palaeomagnetic chronology and vegetational history from Lake George, N.S.W. Journal of the Geological Society of Australia, 28, 435-452.

Swann, G. E. A., Leng, M. J., Juschus, O., Melles, M., Brigham-Grette, J. & Sloane, H. j. 2010: A combined oxygen and silicon diatom isotope record of Late Quaternary change in Lake El'gygytgyn, North East Siberia. Quaternary Science Reviews, 29, 774-786.

Tarasov, P.E., Andreev, A.A., Anderson, P.M., Lozhkin, A.V., Leipe, C., Haltia, E., Nowaczyk, N.R., Wennrich, V., Brigham-Grette, J., Melles, M., 2013. A pollen-based biome reconstruction over the last 3.562 million years in the East Russia Arctic–new insights into climate – vegetation relationships at the regional scale. Climate of the Past, 9, 2759-2775.

Tzedakis, P.C., Hooghiemstra, H., .Pälike, H., 2006. The last 1.35 million years at Tenaghi Philippon: revised chronostratigraphy and long-term vegetation trends. Quaternary Science Reviews, 25, 3416-3430.

van den Bogaard, C., Jensen, B. J. L., Pearce, N. J. G., Froese, D. G., Portnyagin, M. V., Ponomareva, V. V., Wennrich, V. 2014. Volcanic ash layers in Lake El'gygytgyn: eight new regionally significant chronostratigraphic markers for western Beringia. Climate of the Past, 10, 1041-1062

Viereck, L., Little, Jr.E.L., 1975. Atlas of United States trees Volume 2. Alaska trees and common shrubs. U.S. Department of Agriculture Forest Service Miscellaneous Publication No. 1293. Washington, DC, pp: 19 and 82 maps.

Viereck, L., Dryness, C., Batten, A., Wenzlick, K., 1992. The Alaskan vegetation classification. U.S. Department of Agriculture, Portland.

Wennrich, V., Francke, A., Dchnert, A., Juschus, O., Leipe, T., Vogt, C., Brigham-Grette, J., Minyuk, P.S., Melles, M., and El'gygytgyn Scienece Party, 2013. Modern sedimentation patterns in Lake

El'gygytgyn, NE Russia, derived from surface sediment and inlet streams samples. Climate of the Past, 9, 135-148.

Wennrich, V., Andreev, A. A., Tarasov, P. E., Fedorov, G., Zhao, W. W., Gebhardt, C. A., Meyer-Jacob, C., Snyder, J. A., Nowaczyk, N. R., Chapligin, B., Anderson, P. M., Lozhkin, A. V., Minyuk, P. S., Koeberl, C., Melles, M., 2016. Impact processes, permafrost dynamics, and climate and environmental variability in the terrestrial Arctic as inferred from the unique 3.6 Myr record of Lake El'gygytgyn, Far East Russia - a review. Quaternary Science Reviews, 147, 221-244.

Williams, J.W., Shuman, B.N., Webb III, T., Bartlein, P.J., Leduc, P.L., 2004. Late Quaternary vegetation dynamics in North America: scaling from taxa to biomes, Ecological Monographs, 74, 309-334.

Zander, A., Hilgers, A., 2013. Potential and limits of OSL, TT-OSL, IRSL and pIRIR290 dating methods applied on a Middle Pleistocene sediment record of Lake El'gygytgyn, Russia. Climate of the Past, 9, 719-733.

Zhao, W. W., Andreev, A. A., Wennrich, V., Tarasov, P. E., Anderson, P., Lozhkin, A. V., Melles, M., 2015. The Réunion Subchron vegetation and climate history of the northeastern Russian Arctic inferred from the Lake El'gygytgyn pollen record. Palaeogeography, Palaeoclimatology, Palaeoecology, 436, 167-177.

Zhao, W.W., Tarasov, P.E., Lozhkin, A.V., Anderson, P., Andreev, A.A., Korzun, J.A., Matrin M., Nedorubova, E.Yu., Wennrich, V., 2017. High-latitude vegetation and climate changes during the Mid-Pleistocene Transition inferred from a palynological record from Lake El'gygytgyn, NE Russian Arctic. Boreas, doi: 10.1111/bor. 12262.

Summary

The thesis aims to reconstruct the Arctic vegetation during the Quaternary and to provide insights into the orbital and internal forcings of the regional climate changes. The sedimentary record of the Lake El'gygytgyn is vital for understanding the response of the vulnerable ecosystems in the Northeast Siberia to climate variations. With the successful recovery of the deep-drilled ICDP 5011-1 sediment cores, high-resolution palynological analysis and biome reconstruction are applied to the time intervals of ~2150 to 2100 ka (MIS 82-79, including the Réunion Subchron polarity reversal event), ~1091 to 715 ka (MIS 31-18, encompassing the Mid-Pleistocene Transition), and ~240.5 to 181.5 ka (MIS 7.5-6.6; mainly the penultimate interglacial).

For the interval of 2150-2100 ka (MIS 82-79) during the early Quaternary, the tundra (TUND) biome generally has higher affinity scores as compared to cold steppe (STEP) or cold deciduous forest (CLDE). An exception is a climatic optimum between ~2139-2131 ka, coinciding with MIS 81 (approximately the Réunion Subchron) when the CLDE biome has the highest scores. The coeval pollen spectra indicate that deciduous forest and shrubs expanded in the regional vegetation and the climate was relatively warm and wet.

Over the Mid-Pleistocene Transition (1091-715 ka), the pollen spectra reveal seven vegetation successions that have clearly distinguishable glacial-interglacial cycles. Comparing the interglacials during the course of the Mid-Pleistocene Transition, a tendency of a gradual replacement of trees and shrubs by open herbaceous communities can be observed. Since the first large glaciation (MIS 24-22), the long-term tendency of decreasing CLDE biome scores and landscape openness index indicates a prominent aridification in the Northeast Siberia.

During the late Quaternary at 240.5-181.5 ka (MIS 7.5-6.6), mixed herbs and shrubs (mainly alder and birch) dominated the regional vegetation. The high affinity scores of the TUND biome show that the vegetation landscape was generally open. The warm intervals (MIS 7.5, 7.3, and 7.1) were marked by an increase in the CLDE biome scores and a synchronous decrease in the STEP biome scores. Among them, the MIS 7.1 was a climatic optimum phase marked by the highest CLDE biome scores and lasted ~10 ka.

The vegetation of cold intervals (glacials/stadials) were dominated by herb tundra. Some of the cold intervals were relatively wet supporting the survival of some stone pines with a sufficient snow cover. In contrast, interglacials/interstadials can be distinguished by the shrub

dominated regional vegetation (*Betula-Alnus-Salix*). Correspondingly, increases in CLDE biome affinity scores and simultaneous decreases in STEP biome scores characterized the interglacials and vice versa for the glacials.

The cyclic pattern of glacial-interglacial climates was primarily forced by the earth's orbital parameters. The nearly simultaneous peaks of obliquity and precession-related summer insolation probably triggered the onset of most interglacials. The high CLDE biome scores during interglacial periods were basically in phase with the intervals of obliquity values shifting from maxima to minima, highlighting the key role of obliquity cycle driving Arctic vegetation successions during the Quaternary.

The internal forcings of the earth system further modulated the regional vegetation and climate. The global cooling during the first large glaciation may have prevented snow from melting and led to an extended ice volume. It in turn have caused strong snow- and ice-albedo feedback effect that aggravated glacial conditions causing the significant decline in the diversity and populations of trees and shrubs. The climatic optimum at the substage MIS 7.1 benefited from the preceding mild short-lived MIS 7.2 stadial, whereas the long and cold MIS 7.4 and 8 resulted in extensive and stabilized permafrost preventing vegetation development during MIS 7.3 and 7.5, respectively. It shows the strong imprints of glacials/stadials on the subsequent warm intervals in the high latitudes.

This thesis fills the gap of the Arctic vegetation history for the concerned time intervals. It underlines pollen analysis and biome reconstruction as invaluable methods and highlights the potential of Lake El'gygytgyn as a key archive for establishing the framework of long-term Arctic paleoenvironmental changes. This study offers insights into potential scenarios for future climate pattern in the high latitudes and allows a better understanding of the relationship between vegetation, climate, and possible mechanisms.

Zusammenfassung

Das Ziel dieser Doktorarbeit ist es, die arktische Vegetation während des Quartärs zu rekonstruieren und neue Erkenntnisse über die orbitalen und internen Einflüsse auf regionale Klimaänderungen zu erlangen. Das Sedimentprofil des El'gygytgyn-Sees eignet sich hervorragend, um die Auswirkungen von Klimaänderungen auf das verwundbare Ökosystem Nordost-Sibiriens zu untersuchen. Die erfolgreiche Bergung des langen ICDP 5011-1 Sedimentbohrkerns machte es möglich, eine hochauflösende palynologische Analyse und Biomrekonstruktion für den Zeitraum von ~2150 bis 2100 ka (MIS 82-79, inklusive des Réunion-Subchron-Polaritätswechsel-Ereignisses), ~1091 bis 715 ka (MIS 31-18, inklusive des Mittelpleistozänen Übergangs) und ~240,5 bis 181,5 ka (MIS 7.5-6.6; überwiegend das vorletzte Interglazial) anzuwenden.

Für den Zeitraum von ~2150 bis 2100 ka (MIS 82-79) während des frühen Quartärs hat das Tundra-Biom (TUND) generell höhere Zugehörigkeitswerte im Vergleich zur kalten Steppe (STEP) oder zum kalten sommergrünen Wald (CLDE). Eine Ausnahme bildet das Klimaoptimum zwischen ~2139 und 2131 ka, welches mit MIS 81 übereinstimmt (ungefähr das Réunion-Subchron). Hier zeigt das CLDE-Biom höchste Werte. Das gleichaltrige Pollenspektrum deutet auf eine Ausbreitung sommergrüner Wälder und Sträucher in der regionalen Vegetation sowie auf ein relativ warmes und feuchtes Klima.

Zur Zeit des Mittelpleistozänen Übergangs (1091-715 ka) offenbart das Pollenspektrum sieben Vegetationssukzessionen, die deutlich abgrenzbare Glazial-Interglazial-Zyklen anzeigen. Beim Vergleich der Interglaziale des Mittelpleistozänen Übergangs wird eine Tendenz zum schrittweisen Austausch der Bäume und Sträucher durch offene Krautvergesellschaftungen deutlich. Seit der ersten langen Vergletscherung (MIS 24-22) weist die Langzeittendenz des rückläufigen CLDE-Biomwerts und Offenlandschaft-Indexes auf eine starke Austrocknung in Nordost-Sibirien hin.

Während des späten Quartärs bei 240,5-181,5 ka (MIS 7.5-6.6) dominierten gemischte Kräuter und Sträucher (vor allem Erle und Birke) die regionale Vegetation. Der hohe Zugehörigkeitswert des TUND-Bioms zeigt, dass die Vegetationslandschaft generell offen war. Die warmen Zeitspannen (MIS 7.5, 7.3 und 7.1) zeichneten sich durch einen Anstieg der CLDE-Biomwerte und eine gleichzeitige Abnahme der STEP-Biomwerte aus. Darunter war MIS 7.1 eine Phase klimatischen Optimums mit höchsten CLDE-Biomwerten und einer Dauer von ~10 ka.

Die Vegetation kalter Zeitintervalle (Glaziale/Stadiale) wurde von Krauttundra dominiert. Manche dieser Kältephasen waren relativ feucht, was das Überleben von Haploxylon-Kiefern durch eine ausreichend dicke Schneedecke begünstigte. Im Gegensatz dazu können Interglaziale/Interstadiale durch eine Strauch-dominierte regionale Vegetation (*Betula-Alnus-Salix*) unterschieden werden. Dementsprechend werden Interglaziale durch Anstiege der CLDE-Biomwerte und zeitgleiche Rückgänge der STEP-Biomwerte gekennzeichnet, während umgekehrte Verhältnisse Glaziale charakterisieren.

Das zyklische Muster glazialer-interglazialer Klimate wurde primär durch orbitale Erdparameter bestimmt. Die nahezu zeitgleichen Peaks der Obliquität- und Präzession-abhängigen Sommerinsolation verursachte wahrscheinlich den Anfang der meisten Interglaziale. Die hohen CLDE-Biomwerte während der Interglaziale waren grundsätzlich phasengleich mit Zeitabschnitten, in denen Obliquitätswerte von Maxima zu Minima wechselten. Dies unterstreicht die Schlüsselfunktion der Obliquitätszyklen für arktische Vegetationssukzessionen während des Quartärs.

Die internen Einflüsse auf das Erdsystem modulierten zusätzlich die regionale Vegetation und das regionale Klima. Die globale Abkühlung während der ersten langen Vergletscherung könnte eine Schneeschmelze verhindert und zu einem ausgedehnteren Eisvolumen geführt haben. Dies wiederum führte zu starken Schnee- und Eis-Albedo-Rückkopplungen, die glaziale Bedingungen verschärften und dadurch einen signifikanten Rückgang der Diversität und Populationen von Bäumen und Sträuchern verursachten. Das Klimaoptimum von MIS 7.1 wurde von dem vorangegangenen milden und kurzen MIS 7.2-Stadial begünstigt. Hingegen verursachten die langen und kalten MIS 7.4 und 8 ausgedehnte und stabilisierende Permafröste, die die Vegetationsentwicklung während MIS 7.3 bzw. 7.5 verhinderten. Dies zeigt den starken Einfluss von Glazialen/Stadialen auf die darauffolgenden Warmphasen in den hohen Breiten.

Diese Doktorarbeit schließt eine Wissenslücke über die arktische Vegetationsgeschichte für den untersuchten Zeitraum. Sie stellt die Wichtigkeit der Pollenanalyse und Biomrekonstruktion als unschätzbare Methode heraus und zeigt das Potenzial des El'gygytgyn-Sees als Schlüsselarchiv für die Etablierung eines Rahmenkonzepts für Langzeitänderungen der arktischen Paläoumwelt. Durch diese Studie wurden Erkenntnisse über potenzielle Szenarien zukünftiger Klimamuster in den hohen Breiten gewonnen. Außerdem ermöglicht sie ein besseres Verständnis der Zusammenhänge zwischen Vegetation, Klima und möglichen Mechanismen.

Appendix

Table A.1. Counts of fossil pollen and non-pollen-palynomorphs of the sediment core 5011-1 from Lake El'gygytgyn.

Age (yr)	*Pinus*	*Pinus DiploxylonDiploxylon*	*Pinus Haploxylon*	*Picea*	*Picea sect. Eupicea*	*Picea sect. Omorica*	*Larix*	*Abies*	*Alnus*	*Betula Nana-type*	*Betulaceae undiff.*	*Myrica*	*Corylus*	*Ostrya/Carpinus*	*Juglans*	Salix	Ericales
181500	0	0	6	0	0	0	2	0	16	68	5	0	0	0	0	0	1
182696	0	0	2	0	0	0	0	0	7	39	0	0	0	0	0	0	0
183637	0	0	4	0	0	0	0	0	2	31	0	0	0	0	0	1	1
184592	0	0	3	0	0	0	1	0	11	129	0	0	0	0	0	1	3
185548	0	0	5	0	0	0	2	0	3	32	0	0	0	0	0	1	0
186503	0	0	5	0	0	0	2	0	6	61	0	0	0	0	0	0	0
187459	0	0	2	0	0	0	1	0	9	67	0	0	0	0	0	0	2
188696	0	0	0	0	0	0	0	0	8	54	1	0	0	0	0	1	2
189682	0	0	1	0	0	0	2	0	4	36	0	0	0	0	0	2	2
190595	0	0	1	0	0	0	0	0	5	19	0	0	0	0	0	0	0
191483	0	0	5	0	0	0	0	0	17	78	0	0	0	0	0	6	2
192469	0	0	4	0	0	0	0	0	30	91	0	0	0	0	0	1	4
193160	0	0	4	0	0	0	3	0	55	111	0	0	0	0	0	3	2
194311	0	0	0	0	0	0	0	0	16	42	0	0	0	0	0	0	0
195462	0	0	0	0	0	0	0	0	34	43	0	0	0	0	0	0	0
197765	0	0	0	0	0	0	0	0	55	48	0	0	0	0	0	0	2
198916	0	0	1	0	0	0	0	0	38	26	0	0	0	0	0	0	3
200067	0	0	4	0	0	0	0	0	90	114	1	0	0	0	0	1	4
201218	0	0	5	0	0	0	0	0	55	88	0	0	0	0	0	1	5
202369	0	1	0	0	0	0	0	0	27	59	0	0	0	0	0	0	4
203520	0	0	0	0	0	0	0	0	15	60	0	0	0	0	0	0	3
204112	0	0	0	0	0	0	0	0	0	11	0	0	0	0	0	0	1
205208	0	0	0	0	0	0	0	0	0	2	0	0	0	0	0	0	0
206303	0	0	0	0	0	0	0	0	0	0	0	0	0	0	0	0	0
206577	0	2	0	0	0	0	0	0	0	16	0	0	0	0	0	0	0
206960	0	0	0	0	0	0	0	0	0	0	0	0	0	0	0	0	0
209580	0	0	0	0	0	0	0	0	0	6	0	0	0	0	0	0	0
210071	0	0	0	0	0	0	0	0	52	111	3	0	0	0	0	0	2
210533	0	0	0	0	0	0	0	0	27	43	0	0	0	0	0	2	2
211579	0	0	0	0	0	0	0	0	8	15	0	0	0	0	0	0	4
212102	0	0	0	0	0	0	0	0	0	4	0	0	0	0	0	0	2
212625	0	0	0	0	0	0	0	0	0	5	0	0	0	0	0	1	4
213148	0	1	0	0	0	1	0	0	1	57	0	0	0	0	0	0	3
213671	0	1	0	0	0	0	0	0	1	30	0	0	0	0	0	4	1
214194	0	0	0	0	0	0	0	0	1	11	0	0	0	0	0	0	0
215240	0	0	0	0	0	0	0	0	0	3	0	0	0	0	0	0	0

Age (yr)	*Pinus*	*Pinus DiploxylonDiploxylon*	*Pinus Haploxylon*	*Picea*	*Picea sect. Eupicea*	*Picea sect. Omorica*	*Larix*	*Abies*	*Alnus*	*Betula Nana-type*	*Betulaceae undiff.*	*Myrica*	*Corylus*	*Ostrya/Carpinus*	*Juglans*	Salix	Ericales
216286	0	0	0	0	0	0	0	0	1	14	1	0	0	0	0	3	0
217220	0	0	0	0	0	0	0	0	0	1	0	0	0	0	0	1	0
218235	0	1	0	0	0	0	0	0	0	22	0	0	0	0	0	5	0
219251	0	3	0	0	0	0	0	1	6	34	0	0	0	0	0	8	1
220151	0	2	0	0	0	0	0	0	1	16	0	0	0	0	0	6	0
221310	0	0	0	0	0	0	0	0	1	7	0	0	0	0	0	0	0
222082	0	0	0	0	0	0	0	0	1	24	0	0	0	0	0	1	0
223241	0	2	0	0	0	0	0	0	2	14	0	0	0	0	0	0	0
224014	0	1	0	0	0	0	0	0	1	19	0	0	0	0	0	2	1
225128	0	2	0	0	0	0	0	0	0	49	0	0	0	0	0	1	0
226155	0	5	0	0	0	0	0	0	5	60	0	0	0	0	0	0	0
227182	0	5	0	0	0	0	0	0	1	33	0	0	0	0	0	0	1
228209	0	4	0	0	0	0	0	0	0	36	0	0	0	0	0	0	0
229181	0	0	0	0	0	0	0	0	1	17	0	0	0	0	0	0	0
230228	0	0	0	0	0	0	0	0	3	32	0	0	0	0	0	0	1
231229	0	0	0	0	0	0	0	0	2	64	0	0	0	0	0	0	4
233633	0	3	0	0	0	1	0	0	1	20	0	0	0	3	0	1	4
234438	0	0	0	0	0	0	0	0	0	5	0	0	0	0	0	0	1
235244	0	0	0	0	0	0	0	0	0	2	0	0	0	0	0	0	0
236854	0	0	0	0	0	0	0	0	1	17	0	0	0	0	0	0	3
238674	0	0	0	0	0	0	0	0	0	81	0	0	0	0	0	1	2
239587	0	0	0	0	0	0	0	0	0	19	0	0	0	0	0	0	0
240499	0	0	0	0	0	0	0	0	0	17	0	0	0	0	0	0	0
715202	0	0	0	0	0	1	0	0	0	4	0	0	1	0	0	0	0
717253	0	0	0	0	0	1	0	0	1	1	0	0	0	0	0	0	0
718205	1	0	0	0	0	3	0	0	1	4	0	0	0	0	0	0	0
719218	2	0	0	0	0	1	0	0	4	16	0	1	0	0	1	5	1
720231	0	0	0	0	0	0	0	0	0	5	0	0	0	0	0	0	1
721244	0	0	0	0	0	2	0	0	5	52	0	0	2	0	0	3	9
722257	0	0	0	0	0	1	0	0	5	36	0	1	0	0	0	1	3
723270	0	0	0	0	0	0	0	0	0	15	0	0	0	0	0	0	7
724320	0	0	0	0	0	0	0	0	3	59	0	0	0	1	2	3	6
725400	0	0	0	0	0	0	0	0	5	29	0	1	0	0	0	4	2
726481	2	0	0	0	0	1	0	0	13	73	0	0	0	0	0	4	9
727561	0	0	0	0	0	0	0	0	14	99	0	1	0	0	1	1	8
728479	0	0	0	0	0	0	0	0	1	44	0	0	0	0	1	0	2
731888	0	0	0	0	0	0	0	0	3	138	0	0	1	0	1	1	4
732400	0	0	0	0	0	0	0	0	3	64	0	0	1	1	0	3	3
733890	0	0	0	0	0	0	0	0	0	10	0	0	0	1	0	1	0

Table A.1. Continued

Age (yr)	*Pinus*	*Pinus Diploxylon Diploxylon*	*Pinus Haploxylon*	*Picea*	*Picea sect. Eupicea*	*Picea sect. Omorica*	*Larix*	*Abies*	*Alnus*	*Betula Nana-type*	*Betulaceae undiff.*	*Myrica*	*Corylus*	*Ostrya/Carpinus*	*Juglans*	Salix	Ericales
737700	0	0	0	0	0	7	0	0	2	7	0	0	0	0	0	0	1
738543	0	0	0	0	0	0	0	0	2	3	0	0	0	0	0	2	1
740458	0	0	0	0	0	0	0	0	0	4	0	0	0	0	0	0	0
741412	0	0	0	0	0	0	0	0	1	4	0	0	0	0	0	2	0
742365	0	0	0	0	0	0	0	0	3	0	0	0	0	0	0	0	0
747215	0	0	0	0	0	0	0	0	0	0	0	0	0	0	0	1	1
748018	0	0	0	0	0	0	0	0	0	0	0	0	0	0	0	0	0
755500	0	0	0	0	0	0	0	0	14	19	0	0	0	0	0	10	1
767500	0	0	0	0	0	1	0	0	35	29	0	0	0	0	0	37	0
767560	1	0	0	0	0	1	0	0	0	2	0	0	0	0	0	1	0
772280	0	0	0	0	0	0	0	0	1	27	0	0	0	0	0	3	2
775100	0	2	0	0	0	0	0	0	19	23	0	0	0	0	0	24	0
780100	0	9	0	0	0	0	0	0	39	54	0	0	0	0	0	4	3
786400	0	0	0	0	0	0	0	0	4	13	0	0	0	0	0	2	1
796517	0	0	0	0	0	0	0	0	5	7	0	0	0	0	0	0	0
797429	1	0	0	0	0	0	0	0	3	8	0	0	0	0	0	0	0
798341	0	0	0	0	0	0	0	0	0	3	0	0	0	1	0	0	0
799378	0	0	0	0	0	0	0	0	0	2	0	0	0	0	0	0	0
801729	0	0	0	0	0	0	0	0	1	4	0	0	0	0	0	0	0
802893	1	0	0	0	0	0	0	0	6	26	0	0	0	0	0	1	2
804056	0	0	0	0	0	0	0	0	0	1	0	0	0	0	0	0	0
805220	2	0	0	0	0	0	0	0	1	16	0	0	0	0	0	0	1
806384	0	0	0	0	0	0	0	0	3	14	0	0	0	0	0	0	1
809389	0	0	0	0	0	0	0	0	0	0	0	0	0	0	0	0	0
812900	0	0	0	0	0	0	0	0	0	7	0	0	0	0	0	0	1
813577	2	0	0	0	0	0	0	0	1	63	22	0	5	0	0	0	4
814670	2	0	0	0	0	0	0	0	5	25	2	0	0	0	0	0	1
815822	0	0	0	0	0	0	0	0	5	67	33	0	0	6	0	1	6
816975	0	0	0	0	0	0	0	0	1	8	0	0	0	0	0	2	1
817551	0	0	0	0	0	1	0	0	0	5	0	0	0	0	0	1	0
818703	0	0	0	0	0	0	0	0	6	16	4	0	0	0	0	3	1
819856	0	0	0	0	0	0	0	0	0	0	1	0	0	0	0	1	0
820432	0	0	0	0	0	0	0	0	4	15	3	0	0	0	0	0	0
822737	0	0	0	0	0	0	0	0	4	75	21	0	0	2	0	1	2
823314	2	0	0	0	0	0	0	0	3	63	25	0	1	0	1	0	6
824005	3	0	0	0	0	0	0	0	3	27	10	0	0	0	0	0	2
826299	4	0	0	0	0	0	0	0	15	147	5	0	0	0	0	0	2
828795	3	0	0	0	0	0	0	0	1	19	0	0	0	0	0	0	2
830821	0	0	0	0	0	0	0	0	4	19	0	0	0	0	0	0	0
832461	1	0	0	0	0	0	0	0	7	29	0	1	0	0	0	0	2

Table A.1. Continued

Age (yr)	*Pinus*	*Pinus DiploxylonDiploxylon*	*Pinus Haploxylon*	*Picea*	*Picea sect. Eupicea*	*Picea sect. Omorica*	*Larix*	*Abies*	*Alnus*	*Betula Nana-type*	*Betulaceae undiff.*	*Myrica*	*Corylus*	*Ostrya/Carpinus*	*Juglans*	Salix	Ericales
834102	1	0	0	0	0	2	0	0	5	25	5	0	0	0	0	3	0
835743	3	0	0	0	0	0	0	0	7	27	10	0	0	0	0	0	0
840161	1	0	0	0	0	0	0	0	10	30	3	0	0	0	0	0	0
844437	0	0	0	0	0	0	0	0	0	2	0	0	0	0	0	0	0
846186	2	0	0	0	0	0	0	0	18	26	3	0	0	0	0	0	4
847936	1	0	0	0	0	0	0	0	5	24	5	0	0	0	0	0	1
849711	2	0	0	0	0	0	0	0	45	84	29	0	0	0	0	0	0
851510	1	0	0	0	0	0	0	0	3	14	0	0	0	0	0	0	1
853310	8	0	0	0	0	0	0	0	154	173	12	0	0	0	0	0	6
854756	11	0	0	0	0	2	0	0	107	209	3	0	0	0	0	0	3
855848	22	0	0	0	0	2	0	0	47	109	4	0	0	0	0	0	5
856939	4	0	0	0	0	0	0	0	22	68	0	0	0	0	0	0	2
857943	4	0	0	0	0	1	0	0	12	33	0	0	0	0	0	0	2
858970	0	0	0	0	0	0	0	0	8	19	0	0	0	0	0	0	0
860834	0	0	0	0	0	0	0	0	0	11	0	0	0	0	0	0	2
861000	0	2	0	0	0	14	0	0	51	31	0	0	0	0	0	21	20
863100	0	0	0	0	0	0	0	0	46	99	0	0	0	0	0	3	5
867260	0	0	0	0	0	0	0	0	0	4	0	0	0	0	0	0	0
867800	0	0	0	0	0	0	0	0	4	22	0	0	0	0	0	3	2
872300	0	0	0	0	0	2	0	0	1	0	0	0	0	0	0	8	2
875600	2	0	0	0	0	0	0	0	0	3	0	0	0	0	0	1	0
881600	0	0	0	0	0	0	0	0	0	2	0	0	0	0	0	9	0
891300	1	0	0	0	0	8	0	0	17	11	0	0	0	0	0	33	9
892970	0	0	0	0	0	0	0	0	0	4	0	0	0	0	0	2	0
918100	1	0	0	0	0	0	0	0	6	7	0	0	0	0	0	2	1
918900	0	0	0	0	0	0	0	0	2	2	0	0	0	0	0	13	0
920270	0	0	0	0	0	0	0	0	1	6	0	0	0	0	0	0	0
921000	0	0	0	0	0	7	0	0	16	47	0	0	0	0	0	4	3
924500	2	0	0	0	0	5	0	0	20	60	0	0	2	0	0	20	10
924860	0	0	0	0	0	0	0	0	2	12	0	0	0	0	0	0	0
927800	8	0	0	0	0	5	0	0	51	58	0	0	0	0	0	40	7
930155	2	0	0	0	0	0	0	0	13	48	0	0	0	0	0	0	0
933500	12	14	0	0	0	18	0	0	12	15	0	0	2	0	0	1	4
937900	0	0	0	0	0	5	0	0	0	43	0	0	0	0	0	0	4
942500	40	25	0	15	0	18	0	0	61	102	0	0	13	0	0	9	14
951510	0	0	0	0	0	2	0	0	99	562	0	0	0	0	0	7	2
952500	0	0	0	0	0	2	0	0	140	173	0	0	8	3	0	5	1
962600	6	0	0	0	0	7	0	0	30	27	0	0	0	0	0	3	2
964000	10	0	0	0	0	1	0	0	26	68	0	0	0	0	0	4	11
964060	0	0	0	0	0	0	0	0	0	5	0	0	0	0	0	0	0

Table A.1. Continued

Age (yr)	*Pinus*	*Pinus DiploxylonDiploxylon*	*Pinus Haploxylon*	*Picea*	*Picea sect. Eupicea*	*Picea sect. Omorica*	*Larix*	*Abies*	*Alnus*	*Betula Nana-type*	*Betulaceae undiff.*	*Myrica*	*Corylus*	*Ostrya/Carpinus*	*Juglans*	Salix	Ericales
974200	9	5	0	0	0	11	0	0	54	48	0	0	0	0	0	1	3
987400	3	0	0	0	0	13	0	0	32	34	0	0	0	0	0	2	22
988880	0	0	0	0	0	0	0	0	3	10	0	0	0	0	0	1	0
992526	15	0	0	0	0	0	0	0	1	7	0	0	0	0	0	0	1
993451	21	0	0	0	0	0	0	0	68	119	20	0	0	0	0	0	1
994376	9	0	0	0	0	0	0	0	38	75	22	0	0	0	0	0	0
996226	0	0	0	0	0	0	0	0	6	20	3	0	0	0	0	0	0
999639	0	0	0	0	0	2	0	0	0	3	0	0	0	0	0	0	1
1003539	1	0	0	0	0	0	0	0	4	18	0	0	0	0	0	1	0
1004745	0	0	0	0	0	0	0	0	0	6	0	0	0	0	0	0	0
1005953	3	0	0	0	0	0	0	0	2	8	0	0	0	0	0	1	0
1006573	2	0	0	0	0	0	0	0	1	11	0	0	0	0	0	0	0
1009000	0	3	0	0	0	11	0	0	33	56	0	0	0	0	0	38	18
1009675	0	0	0	0	0	0	0	0	1	3	0	0	0	0	0	0	0
1012157	2	0	0	0	0	0	0	0	0	2	0	0	0	0	0	0	1
1013647	5	0	0	0	0	0	0	0	1	8	0	0	0	0	0	0	0
1014400	3	4	0	0	0	10	0	0	11	38	0	0	5	3	0	7	11
1016391	0	0	0	0	0	3	0	0	6	24	2	0	0	0	0	0	2
1017368	0	0	0	0	0	0	0	0	6	10	0	0	0	0	0	0	0
1018346	0	0	0	0	0	2	0	0	12	26	4	0	0	0	0	0	1
1021278	2	0	0	0	0	0	0	0	53	91	14	0	0	0	0	3	2
1022255	2	0	0	0	0	1	0	0	64	156	22	0	0	0	0	2	5
1023598	0	0	0	0	0	0	0	0	148	192	26	0	0	0	1	1	1
1024485	0	0	0	0	0	0	0	0	8	7	0	0	0	0	0	0	0
1025372	0	0	0	0	0	0	0	0	11	30	3	0	0	0	0	0	0
1026370	0	0	0	0	0	0	0	0	0	3	0	0	0	0	0	0	0
1027928	5	0	0	0	0	0	0	0	2	140	6	0	1	0	0	1	1
1028975	6	0	0	0	0	0	0	0	7	223	1	0	0	0	0	2	4
1030255	3	0	0	0	0	0	0	0	2	20	0	0	0	0	0	1	0
1031534	1	0	0	0	0	0	0	0	1	17	0	0	0	0	0	0	0
1032814	0	0	0	0	0	0	0	0	1	17	0	0	0	0	0	0	0
1037359	0	0	0	0	0	0	0	0	0	0	0	0	0	0	0	0	0
1038551	13	0	0	0	0	0	0	0	13	41	0	0	0	0	0	2	0
1039743	31	0	0	0	0	1	0	0	8	24	0	0	0	0	0	1	0
1040339	3	0	0	0	0	0	0	0	0	7	0	0	0	0	0	1	0
1041531	7	0	0	0	0	2	0	1	5	47	0	0	0	0	0	2	0
1042977	0	0	0	0	0	0	0	0	2	10	0	0	0	0	0	0	0
1043919	1	0	0	0	0	1	0	1	2	12	0	0	0	0	0	0	0
1045800	0	0	0	0	0	5	0	0	5	5	0	0	0	0	0	1	0
1047573	0	0	0	0	0	2	0	0	0	3	0	0	0	0	0	0	0

Table A.1. Continued

Age (yr)	*Pinus*	*Pinus DiploxylonDiploxylon*	*Pinus Haploxylon*	*Picea*	*Picea sect. Eupicea*	*Picea sect. Omorica*	*Larix*	*Abies*	*Alnus*	*Betula Nana-type*	*Betulaceae undiff.*	*Myrica*	*Corylus*	*Ostrya/Carpinus*	*Juglans*	Salix	Ericales
1049333	0	0	0	0	0	1	0	0	1	3	0	0	0	0	0	0	0
1051878	0	0	1	0	0	0	0	0	0	4	0	0	0	0	0	0	0
1054596	1	0	0	0	0	0	0	5	6	36	0	0	0	0	0	1	0
1055813	23	0	0	0	0	0	0	6	1	35	0	0	0	0	0	0	0
1057190	20	4	2	0	0	8	0	0	95	84	0	0	0	0	0	5	7
1058490	15	3	0	0	0	5	0	0	89	132	0	0	0	0	0	2	11
1059595	0	0	0	0	0	6	0	22	77	111	0	0	1	0	0	7	11
1061800	3	2	0	0	0	5	0	20	93	105	0	0	0	0	0	4	8
1062580	12	12	4	3	0	9	0	9	151	152	0	0	0	1	0	5	11
1063210	0	36	0	11	0	9	0	24	204	307	0	1	0	0	0	9	19
1064560	13	22	11	20	15	1	0	0	222	150	0	0	15	2	0	13	4
1066560	21	89	17	24	0	7	0	41	350	310	0	0	0	0	0	16	12
1067420	26	128	2	60	7	6	2	0	287	281	0	1	12	2	0	11	5
1068240	2	70	0	49	0	5	0	60	189	346	0	0	0	0	0	18	3
1070530	16	158	7	137	23	4	0	0	153	255	0	0	2	0	0	8	2
1072920	40	55	17	135	14	2	1	0	180	298	0	0	1	0	0	10	4
1074460	19	68	31	65	3	10	0	92	112	417	0	0	0	0	0	5	1
1074970	46	63	29	76	35	4	2	0	98	231	0	3	3	1	0	5	2
1077580	0	20	30	31	1	4	0	0	98	333	0	0	0	0	0	7	1
1083930	4	0	0	1	0	11	0	0	152	305	0	2	8	13	0	7	3
1085990	0	4	0	0	0	4	0	5	353	218	0	0	0	4	0	19	2
1091420	0	1	0	0	0	0	0	0	6	19	0	0	0	0	0	3	1
2099100	9	0	0	0	0	0	0	0	46	64	0	7	19	0	0	0	0
2100143	5	0	0	0	0	4	0	0	19	93	0	8	17	9	13	4	0
2101185	0	0	0	0	0	0	0	0	33	140	0	3	12	2	9	17	2
2102149	0	0	0	0	0	1	0	0	16	61	0	2	5	1	3	8	2
2104258	4	0	0	0	0	0	0	0	5	41	0	0	4	0	2	13	0
2105105	1	0	0	0	0	3	0	0	3	14	0	3	2	0	0	4	0
2106376	0	0	0	0	0	3	0	0	7	28	0	1	4	0	4	12	0
2107224	2	0	0	0	0	1	0	0	3	8	0	0	0	0	0	5	0
2108071	1	0	0	0	0	1	0	0	0	4	0	0	0	0	0	0	0
2108993	1	0	0	0	0	4	0	0	10	19	0	0	3	0	0	12	4
2110015	3	0	0	0	0	2	0	0	26	114	0	2	7	0	13	6	5
2111038	0	0	0	0	0	0	0	0	0	7	0	0	0	0	1	1	1
2112061	1	0	0	0	0	1	0	0	35	190	0	0	2	2	11	11	6
2113083	1	0	0	0	0	1	0	0	88	172	0	0	25	0	19	5	2
2114055	0	0	0	0	0	2	0	0	49	95	0	4	26	2	8	4	0
2115151	0	0	0	0	0	4	0	0	21	81	0	1	5	0	6	3	3
2116247	0	0	0	0	0	0	0	0	25	197	0	1	5	0	4	8	3
2117307	0	0	0	0	0	1	0	0	13	36	0	3	1	0	1	6	0

Table A.1. Continued

Age (yr)	*Pinus*	*Pinus DiploxylonDiploxylon*	*Pinus Haploxylon*	*Picea*	*Picea sect. Eupicea*	*Picea sect. Omorica*	*Larix*	*Abies*	*Alnus*	*Betula Nana-type*	*Betulaceae undiff.*	*Myrica*	*Corylus*	*Ostrya/Carpinus*	*Juglans*	Salix	Ericales
2119152	5	0	0	0	0	1	0	0	20	121	0	5	12	7	7	15	9
2119883	3	0	0	0	0	3	0	0	16	50	0	11	9	0	0	0	0
2120979	5	0	0	0	0	3	0	0	32	106	0	2	9	0	8	9	1
2121902	7	0	0	0	0	0	0	0	19	50	0	0	1	0	3	14	7
2122907	6	0	0	0	0	2	0	0	0	43	0	2	1	0	0	4	1
2123913	4	0	0	0	0	0	0	0	9	71	0	3	4	0	6	13	2
2124918	6	0	0	0	0	2	0	0	5	51	0	0	0	0	4	2	5
2125924	19	0	0	0	0	0	0	0	5	50	0	5	8	0	0	3	5
2126929	45	0	0	0	0	6	0	0	11	168	0	5	7	0	7	7	7
2127934	10	0	0	0	0	6	0	0	41	101	9	3	0	0	1	11	0
2128670	18	0	0	0	0	5	0	0	13	130	0	6	20	0	6	1	1
2129273	22	0	0	0	0	8	0	0	53	166	0	6	0	8	2	6	21
2130322	38	0	0	0	0	2	0	0	42	162	0	8	6	0	2	6	6
2131371	190	0	1	0	0	4	0	8	41	229	0	5	15	0	2	0	2
2132499	133	0	2	0	0	4	0	0	63	188	0	9	17	5	6	2	0
2133548	207	0	0	0	0	2	0	19	35	206	0	6	38	0	18	5	8
2134579	308	0	0	0	0	2	0	24	29	141	0	2	23	0	15	1	1
2135646	250	0	1	0	0	0	0	0	59	86	0	1	19	9	0	3	0
2136695	385	0	0	0	0	3	0	21	18	87	0	1	27	0	3	6	0
2137744	218	0	1	0	0	3	0	0	24	168	0	0	10	8	13	3	3
2138801	14	0	0	0	0	1	0	0	22	109	0	4	4	0	0	0	0
2139805	0	0	0	0	0	2	0	0	31	71	0	0	1	3	1	0	2
2143787	1	0	0	0	0	3	0	0	13	86	0	1	3	5	10	5	2
2144342	3	0	0	0	0	10	0	0	90	198	0	25	24	0	14	7	0
2145174	0	0	0	0	0	0	0	0	58	149	0	0	40	0	0	12	0
2146292	0	0	0	0	0	2	0	0	6	39	0	0	11	0	0	19	2
2147097	0	0	0	0	0	0	0	0	0	3	0	0	0	0	0	3	0
2148169	0	0	0	0	0	0	0	0	7	13	0	0	7	0	0	17	1
2149242	1	0	0	0	0	1	0	0	0	2	0	0	0	0	0	0	1

Age (yr)	Poaceae	Cyperaceae	*Artemisia*	Caryophyllaceae	*Thalictrum*	Ranunculaceae	Asteraceae	Chenopodiaceae	*Rubus*	Polygonaceae	*Polemoniaceae*	Cruciferae	Cichorioideae	*Valeriana*	Geraniaceae	*Gentianaceae*	*Nuphar*
181500	109	25	261	9	0	5	2	1	0	1	0	0	2	1	0	0	0
182696	54	9	157	6	1	4	1	1	0	0	0	0	1	0	0	1	3
183637	15	9	85	8	0	3	2	0	0	1	0	0	0	1	0	0	2
184592	46	53	191	22	0	5	2	2	0	1	0	0	1	1	0	0	0

Table A.1. Continued

Age (yr)	Poaceae	Cyperaceae	*Artemisia*	Caryophyllaceae	*Thalictrum*	Ranunculaceae	Asteraceae	Chenopodiaceae	*Rubus*	Polygonaceae	*Polemoniaceae*	Cruciferae	Cichorioideae	*Valeriana*	Geraniaceae	*Gentianaceae*	*Nuphar*
185548	32	11	109	6	1	5	0	5	0	0	0	0	3	0	0	1	0
186503	54	24	277	13	1	6	2	1	0	0	0	0	2	1	0	1	3
187459	57	21	153	11	1	2	3	0	0	0	0	0	2	0	0	2	2
188696	84	93	151	11	1	8	4	0	0	19	0	0	0	3	0	2	1
189682	52	6	119	9	1	3	0	0	0	10	0	0	2	0	0	8	0
190595	35	11	26	2	1	0	0	0	0	9	0	0	0	0	0	3	0
191483	72	30	123	8	1	2	2	1	0	15	0	0	0	1	0	10	1
192469	71	20	84	13	1	4	0	0	0	6	0	0	0	1	0	12	0
193160	50	44	37	3	3	5	1	0	0	1	0	0	0	0	0	0	0
194311	24	7	28	3	1	1	0	0	0	1	0	0	0	0	0	1	0
195462	20	19	29	2	0	3	0	0	0	2	0	0	0	0	0	1	0
197765	24	17	23	1	0	3	0	0	0	1	0	0	0	0	0	0	0
198916	8	9	14	0	1	1	0	0	0	0	0	0	0	0	0	2	0
200067	38	55	22	0	1	0	0	0	0	3	0	0	0	0	0	0	0
201218	31	62	24	5	3	3	1	0	0	2	0	0	0	0	0	0	0
202369	36	50	37	1	1	1	1	0	0	5	0	0	0	0	0	0	0
203520	59	60	31	2	3	0	1	0	0	5	0	0	0	0	0	0	0
204112	116	27	93	8	5	16	2	0	0	8	0	0	0	0	0	0	0
205208	11	3	7	0	0	1	0	0	0	1	0	0	0	0	0	0	0
206303	3	0	5	1	0	0	0	0	0	0	0	0	0	0	0	0	0
206577	31	22	30	3	1	9	1	0	0	5	1	0	0	0	0	0	0
206960	0	0	0	0	0	0	0	0	0	0	0	0	0	0	0	0	0
209580	12	9	15	0	2	2	0	0	0	4	0	0	0	0	0	0	0
210071	58	28	93	2	4	5	0	0	0	1	0	0	1	1	0	1	0
210533	66	77	30	5	0	1	1	0	0	3	0	0	0	0	0	0	0
211579	26	20	22	4	0	4	0	0	0	2	0	0	0	0	0	0	0
212102	10	2	9	1	0	2	0	0	0	0	0	0	0	1	0	0	0
212625	12	24	9	3	0	1	0	0	0	2	0	0	0	0	0	0	0
213148	57	41	63	25	0	6	2	0	0	3	0	0	1	4	0	3	0
213671	72	64	50	15	5	1	0	0	0	3	1	0	0	0	0	2	0
214194	74	20	79	13	1	6	1	1	0	4	0	0	0	1	0	0	0
215240	21	7	22	2	11	1	0	0	0	0	0	0	0	0	0	0	0
216286	86	42	132	20	9	15	2	0	0	3	0	0	0	1	0	1	0
217220	27	6	31	10	3	1	1	0	0	0	0	0	0	0	0	0	0
218235	91	38	156	1	1	10	2	1	0	1	1	0	2	0	0	0	0
219251	147	55	204	20	5	15	1	0	0	5	0	0	0	1	0	0	2
220151	61	18	160	8	2	7	6	3	0	2	1	0	0	0	0	0	1
221310	29	9	76	2	1	3	1	0	0	0	0	0	0	0	0	0	0
222082	68	33	154	12	1	5	1	2	0	2	3	0	0	0	0	0	1
223241	47	15	37	8	0	2	1	0	0	0	3	0	0	0	0	0	0
224014	22	14	97	8	1	4	0	0	0	0	0	0	0	0	0	0	4
225128	28	20	58	12	1	2	1	9	0	2	0	0	1	0	0	0	0
226155	16	23	41	9	0	6	1	1	0	1	0	0	0	0	0	0	3

Table A.1. Continued

Age (yr)	Poaceae	Cyperaceae	*Artemisia*	Caryophyllaceae	*Thalictrum*	Ranunculaceae	Asteraceae	Chenopodiaceae	*Rubus*	Polygonaceae	*Polemoniaceae*	Cruciferae	Cichorioideae	*Valeriana*	Geraniaceae	*Gentianaceae*	*Nuphar*
227182	13	19	39	14	0	3	0	1	0	1	0	0	0	0	0	0	0
228209	14	12	20	8	0	0	4	1	0	0	0	0	0	0	0	3	0
229181	17	7	66	5	0	4	2	0	0	0	0	0	0	0	0	0	0
230228	33	6	45	24	0	0	5	0	0	0	0	0	2	0	0	0	0
231229	93	43	69	8	0	8	1	0	0	12	0	0	0	0	0	0	1
233633	47	60	35	7	0	1	0	0	0	3	0	0	0	0	0	0	0
234438	19	11	11	1	1	1	0	0	0	1	0	0	0	0	0	0	0
235244	9	2	4	1	0	0	0	0	0	0	0	0	0	0	0	0	0
236854	14	13	8	2	0	0	0	0	0	1	0	0	0	0	0	0	1
238674	31	29	8	2	0	0	0	0	0	1	0	0	0	0	0	0	1
239587	20	8	5	3	1	0	0	0	0	1	0	0	0	0	0	0	0
240499	45	12	23	8	1	0	0	0	0	0	0	0	0	0	0	0	0
715202	47	12	128	9	13	3	5	0	0	4	1	0	1	0	0	0	0
717253	17	2	25	0	1	1	0	0	0	1	0	0	0	0	0	0	0
718205	52	6	127	11	1	6	3	0	0	2	0	1	0	0	0	0	0
719218	50	16	138	6	1	9	4	2	0	7	0	1	1	0	0	5	1
720231	4	3	62	0	1	3	0	0	0	0	0	1	1	0	0	1	1
721244	45	34	60	14	3	5	1	0	0	10	0	0	3	0	0	0	1
722257	60	34	59	8	4	7	1	0	0	5	0	0	1	0	0	4	1
723270	34	9	34	2	1	4	2	0	0	13	0	0	0	0	5	0	4
724320	112	46	56	19	2	16	0	1	0	14	0	1	1	0	9	2	4
725400	78	18	39	7	3	4	0	0	0	11	0	0	0	0	9	1	1
726481	177	47	57	15	6	6	3	1	0	6	0	0	1	5	1	0	3
727561	135	34	53	10	1	7	3	0	0	8	0	1	0	3	1	0	0
728479	117	12	25	2	0	4	2	0	0	1	0	0	0	2	0	1	0
731888	113	41	46	10	0	8	2	0	0	5	1	0	0	1	0	0	0
732400	126	2	8	6	5	1	2	0	0	2	1	0	0	0	2	0	0
733890	68	2	8	8	3	1	1	0	0	0	2	0	0	0	0	0	0
737700	108	4	5	5	0	1	0	0	0	0	0	0	0	0	0	0	0
738543	84	4	130	5	3	2	1	0	0	1	0	0	0	0	0	0	0
740458	53	2	38	3	6	2	0	0	0	0	0	0	1	0	0	0	0
741412	57	1	180	5	7	5	0	0	0	1	0	0	0	0	1	0	0
742365	49	7	98	3	7	6	1	0	0	6	0	0	0	0	0	0	0
747215	21	3	78	6	7	3	0	0	0	4	0	0	0	0	0	1	0
748018	15	0	23	0	4	1	1	0	0	0	0	0	0	0	1	0	0
755500	59	12	78	3	6	6	3	0	0	1	0	0	0	0	0	0	0
767500	119	69	38	18	4	4	2	0	0	0	0	0	0	2	0	0	0
767560	12	3	26	3	1	0	0	0	0	0	0	0	0	1	0	2	0
772280	31	6	27	6	1	2	2	0	0	1	0	0	0	0	0	1	2
775100	54	26	5	9	1	0	0	0	0	0	0	0	0	0	0	0	0
780100	40	31	4	4	4	2	0	0	0	0	1	0	0	0	0	0	0
786400	49	3	57	10	0	0	1	0	0	0	0	0	0	0	0	0	0
796517	53	2	65	3	5	5	0	0	0	1	0	0	0	0	0	0	0

Table A.1. Continued

Age (yr)	Poaceae	Cyperaceae	*Artemisia*	Caryophyllaceae	*Thalictrum*	Ranunculaceae	Asteraceae	Chenopodiaceae	*Rubus*	Polygonaceae	*Polemoniaceae*	Cruciferae	Cichorioideae	*Valeriana*	Geraniaceae	*Gentianaceae*	*Nuphar*
797429	57	3	97	10	2	4	2	0	0	1	0	0	0	0	2	1	0
798341	52	3	66	5	21	2	0	0	0	5	1	0	0	0	0	2	0
799378	21	0	16	3	7	1	0	0	0	4	0	0	0	0	0	0	0
801729	23	4	17	6	2	6	4	0	0	4	0	0	0	3	0	0	0
802893	116	33	93	30	5	9	5	0	0	0	0	0	0	2	0	2	9
804056	25	2	39	2	5	1	0	0	0	0	0	0	0	0	2	0	0
805220	106	14	28	22	0	6	2	0	0	3	0	0	0	1	1	1	0
806384	104	17	24	12	5	9	0	0	0	5	0	1	0	4	0	0	0
809389	25	0	6	4	0	2	0	0	0	2	1	0	0	0	0	0	0
812900	34	9	4	4	3	0	0	0	0	0	0	0	0	0	0	0	0
813577	138	58	68	11	4	8	5	0	0	3	1	0	0	0	1	0	0
814670	82	32	64	0	0	14	0	0	0	4	0	0	1	0	1	0	6
815822	110	55	55	0	3	7	2	0	0	6	0	0	0	2	1	0	4
816975	58	32	25	4	4	0	1	0	0	0	0	0	0	1	0	0	0
817551	67	33	50	8	0	8	3	0	0	1	4	0	0	0	1	0	0
818703	76	18	193	5	1	10	4	0	0	0	0	0	0	1	0	0	0
819856	37	24	21	3	2	4	3	2	0	2	0	0	0	0	0	0	0
820432	59	16	24	9	2	4	1	0	0	1	0	0	0	0	0	0	2
822737	78	32	50	4	3	6	2	0	0	0	2	0	0	1	0	0	0
823314	151	70	68	11	3	9	7	0	0	3	0	0	0	0	0	0	1
824005	196	72	89	20	5	17	3	0	0	0	1	0	0	0	0	0	1
826299	32	22	36	20	1	0	2	0	0	8	0	0	0	0	2	1	1
828795	21	5	112	2	0	5	0	0	0	1	1	0	0	0	0	0	0
830821	54	6	108	5	0	1	3	0	0	0	0	0	0	0	0	2	1
832461	54	15	54	4	0	5	1	0	0	3	0	0	0	0	0	0	4
834102	51	21	162	4	5	9	3	0	1	1	0	0	0	0	0	0	2
835743	98	31	75	4	2	7	5	0	0	6	0	0	0	0	0	0	0
840161	127	35	80	11	6	8	7	0	0	2	0	0	0	0	0	0	0
844437	24	3	52	6	1	3	1	0	0	1	0	0	1	0	0	0	1
846186	50	20	24	6	2	7	0	0	0	15	2	0	0	0	0	0	0
847936	41	12	15	5	1	5	4	0	0	1	0	0	0	0	0	0	0
849711	139	58	71	14	2	4	3	0	0	5	0	0	0	0	0	0	0
851510	78	27	31	11	2	9	4	0	0	6	0	0	0	1	0	0	0
853310	107	64	74	9	3	9	3	0	0	5	1	0	0	2	1	0	0
854756	91	68	64	5	1	5	3	0	0	0	0	0	0	0	0	0	0
855848	71	51	44	13	1	4	3	0	0	7	0	0	0	3	0	0	0
856939	28	18	26	3	0	1	0	0	0	1	0	0	0	2	0	0	0
857943	13	16	13	2	0	1	0	0	0	1	0	0	0	0	1	0	0
858970	45	27	29	4	5	3	0	0	0	1	0	0	0	3	1	0	0
860834	26	14	10	0	0	2	0	0	0	0	0	0	0	2	0	2	0
861000	272	35	16	10	0	0	3	0	0	0	0	0	0	1	0	0	0
863100	40	10	16	3	3	3	0	0	0	0	0	0	0	0	0	0	0
867260	20	3	79	8	0	1	0	3	0	0	0	0	0	0	0	0	0

Table A.1. Continued

Age (yr)	Poaceae	Cyperaceae	*Artemisia*	Caryophyllaceae	*Thalictrum*	Ranunculaceae	Asteraceae	Chenopodiaceae	*Rubus*	Polygonaceae	*Polemoniaceae*	Cruciferae	Cichorioideae	*Valeriana*	Geraniaceae	*Gentianaceae*	*Nuphar*
867800	83	27	66	11	4	0	0	0	0	0	0	0	0	0	0	0	0
872300	46	30	32	4	7	4	0	0	0	0	0	0	0	0	0	0	0
875600	27	4	157	3	2	3	1	2	0	0	0	0	0	1	0	0	0
881600	68	18	6	3	2	0	0	0	0	0	0	0	0	0	0	0	0
891300	148	27	20	6	4	0	8	4	0	3	0	0	0	0	0	0	0
892970	12	5	44	10	0	5	0	1	0	3	0	0	1	0	0	0	0
918100	50	4	13	1	6	2	2	1	0	0	0	0	0	0	0	0	0
918900	75	16	10	3	1	0	0	2	0	0	0	0	0	0	0	0	0
920270	6	1	35	0	0	1	0	0	0	0	0	0	0	0	0	0	0
921000	177	10	49	4	7	5	2	0	0	0	0	0	2	0	0	0	0
924500	108	1	2	17	5	0	4	9	0	0	0	0	2	0	0	0	0
924860	19	7	81	6	1	0	1	1	0	0	0	0	3	0	0	2	0
927800	199	11	14	13	4	0	5	13	0	0	0	0	0	0	0	0	0
930155	79	41	28	13	6	5	0	0	0	8	0	0	0	0	0	6	0
933500	55	6	2	1	3	0	0	0	0	0	0	0	0	0	0	0	0
937900	176	19	3	10	0	0	10	0	0	0	0	0	0	0	0	0	0
942500	33	3	5	1	2	0	0	0	0	0	0	0	0	1	0	0	0
951510	4	7	4	0	0	1	0	0	0	1	0	0	0	0	0	0	0
952500	13	3	0	1	0	0	0	0	0	0	0	0	0	0	0	0	0
962600	137	15	34	5	7	4	2	1	0	0	0	0	2	0	0	0	0
964000	34	11	12	11	3	0	12	0	0	0	0	0	0	0	0	0	0
964060	2	0	1	1	0	0	0	1	0	1	0	0	1	0	0	0	0
974200	96	26	38	11	3	2	2	0	0	0	0	0	0	0	0	0	0
987400	143	8	14	15	1	3	3	0	0	0	0	0	4	0	0	0	0
988880	6	9	6	3	1	0	0	0	0	0	0	0	1	0	0	0	0
992526	19	19	12	14	0	3	4	0	0	0	0	0	0	0	1	0	0
993451	72	40	63	19	2	4	2	0	0	0	0	0	0	0	0	0	0
994376	56	25	46	21	3	4	4	0	0	3	0	0	0	0	0	2	0
996226	19	20	8	5	0	2	0	0	0	0	0	0	0	0	1	0	0
999639	5	1	0	0	0	0	0	0	2	1	0	0	0	0	0	0	0
1003539	60	24	116	21	12	8	1	0	2	2	0	0	0	1	0	0	0
1004745	46	6	34	5	3	3	0	2	0	0	1	0	0	0	0	1	0
1005953	44	7	111	6	0	6	0	0	0	1	2	0	1	0	0	0	1
1006573	24	2	82	4	3	9	0	0	0	0	1	0	0	0	0	0	0
1009000	162	43	18	16	5	6	6	1	0	1	0	0	2	0	0	0	0
1009675	20	13	26	5	1	0	0	0	0	0	0	0	0	1	0	1	0
1012157	4	1	20	6	0	0	1	0	0	0	0	0	1	0	0	2	0
1013647	11	7	20	13	0	2	0	0	0	0	0	0	0	2	0	1	0
1014400	68	18	9	7	4	0	2	1	0	2	2	0	0	2	0	0	0
1016391	21	4	10	2	2	0	1	0	0	1	0	0	0	1	0	3	0
1017368	8	3	6	3	0	2	0	0	0	1	0	0	0	0	0	1	0
1018346	22	3	9	5	0	1	0	0	0	0	0	0	0	0	0	0	0
1021278	74	26	44	14	2	2	0	0	0	3	0	0	0	0	0	3	0

Table A.1. Continued

Age (yr)	Poaceae	Cyperaceae	*Artemisia*	Caryophyllaceae	*Thalictrum*	Ranunculaceae	Asteraceae	Chenopodiaceae	*Rubus*	Polygonaceae	*Polemoniaceae*	Cruciferae	Cichorioideae	*Valeriana*	Geraniaceae	*Gentianaceae*	*Nuphar*
1022255	123	33	94	24	1	7	5	0	1	2	0	0	0	1	0	0	0
1023598	42	26	20	5	0	4	0	0	0	1	0	0	0	0	0	0	0
1024485	3	3	0	0	0	0	0	0	0	0	0	0	0	0	0	0	0
1025372	10	12	3	3	0	0	0	0	0	0	0	0	0	0	0	0	0
1026370	11	2	0	0	0	0	0	0	0	0	0	0	0	0	0	0	0
1027928	24	46	39	11	0	3	1	0	0	0	0	0	0	0	0	0	0
1028975	117	60	74	20	3	6	5	2	0	1	0	0	0	0	0	1	0
1030255	60	11	79	20	2	4	6	2	0	4	0	0	0	0	0	5	0
1031534	56	10	33	13	6	2	4	0	0	0	2	0	0	4	0	4	0
1032814	35	1	13	6	2	1	1	0	0	3	3	0	0	0	0	1	0
1037359	7	0	25	1	1	3	1	1	0	0	0	0	0	0	0	0	0
1038551	53	17	113	6	1	7	1	1	0	0	0	0	0	0	0	0	0
1039743	8	0	44	8	0	3	0	1	0	1	0	0	0	0	0	0	0
1040339	0	0	71	1	2	1	0	0	0	0	0	0	0	0	0	0	0
1041531	37	17	115	9	10	6	0	0	0	0	0	0	0	0	0	2	0
1042977	22	4	25	4	11	2	0	0	0	2	0	0	0	0	0	1	0
1043919	21	3	19	4	3	0	0	0	0	2	1	0	0	0	0	0	0
1045800	42	0	4	2	1	0	0	0	0	0	0	0	1	0	0	0	0
1047573	8	0	2	0	3	2	0	0	0	0	0	0	0	0	0	0	0
1049333	5	1	10	2	4	1	1	1	0	0	1	0	0	0	0	1	0
1051878	0	0	1	0	0	0	0	0	0	0	0	0	0	0	0	1	0
1054596	19	2	27	4	3	0	1	0	0	0	0	0	0	0	0	1	0
1055813	11	4	23	6	1	2	0	0	0	0	0	0	0	0	0	0	1
1057190	106	8	4	1	1	3	1	0	0	0	0	0	0	0	0	0	0
1058490	136	3	13	0	0	1	1	0	0	0	0	0	2	0	0	0	0
1059595	78	4	12	3	0	5	3	0	0	1	1	0	0	0	0	0	0
1061800	82	7	8	0	1	3	2	0	0	10	0	0	2	0	0	0	0
1062580	46	16	3	4	2	1	1	0	0	0	0	0	0	0	0	0	0
1063210	24	14	10	2	1	2	2	0	0	1	0	0	0	0	0	0	0
1064560	13	25	2	2	1	0	1	0	0	0	0	0	0	0	0	0	0
1066560	10	16	1	0	0	0	0	0	0	0	0	0	0	0	0	0	0
1067420	16	23	0	0	0	3	0	0	0	0	0	0	0	0	0	0	0
1068240	3	8	1	0	0	0	0	0	0	0	0	0	0	0	0	0	0
1070530	4	5	0	0	0	0	0	0	0	0	0	0	0	0	0	0	0
1072920	7	10	0	0	0	1	0	0	0	0	0	0	0	0	0	0	0
1074460	3	16	1	0	0	0	0	0	0	0	0	0	0	0	0	0	0
1074970	0	12	0	0	0	0	0	0	0	0	0	0	0	0	0	0	0
1077580	2	16	0	0	0	0	0	0	0	0	0	0	0	0	0	0	0
1083930	5	17	0	0	0	0	0	0	0	0	0	0	0	0	0	0	0
1085990	7	19	0	1	0	0	0	0	0	0	0	0	0	0	0	0	0
1091420	48	0	1	3	0	1	1	0	0	0	1	0	0	0	0	0	0
2099100	49	74	8	2	0	0	1	0	0	7	0	0	0	0	0	0	0
2100143	29	83	2	4	0	0	0	0	0	3	0	0	0	0	0	0	0

Table A.1. Continued

Age (yr)	Poaceae	Cyperaceae	*Artemisia*	Caryophyllaceae	*Thalictrum*	Ranunculaceae	Asteraceae	Chenopodiaceae	*Rubus*	Polygonaceae	*Polemoniaceae*	Cruciferae	Cichorioideae	*Valeriana*	Geraniaceae	*Gentianaceae*	*Nuphar*
2101185	43	66	22	10	4	0	1	0	0	4	0	0	0	0	0	0	0
2102149	68	27	67	24	3	1	6	0	0	7	0	0	0	6	0	0	4
2104258	30	11	68	9	2	1	6	0	0	6	0	0	0	0	2	0	0
2105105	35	16	10	8	1	3	2	0	1	1	0	0	0	0	0	0	0
2106376	69	16	28	5	1	2	2	0	0	2	0	0	0	1	0	0	4
2107224	10	4	2	0	0	0	0	0	0	2	0	0	0	0	0	0	0
2108071	12	1	4	2	0	0	0	0	0	1	0	0	0	0	0	0	0
2108993	26	49	15	5	0	4	3	0	3	6	0	1	0	0	0	0	0
2110015	57	33	40	24	1	2	3	0	1	15	0	0	0	2	0	0	1
2111038	46	10	24	4	0	2	3	0	0	0	0	0	0	0	0	0	0
2112061	27	43	12	9	3	0	1	0	1	3	0	0	0	0	0	0	0
2113083	25	36	17	9	1	2	0	0	0	4	0	0	0	1	1	0	1
2114055	13	30	2	4	1	0	0	0	3	0	0	0	0	0	0	0	0
2115151	20	66	6	4	0	1	0	0	0	4	1	0	0	0	0	0	2
2116247	39	72	1	3	0	0	3	0	1	4	1	0	0	0	0	0	0
2117307	36	16	16	7	0	1	0	0	0	0	0	0	0	3	0	0	2
2119152	57	43	37	7	6	2	0	0	0	6	0	0	0	3	4	0	0
2119883	71	57	23	17	2	18	0	0	0	3	1	0	0	0	0	0	0
2120979	78	45	38	11	4	4	0	0	0	13	1	0	0	0	3	0	4
2121902	52	5	38	6	2	0	1	0	1	2	0	0	0	0	0	0	0
2122907	8	9	40	5	0	0	0	0	0	0	0	0	0	0	0	0	0
2123913	48	19	51	5	1	4	0	0	1	2	0	0	0	1	0	0	3
2124918	39	12	13	1	0	0	0	0	0	6	0	0	0	0	0	0	0
2125924	24	4	21	4	0	1	0	0	0	2	0	0	0	2	0	0	0
2126929	35	18	14	6	0	2	3	0	0	7	0	0	0	2	2	0	1
2127934	40	40	10	4	1	4	3	0	0	4	0	0	0	0	0	0	0
2128670	33	13	6	8	0	7	1	0	0	2	0	0	0	2	0	0	3
2129273	26	17	13	8	0	6	2	0	0	10	0	0	0	1	0	0	0
2130322	33	17	10	6	0	4	3	0	0	8	0	0	0	0	0	0	0
2131371	38	34	16	3	1	0	0	0	0	4	0	0	1	1	0	0	0
2132499	9	23	0	0	0	1	0	0	0	0	0	0	0	0	0	0	0
2133548	11	14	2	2	1	1	0	0	0	2	0	1	0	2	0	0	0
2134579	4	18	4	6	0	0	0	0	0	4	0	0	1	0	0	0	0
2135646	6	12	2	1	0	0	0	0	2	0	0	0	0	0	0	0	0
2136695	7	27	0	0	0	0	0	0	0	0	0	0	0	0	0	0	0
2137744	27	14	1	0	1	0	0	0	0	1	0	0	0	0	0	0	0
2138801	14	26	1	2	0	0	1	0	0	0	0	0	0	0	0	0	0
2139805	9	8	1	0	0	0	0	0	0	0	1	0	0	0	0	0	1
2143787	3	12	4	2	0	3	0	0	1	2	0	0	0	4	0	0	2
2144342	52	25	1	3	1	1	1	0	0	3	0	0	0	0	0	0	0
2145174	49	68	7	6	0	4	0	0	0	3	2	0	0	1	0	0	0
2146292	115	92	15	8	22	0	2	0	0	1	2	0	0	0	0	0	0
2147097	21	11	5	3	1	2	0	0	0	2	2	0	0	0	0	0	0

Table A.1. Continued

Age (yr)	Poaceae	Cyperaceae	*Artemisia*	Caryophyllaceae	*Thalictrum*	Ranunculaceae	Asteraceae	Chenopodiaceae	*Rubus*	Polygonaceae	*Polemoniaceae*	Cruciferae	Cichorioideae	*Valeriana*	Geraniaceae	*Gentianaceae*	*Nuphar*
2148169	200	57	16	4	40	6	0	0	0	0	0	0	1	0	0	0	0
2149242	14	1	35	1	4	0	1	0	1	2	0	0	0	0	0	0	0

Age (yr)	*Nelumbo*	Papaveraceae	*Saxifraga*	Onagraceae	*Lamiaceae*	*Sphagnum*	*Selaginella.sanguinolepta*	*Selaginella.rupestris*	*Selaginella.sibrica*	*Encalypta*	Polypodiaceae	*Gelasinospora*	*Sporormiella*	*Sordaria*	*Botryococcus*	*Zygnema*-type
181500	0	0	0	0	0	14	0	8	0	0	0	0	1	0	0	0
182696	0	0	0	1	0	4	1	5	0	0	0	0	1	0	0	0
183637	0	0	0	0	0	1	1	3	0	0	0	1	0	0	0	0
184592	0	0	0	0	0	0	0	1	0	0	0	0	0	3	0	0
185548	0	0	0	0	0	4	1	6	0	1	0	1	0	0	0	0
186503	0	0	0	0	0	3	0	7	0	1	0	0	1	0	0	0
187459	0	0	0	0	0	8	0	14	0	1	0	1	0	2	0	2
188696	0	0	4	0	0	0	2	18	0	0	0	1	0	4	0	0
189682	0	0	1	0	0	0	0	25	0	0	0	0	0	1	0	0
190595	0	0	0	0	0	0	0	8	0	0	0	0	0	0	0	0
191483	0	0	4	0	0	0	0	35	0	0	0	2	1	4	0	0
192469	0	0	1	2	0	0	0	28	0	1	0	0	0	0	0	0
193160	0	0	0	0	0	1	0	27	0	0	1	7	0	1	0	0
194311	0	0	0	0	0	2	0	18	0	0	0	0	0	0	0	0
195462	0	0	0	0	1	4	0	4	0	0	1	0	0	1	0	0
197765	0	0	0	0	0	0	0	12	0	1	6	6	0	0	0	0
198916	0	0	0	0	0	7	0	6	0	0	0	5	0	0	0	0
200067	0	0	0	0	0	27	0	6	0	2	0	2	0	1	0	1
201218	0	0	0	0	0	44	0	6	0	0	0	6	0	2	0	0
202369	0	0	0	0	0	48	0	16	0	1	0	5	0	1	0	3
203520	0	0	0	1	0	19	0	4	0	0	0	7	0	5	0	0
204112	0	0	0	0	0	2	0	12	0	0	0	0	0	1	0	3
205208	0	0	0	0	0	0	0	0	0	0	0	0	0	0	0	0
206303	0	0	0	0	0	0	0	0	0	0	0	1	0	0	0	0
206577	0	0	0	0	0	2	0	3	0	1	0	0	0	0	0	1
206960	0	0	0	0	0	0	0	0	0	0	0	0	0	0	0	0
209580	0	0	0	0	0	0	0	2	0	0	0	0	0	0	0	1
210071	0	0	0	0	0	1	0	1	0	0	0	8	0	2	0	0
210533	0	0	0	0	0	32	0	6	0	2	0	10	0	6	0	2
211579	0	0	0	0	0	27	0	0	0	1	0	0	0	0	0	4
212102	0	0	0	0	0	0	0	1	0	0	0	0	0	0	0	1
212625	0	0	0	0	0	47	0	3	0	2	0	1	0	2	0	0

Table A.1. Continued

Age (yr)	*Nelumbo*	Papaveraceae	*Saxifraga*	Onagraceae	*Lamiaceae*	*Sphagnum*	*Selaginella.sanguinolepta*	*Selaginella.rupestris*	*Selaginella.sibrica*	*Encalypta*	Polypodiaceae	*Gelasinospora*	*Sporormiella*	*Sordaria*	*Botryococcus*	*Zygnema*-type
213148	0	0	0	0	0	3	0	6	0	0	0	0	0	1	0	1
213671	0	0	0	1	0	5	0	2	0	1	0	6	0	6	0	3
214194	0	0	1	1	0	0	0	4	0	1	0	5	0	2	0	0
215240	0	0	0	1	0	0	0	2	0	0	0	0	0	1	0	0
216286	0	0	0	1	0	0	0	4	0	0	0	3	0	1	0	0
217220	0	0	1	0	0	0	0	0	0	0	0	0	0	0	0	0
218235	0	0	4	1	0	1	0	6	0	2	0	1	0	5	0	0
219251	0	0	5	0	0	2	0	9	0	2	0	0	0	0	0	0
220151	0	0	0	0	0	0	0	6	0	0	0	1	0	6	0	0
221310	0	0	1	0	0	0	0	1	0	1	0	0	0	2	0	0
222082	0	0	2	1	0	2	0	14	0	0	0	0	0	0	0	0
223241	0	0	0	0	0	6	0	4	0	0	0	0	0	0	0	0
224014	0	0	0	0	0	0	0	5	0	1	0	0	0	0	0	0
225128	0	0	0	0	0	6	0	5	0	0	0	0	0	1	0	0
226155	0	0	0	0	0	6	0	5	0	0	0	0	0	2	0	0
227182	0	0	0	0	0	0	0	9	0	2	0	0	0	3	0	2
228209	0	0	0	0	0	1	0	2	0	0	0	0	0	5	0	0
229181	0	0	0	0	0	2	0	5	0	1	0	0	0	5	0	0
230228	0	0	0	0	0	3	0	3	0	0	0	0	0	1	0	0
231229	0	0	0	0	0	2	0	43	0	0	0	0	0	1	15	0
233633	0	0	1	2	0	1	0	56	0	0	1	0	0	0	2	2
234438	0	0	0	1	0	1	0	23	0	0	0	0	0	0	0	0
235244	0	0	0	1	0	1	0	13	0	1	0	0	0	0	0	0
236854	0	0	0	0	0	2	0	12	0	0	0	0	0	0	0	0
238674	0	0	0	0	0	24	0	36	0	0	4	21	0	1	0	0
239587	0	0	0	0	0	5	0	19	0	0	0	4	0	0	0	0
240499	0	0	0	0	0	61	0	22	0	0	0	7	0	2	0	0
715202	0	0	0	0	0	4	0	0	3	0	0	1	0	0	0	2
717253	0	0	0	0	2	0	0	0	3	0	0	0	0	0	0	0
718205	0	0	0	0	4	9	1	0	2	0	0	0	0	0	0	0
719218	0	3	0	0	2	9	0	0	8	0	0	0	0	0	0	1
720231	0	3	0	0	0	1	0	0	1	0	0	0	1	0	0	0
721244	0	3	0	0	0	36	1	0	26	10	3	0	0	4	0	5
722257	0	2	1	0	1	20	0	0	27	7	0	0	0	0	0	0
723270	0	1	0	0	0	7	1	0	16	5	0	0	0	1	0	0
724320	0	0	0	0	0	17	0	0	57	17	2	0	0	0	0	5
725400	0	0	1	0	0	14	0	0	26	11	4	0	0	0	0	4
726481	0	0	8	0	0	28	1	0	19	3	1	2	0	3	0	0
727561	0	0	11	0	0	29	2	0	20	6	0	0	0	0	0	0
728479	0	0	1	1	0	48	0	0	15	9	2	3	0	0	0	0

Table A.1. Continued

Age (yr)	*Nelumbo*	Papaveraceae	*Saxifraga*	Onagraceae	*Lamiaceae*	*Sphagnum*	*Selaginella.sanguinolepta*	*Selaginella.rupestris*	*Selaginella.sibrica*	*Encalypta*	Polypodiaceae	*Gelasinospora*	*Sporormiella*	*Sordaria*	*Botryococcus*	*Zygnema*-type
731888	0	0	2	0	0	9	0	0	24	7	1	5	1	6	0	0
732400	0	0	0	1	0	30	0	0	10	3	0	7	0	4	0	0
733890	0	0	1	0	0	17	0	0	10	0	1	0	0	0	0	0
737700	0	0	4	0	0	22	0	0	9	0	3	0	0	0	0	0
738543	0	0	2	1	0	9	0	0	13	4	1	0	0	0	0	0
740458	0	0	0	0	0	3	0	0	11	0	0	0	0	0	0	0
741412	0	0	0	0	0	5	0	0	19	2	0	0	0	0	0	2
742365	0	0	0	0	0	0	0	0	13	0	1	0	0	0	0	1
747215	0	0	0	0	0	0	0	0	8	0	0	0	0	0	0	0
748018	0	0	1	0	0	0	0	0	3	0	0	0	0	0	0	0
755500	0	4	11	0	0	11	0	0	1	0	3	0	0	0	0	0
767500	0	0	4	0	0	26	0	0	13	0	5	0	0	0	0	0
767560	0	0	0	0	0	0	0	0	0	0	0	0	0	0	0	0
772280	0	0	0	0	0	6	0	0	25	2	0	0	0	0	0	0
775100	0	0	0	0	0	36	0	0	2	0	4	0	0	0	0	0
780100	0	0	0	1	0	145	0	0	7	0	15	0	0	0	0	0
786400	0	0	0	0	0	7	0	0	10	0	5	0	0	0	0	0
796517	0	0	0	0	0	3	0	0	4	0	0	0	0	0	2	0
797429	0	0	0	0	0	3	0	0	9	1	0	0	0	0	5	0
798341	0	0	0	0	0	0	0	0	30	1	0	0	0	0	0	1
799378	0	0	0	1	0	0	0	0	12	2	0	0	0	0	3	1
801729	0	0	1	0	0	1	0	0	31	4	0	0	0	0	0	1
802893	0	1	3	0	0	7	0	0	78	0	0	0	0	0	0	2
804056	0	0	0	0	0	1	0	0	10	1	0	0	0	0	0	0
805220	0	2	0	1	0	19	0	0	30	0	0	1	1	1	0	0
806384	0	0	4	1	0	18	0	0	36	4	3	1	0	0	0	0
809389	0	0	0	0	0	4	0	0	11	2	0	0	0	0	0	0
812900	0	0	0	0	0	19	0	0	5	0	5	0	0	0	0	0
813577	0	0	2	0	0	25	1	0	9	3	1	9	1	3	3	0
814670	0	0	3	0	0	8	1	0	18	5	1	1	0	2	121	0
815822	0	0	2	0	0	21	0	0	12	2	0	1	0	0	31	0
816975	0	0	2	0	1	0	0	0	7	4	0	2	0	4	1	1
817551	0	0	1	0	0	4	0	0	0	8	2	0	0	2	3	0
818703	0	0	0	0	0	19	0	0	3	1	0	0	0	0	30	0
819856	0	0	0	0	0	0	0	0	12	1	0	0	0	0	3	2
820432	0	0	2	0	0	5	0	0	19	0	0	1	0	1	17	0
822737	0	0	1	0	0	19	0	0	4	1	0	3	0	5	0	1
823314	0	0	4	0	0	22	0	0	11	1	0	3	0	6	1	0
824005	0	0	6	0	0	17	0	0	11	0	0	4	0	0	0	2
826299	0	0	0	0	0	29	0	0	25	0	0	0	0	1	3	1

Table A.1. Continued

Age (yr)	*Nelumbo*	Papaveraceae	*Saxifraga*	Onagraceae	*Lamiaceae*	*Sphagnum*	*Selaginella.sanguinolepta*	*Selaginella.rupestris*	*Selaginella.sibrica*	*Encalypta*	Polypodiaceae	*Gelasinospora*	*Sporormiella*	*Sordaria*	*Botryococcus*	*Zygnema*-type
828795	0	0	0	0	0	4	1	0	6	1	0	0	0	0	29	0
830821	0	0	0	0	0	19	0	0	0	2	0	1	0	0	18	1
832461	0	3	0	0	1	8	0	0	8	5	0	0	0	1	18	0
834102	0	0	3	0	1	16	0	0	3	0	1	0	0	0	26	0
835743	0	0	3	0	0	8	1	0	20	2	0	0	0	0	32	2
840161	0	0	2	0	1	10	1	0	11	14	2	2	0	1	13	1
844437	0	0	0	0	0	0	0	0	0	0	0	0	0	0	15	0
846186	0	0	1	0	0	14	0	0	8	0	0	0	0	0	23	0
847936	0	0	0	3	0	8	0	0	19	10	0	0	0	0	9	1
849711	0	0	7	0	0	7	0	0	24	3	1	2	0	0	1	1
851510	0	0	2	0	0	3	0	0	18	3	1	0	0	0	5	2
853310	0	0	8	1	0	6	0	0	24	0	0	10	0	5	0	0
854756	0	0	6	1	0	34	0	0	6	0	0	0	0	0	0	0
855848	0	0	1	0	0	52	0	0	20	11	1	0	0	0	3	0
856939	0	0	0	1	0	43	0	0	9	0	1	0	0	0	0	0
857943	0	0	0	1	0	14	0	0	9	4	1	0	0	0	5	0
858970	0	0	0	0	0	6	0	0	11	0	0	1	0	1	6	0
860834	0	0	0	0	0	4	0	0	6	0	4	0	0	0	7	1
861000	0	0	19	0	0	44	0	0	26	0	33	0	0	0	0	0
863100	0	1	3	0	0	40	0	0	2	0	6	0	0	0	0	0
867260	0	0	0	0	0	1	0	0	27	0	0	3	0	1	0	0
867800	0	0	0	0	0	2	0	0	13	0	0	0	0	0	0	0
872300	0	0	2	0	0	2	0	0	1	0	0	0	0	0	0	0
875600	0	0	1	0	0	2	0	0	24	0	0	0	0	0	0	1
881600	0	0	2	0	0	0	0	0	4	0	1	0	0	0	0	0
891300	0	1	21	0	0	30	0	0	7	0	8	0	0	0	0	0
892970	0	0	1	0	0	2	0	0	16	1	0	0	0	1	0	0
918100	0	6	10	0	0	5	0	0	2	0	0	0	0	0	0	0
918900	0	0	1	0	0	5	0	0	2	0	6	0	0	0	0	0
920270	0	0	0	0	0	2	0	0	1	0	0	0	0	0	0	0
921000	0	6	32	0	0	20	0	0	2	0	2	0	0	0	0	0
924500	0	0	17	0	0	52	0	0	3	0	6	0	0	0	0	0
924860	0	0	0	0	0	6	0	0	5	0	0	0	0	2	0	1
927800	0	0	52	0	0	56	0	0	4	0	1	0	0	0	0	0
930155	0	0	0	0	0	18	3	0	24	5	0	0	0	0	1	4
933500	0	0	0	1	0	81	0	0	6	0	4	0	0	0	0	0
937900	0	0	0	0	0	73	0	0	3	0	5	0	0	0	0	0
942500	0	3	5	0	0	41	0	0	3	0	23	0	0	0	0	0
951510	0	0	0	0	0	20	0	0	2	0	0	4	0	2	0	0
952500	0	0	0	0	0	24	0	0	1	0	26	0	0	0	0	0

Table A.1. Continued

Age (yr)	*Nelumbo*	Papaveraceae	*Saxifraga*	Onagraceae	*Lamiaceae*	*Sphagnum*	*Selaginella.sanguinolepta*	*Selaginella.rupestris*	*Selaginella.sibrica*	*Encalypta*	Polypodiaceae	*Gelasinospora*	*Sporormiella*	*Sordaria*	*Botryococcus*	*Zygnema*-type
962600	0	4	18	0	0	31	0	0	4	0	0	0	0	0	0	0
964000	0	0	0	0	0	49	0	0	3	0	1	0	0	0	0	0
964060	0	0	0	0	0	9	0	0	2	0	0	0	0	2	0	0
974200	0	2	1	0	0	25	0	0	16	0	3	0	0	0	0	0
987400	0	0	7	0	0	14	0	0	12	0	4	0	0	0	0	0
988880	0	0	0	0	0	2	0	0	7	0	0	0	0	0	0	0
992526	0	0	0	0	0	4	0	0	8	2	0	1	0	0	0	1
993451	0	0	1	0	0	33	0	0	22	5	2	3	0	1	0	0
994376	0	0	0	0	0	22	0	0	23	1	0	4	0	3	0	0
996226	0	0	0	1	0	12	0	0	16	0	0	0	0	0	0	0
999639	0	0	0	0	0	46	0	0	8	0	0	0	0	0	0	1
1003539	0	0	2	0	0	6	0	0	20	1	0	3	1	8	0	1
1004745	0	0	0	1	0	3	0	0	15	4	0	0	0	1	0	0
1005953	0	0	0	0	0	5	0	0	2	1	0	0	0	0	2	0
1006573	0	0	0	0	0	0	0	0	3	0	0	0	0	0	0	0
1009000	0	0	10	0	0	61	0	0	9	0	10	0	0	0	0	0
1009675	0	0	0	0	0	3	0	0	6	1	0	0	0	0	0	2
1012157	0	0	0	0	0	2	1	0	5	0	0	0	0	2	0	0
1013647	0	0	0	0	0	3	1	0	17	2	0	0	0	0	0	0
1014400	0	0	5	0	0	33	0	0	8	0	13	0	0	0	0	0
1016391	0	0	0	0	0	41	0	0	3	1	0	1	0	1	0	0
1017368	0	0	0	0	0	29	0	0	7	2	1	2	0	3	0	0
1018346	0	0	0	1	0	37	2	0	5	0	0	0	0	0	0	0
1021278	0	0	0	1	0	15	1	0	23	1	0	3	2	6	0	0
1022255	0	0	0	0	0	28	1	0	35	1	0	0	2	14	0	0
1023598	0	0	0	0	0	18	1	0	10	0	2	20	0	3	1	0
1024485	0	0	0	0	0	8	0	0	2	0	2	0	0	0	0	0
1025372	0	0	1	0	0	30	0	0	3	1	8	2	0	0	0	0
1026370	0	0	0	0	0	27	0	0	2	0	0	1	0	1	0	0
1027928	0	0	1	0	0	26	0	0	15	0	2	13	0	10	0	2
1028975	0	0	6	0	1	8	0	0	13	0	1	12	0	12	0	0
1030255	0	0	0	0	0	3	0	0	27	0	0	6	0	10	0	0
1031534	0	0	0	0	0	5	0	0	14	0	0	3	0	0	0	0
1032814	0	0	0	0	0	8	0	0	5	1	0	2	0	0	0	1
1037359	0	0	0	0	0	0	0	0	0	0	0	0	0	0	0	0
1038551	0	1	1	0	0	22	2	0	6	0	0	0	0	0	0	0
1039743	0	0	0	0	0	13	0	0	6	0	0	2	0	2	0	0
1040339	0	0	0	0	0	2	0	0	2	0	1	0	0	0	0	1
1041531	0	0	3	0	0	10	1	0	10	1	0	0	0	0	0	0
1042977	0	0	0	0	0	5	0	0	3	0	0	0	0	0	0	1

Table A.1. Continued

Age (yr)	*Nelumbo*	Papaveraceae	*Saxifraga*	Onagraceae	*Lamiaceae*	*Sphagnum*	*Selaginella.sanguinolepta*	*Selaginella.rupestris*	*Selaginella.sibrica*	*Encalypta*	Polypodiaceae	*Gelasinospora*	*Sporormiella*	*Sordaria*	*Botryococcus*	*Zygnema*-type
1043919	0	0	0	0	0	8	0	0	1	1	0	0	0	0	0	0
1045800	0	0	0	0	0	17	0	0	4	0	1	0	0	0	0	0
1047573	0	0	0	0	0	22	1	0	0	1	0	0	0	0	0	0
1049333	0	0	0	0	0	3	0	0	2	0	0	0	0	0	0	0
1051878	0	0	0	0	0	1	0	0	1	0	0	0	0	0	0	0
1054596	0	0	0	0	1	17	0	0	2	1	0	0	0	0	0	1
1055813	0	0	1	0	0	16	0	0	4	0	0	0	0	0	0	0
1057190	0	3	6	0	0	100	0	0	2	0	5	0	0	0	0	0
1058490	0	9	7	0	0	131	0	0	2	0	6	0	0	0	0	0
1059595	0	3	7	0	0	138	1	0	2	0	4	0	0	0	0	0
1061800	0	4	2	0	0	112	0	0	2	0	5	0	0	0	0	0
1062580	0	0	2	0	0	120	0	0	4	0	10	0	0	0	0	0
1063210	0	0	0	0	0	205	0	0	5	0	16	0	0	0	0	0
1064560	0	7	2	0	0	69	0	0	5	0	4	0	0	0	0	0
1066560	0	0	2	0	0	48	0	0	1	0	7	0	0	0	0	0
1067420	0	0	2	0	0	33	0	0	4	0	7	0	0	0	0	0
1068240	0	0	0	0	0	24	0	0	0	0	1	0	0	0	0	0
1070530	0	0	1	0	0	25	0	0	1	0	5	0	0	0	0	0
1072920	0	0	1	0	0	88	0	0	1	0	20	0	0	0	0	0
1074460	0	0	0	0	0	30	0	0	0	0	11	0	0	0	0	0
1074970	0	0	0	0	0	35	0	0	0	0	17	0	0	0	0	0
1077580	0	0	0	0	0	35	0	0	1	0	16	0	0	0	0	0
1083930	0	0	0	0	0	16	0	0	1	0	4	0	0	0	0	0
1085990	0	2	8	0	0	43	0	0	1	0	3	0	0	0	0	0
1091420	0	7	0	0	0	26	0	0	1	0	2	0	0	0	0	0
2099100	0	0	0	0	0	118	0	0	24	0	20	9	0	0	17	0
2100143	0	0	0	0	0	167	0	0	29	10	16	4	0	1	29	0
2101185	0	0	0	0	0	67	0	0	18	2	17	4	0	1	56	0
2102149	0	0	0	0	0	14	4	0	53	2	5	7	10	0	15	5
2104258	0	0	0	0	0	19	3	0	48	5	1	2	6	4	29	0
2105105	0	0	0	0	0	4	0	0	16	0	3	0	0	0	27	0
2106376	0	0	0	0	0	8	0	0	26	1	3	0	0	0	272	2
2107224	0	0	0	0	0	2	0	0	10	0	0	0	0	0	85	2
2108071	0	0	0	0	0	1	0	0	4	0	0	0	0	0	22	0
2108993	0	0	0	0	0	5	0	0	38	0	7	2	0	1	13	2
2110015	0	0	0	0	1	11	11	0	45	7	7	2	0	0	41	2
2111038	0	0	0	0	0	7	0	0	5	3	2	0	1	0	0	1
2112061	0	0	0	0	0	39	0	0	22	2	8	6	1	0	6	3
2113083	0	0	0	0	0	31	2	0	17	3	3	3	0	0	4	1
2114055	0	0	0	0	0	51	0	0	3	0	6	2	0	0	2	0

Table A.1. Continued

Age (yr)	*Nelumbo*	Papaveraceae	*Saxifraga*	Onagraceae	*Lamiaceae*	*Sphagnum*	*Selaginella.sanguinolepta*	*Selaginella.rupestris*	*Selaginella.sibrica*	*Encalypta*	Polypodiaceae	*Gelasinospora*	*Sporormiella*	*Sordaria*	*Botryococcus*	*Zygnema*-type
2115151	0	0	0	0	0	93	3	0	27	6	11	10	2	8	3	2
2116247	0	0	0	0	0	94	0	0	11	0	15	5	0	0	11	0
2117307	0	0	0	0	0	14	0	0	7	3	4	3	2	0	1	2
2119152	0	0	0	0	0	24	0	0	10	1	0	3	7	4	17	1
2119883	0	0	0	0	0	26	0	0	14	0	24	1	0	0	29	3
2120979	0	0	0	0	1	41	1	0	15	1	0	0	0	0	14	1
2121902	0	0	0	0	0	50	0	0	3	1	5	0	0	0	42	0
2122907	0	0	0	0	0	13	1	0	5	2	0	0	0	0	47	0
2123913	0	0	0	0	0	34	0	0	4	2	0	0	0	0	116	3
2124918	0	0	0	0	0	9	0	0	0	1	5	0	0	0	80	1
2125924	0	0	0	0	1	17	0	0	6	1	1	0	0	0	172	1
2126929	0	0	0	0	0	59	1	0	9	1	4	0	0	0	95	3
2127934	0	0	0	0	0	36	0	3	15	0	19	0	0	0	9	3
2128670	0	0	0	0	3	52	2	0	18	2	3	0	0	2	9	2
2129273	0	0	0	0	0	54	0	0	16	2	2	1	0	0	1	1
2130322	0	4	0	0	0	44	0	0	17	3	19	0	0	0	5	6
2131371	0	0	0	0	1	65	3	0	8	4	9	0	0	0	0	0
2132499	0	0	0	0	0	21	0	0	9	0	7	3	0	0	0	0
2133548	0	0	0	0	1	19	0	0	6	3	6	3	2	1	1	0
2134579	0	0	0	0	0	63	0	0	7	1	1	3	0	0	0	0
2135646	0	0	0	0	0	26	3	0	1	0	3	0	0	0	0	0
2136695	0	0	0	0	0	32	0	0	5	1	5	3	0	0	0	0
2137744	0	0	0	0	0	42	0	0	9	0	27	2	0	0	0	1
2138801	0	0	0	0	0	152	0	0	11	3	4	14	0	0	1	3
2139805	1	0	1	0	0	56	14	1	3	0	27	1	0	0	0	0
2143787	0	0	0	0	0	68	0	0	31	3	10	12	4	4	2	0
2144342	0	0	0	0	0	43	0	0	12	0	12	4	0	0	12	5
2145174	0	0	0	0	0	54	0	0	13	0	11	4	0	1	23	6
2146292	0	0	0	0	0	16	0	0	31	1	1	0	0	0	111	26
2147097	0	0	0	0	0	1	0	0	1	0	0	0	0	1	8	6
2148169	0	0	0	0	0	16	0	0	8	0	13	0	0	8	73	14
2149242	0	0	0	0	0	4	0	0	0	0	0	0	0	0	68	1

Table A.1: Continued.

List of abbreviations

^{14}C	radiocarbon dated
℃	degree Celsius
AP	arboreal pollen
a.s.l	above sea level
BP	before present (before 1950)
c.	circa
ChRM	characteristic remanent magnetization
CLDE	cold deciduous forest
COCO	cold conifer forest
CONISS	constrained incremental sums of squares cluster analysis
ICDP	International Continental Scientific Drilling Program
e.g.	*exempli gratia*, for example
FTIRS	fourier transform infrared spectroscopy
km	kilometer
ka	kilo years
LW	low boundary
m	meter
MPT	middle Pleistocene transition
Myr	million years
mblf	meters below lake floor
Ma	million years
MIS	marine isotope stage
MS	magnetic susceptibility
NAP	non-arboreal pollen
NE	north-east
NPP	non-pollen-palynomorph
PAZ	pollen assemblage zone
PGTM	postglacial thermal maximum
SST	sea surface temperature
STEP	cold steppe
TAIG	taiga
TUND	tundra

Acknowledgment

I owe a lot to Dr. Andrei Andreev for giving me the opportunity to initiate my Ph.D. thesis at the University of Cologne. Since I arrived in Germany, Andrei offered substantial help to start my life and study here. I shared countless hours with him in the same office, working on the identification of my pollen samples as well as on my publications. No words can really express my gratitude to him whether in life or research. I greatly thank my supervisor Prof. Dr. Martin Melles who allowed me to become a member of his research group and gave invaluable suggestions on my work.

I appreciate the help of Prof. Dr. Pavel Tarasov, who is a referee of my thesis and also a co-author of my publications. Thanks to his work in pollen-based biomization, I can better analyze and interpret the pollen data. Dr. Volker Wennrich is acknowledged for his great support of sampling the cores from the "Lake El'gygytgyn Drilling Project" so that my work became possible. I am grateful to my co-authors Prof. Dr. Patricia Anderson and Prof. Dr. Anatoly V. Lozhkin whose expertise greatly improved the quality of my publications.

My work would not have come true without the close collaboration within the ICDP 5011 program and the support of the funding agencies. The China Scholarship Council gave me the opportunity to experience life and study in Germany. PD Dr. Finn Viehberg in my institute helped me a lot in life. Dr. Andrea Miebach from University of Bonn kindly translated the summary of this thesis into German. I also owe appreciation to my colleagues/ex-colleagues Prof. Dr. Yan Zhao, Dr. Ke Zhang, Dr. Xianyong Cao, Dr. Jonathan Hense, and Dr. Yin Yansun for their help.

I benefited incredibly from my parents Mr. Jianfa Zhao and Ms. Xianyun Yu who constantly encouraged me. A special thank goes to my girlfriend Ms. Chunzhu Chen for her wonderful support during my studies over the past seven years.

Chapter contribution

Chapter 2: The Réunion Subchron vegetation and climate history of the northeastern Russian Arctic inferred from the Lake El'gygytgyn pollen record

Zhao conducted palynological and biome reconstruction analyses and provided relevant data sets and interpretation. Zhao wrote the manuscript and Anderson provided constructive suggestions for the discussion part. Andreev, Wennrich, Tarasov, Anderson, Lozhkin, and Melles were all involved in commenting and revising the manuscript. The overall contribution of Zhao exceeds 80%.

Chapter 3: High-latitude vegetation and climate changes during the Mid-Pleistocene Transition inferred from a palynological record from Lake El'gygytgyn, NE Russian Arctic

Zhao provided original palynological and biomization data sets and interpretation. Lozhkin Anderson, Nedorubova, and Korzun provided published pollen data of 46 samples. Zhao wrote the text and Tarasov, Anderson, Andreev, Wennrich, Lozhkin, and Melles revised the manuscript before submission. The two anonymous reviewers provided constructive suggestions for the improvement of the manuscript. The overall contribution of Zhao exceeds 85%.

Chapter 4: The penultimate interglacial vegetation and climate record of the northeastern Russian Arctic inferred from the Lake El'gygytgyn pollen record

Zhao conducted palynological and biome reconstruction analyses and provided relevant data sets. Zhao undertook the data interpretation and wrote the manuscript. The overall contribution of Zhao to exceeds 90%.

Erkärung

Ich versichere, dass ich die von mir vorgelegte Dissertation selbständing angefertigt, die benutzten Quellen und Hilfsmittel vollständig angegeben und die Stellen der Arbeit – einschließlich Tabellen, Karten und Abbildungen -, die anderen Werken im Wortlaut oder dem Sinn nach entnommen sind, in jedem Einzelfall als Entlehnung kenntlich gemacht habe; dass diese Dissertation noch keiner anderen Fakultät oder Universität zur Prüfung voegelegen hat; dass sie – abgesehen von unten angegebenen Teilpublikationen – noch nicht veröffentlich worden ist, sowie, dass ich eine solche Veröffentlichung vor Abschluss des Promomotionsverfahrens nicht vornehmen werde.

Die Bestimmungen der Promotionsordung sind mir bekannt. Die von mir vorgelegte Disssertation ist von Prof. Dr. Martin Melles and Dr. Andrei Andreev betreut worden.

Folgende Teilpublikationen liegen vor:

Zhao, W.W., Andreev, A.A., Wennrich, V., Tarasov, P.E., Anderson, P., Lozhkin, A.V., and Melles, M. (2015): The Réunion Subchron vegetation and climate history of the northeastern Russian Arctic inferred from the Lake El'gygytgyn pollen record. Palaeogeography, Palaeoclimatology, Palaeoecology 436, 167-177.

Zhao, W.W., Tarasov, P.E., Lozhkin, A.V., Anderson, P., Andreev, A.A., Korzun, J.A., Matrin M., Nedorubova, E.Yu., and Wennrich, V. (2017): High-latitude vegetation and climate changes during the Mid-Pleistocene Transition inferred from a palynological record from Lake El'gygytgyn, NE Russian Arctic. Boreas DOI: 10.1111/bor. 12262.

Zhao, W.W., Andreev, A.A., Tarasov, P.E., Wennrich, V., Melles, M. (ready for submission): The penultimate interglacial vegetation and climate record of the northeastern Russian Arctic inferred from the Lake El'gygytgyn pollen record.

Köln, den 09. 18. 2017

Wenwei Zhao